Journal of Medicinal Chemistry

Article

Structure-Based Optimization of N-Substituted Oseltamivir Derivatives as Potent Anti-influenza A Virus Agents with Significantly Improved Potency against Oseltamivir-Resistant N1-H274Y Variant

Jian Zhang, Natarajan Arul Murugan, Ye Tian, Chiara Bertagnin, Zengjun Fang, Dongwei Kang, Xiujie Kong, Haiyong Jia, Zhuosen Sun, Ruifang Jia, Ping Gao, Vasanthanathan Poongavanam, Arianna Loregian, Wenfang Xu, Xiuli Ma, Xiao Ding, bing huang, Peng Zhan, and Xinyong Liu

J. Med. Chem., **Just Accepted Manuscript** • DOI: 10.1021/acs.jmedchem.8b01065 • Publication Date (Web): 26 Oct 2018

ACS Publications

is published by the American Chemical Society. 1155 Sixteenth Street N.W., Washington, DC 20036

Structure-Based Optimization of N-Substituted Oseltamivir Derivatives as Potent Anti-influenza A Virus Agents with Significantly Improved Potency against Oseltamivir-Resistant N1-H274Y Variant

Jian Zhang,[†] Natarajan Arul Murugan,[&] Ye Tian,[†,@] Chiara Bertagnin,[≠] Zengjun Fang,[†,#] Dongwei Kang,[†] Xiujie Kong,[†] Haiyong Jia,[†] Zhuosen Sun,[†] Ruifang Jia,[†] Ping Gao,[†] Vasanthanathan Poongavanam,[|,◊] Arianna Loregian,[≠] Wenfang Xu,[†] Xiuli Ma,[‡] Xiao Ding,[†] Bing Huang,[‡,*] Peng Zhan,[†,*] and Xinyong Liu[†,*]

[†] *Department of Medicinal Chemistry, Key Laboratory of Chemical Biology (Ministry of Education), School of Pharmaceutical Sciences, Shandong University, 44 West Culture Road, 250012 Jinan, Shandong, PR China.*

[&] *Division of Theoretical Chemistry and Biology, School of Biotechnology, KTH Royal Institute of Technology, S-106 91 Stockholm, Sweden.*

[@] *Key Laboratory for Experimental Teratology of Ministry of Education, Key Laboratory of Infection and Immunity of Shandong Province, Department of Immunology, School of Basic Medical Sciences, Shandong University, 44 West Culture Road, 250012 Jinan, Shandong, P. R. China.*

[≠] *Department of Molecular Medicine, University of Padova, via Gabelli 63, 35121 Padova, Italy.*

[‡] *Institute of Poultry Science, Shandong Academy of Agricultural Sciences, 1, Jiaoxiao Road, 250023 Jinan, Shandong, P. R. China.*

[|] *Department of Physics, Chemistry, and Pharmacy, University of Southern Denmark, DK-5230 Odense M. Denmark.*

[◊] *Present Address: [◊] Biomedicinskt Centrum (BMC), Department of Chemistry, Uppsala University, Husargatan 3, 75237 Uppsala, Sweden.*

[#] *The Second Hospital of Shandong University, No. 247 Beiyuan Avenue, Jinan250033, China.*

ABSTRACT: Due to the emergence of highly pathogenic and oseltamivir-resistant influenza viruses, there is an urgent need to develop new anti-influenza agents. Herein, five sub-series of oseltamivir derivatives were designed and synthesized to improve their activity towards drug-resistant viral strains by further exploiting the 150-cavity in the neuraminidases (NAs). The bioassay results showed that compound **21h** exhibited antiviral activities similar to or better than those of oseltamivir carboxylate (OSC) against H5N1, H5N2, H5N6 and H5N8. Besides, **21h** was 5- to 86-fold more potent than OSC toward N1, N8, and N1-H274Y mutant NAs in the inhibitory assays. Computational studies provided a plausible rationale for the high potency of **21h** against group-1 and N1-H274Y NAs. In addition, **21h** demonstrated acceptable oral bioavailability, low acute toxicity and potent antiviral activity *in vivo*, and high metabolic stability. Overall, above excellent profiles make **21h** a promising drug candidate for the treatment of influenza virus infection.

INTRODUCTION

Despite the availability of vaccines and antiviral drugs, influenza A virus frequently causes severe respiratory disease.[1] The worldwide spread of swine-origin 2009 pandemic H1N1 (H1N1pdm09) and avian influenza virus (AIV), especially the H5 subtypes of highly pathogenic avian influenza (HPAI), have raised public concern globally due to their high morbidity and mortality rates.[2,3] For example, H5N1 subtype of AIV is a deadly disease in birds, mammals, and humans, with a 63% mortality rate in humans.[4] Although the H5N1 virus has not yet acquired the ability to bind efficiently to the human receptor, it might eventually overcome the species barrier and achieve human-to-human transmission.[5,6]

Influenza virus neuraminidase (NA) is an important surface antigenic glycoprotein, which facilitates viral shedding by cleaving terminal sialic acid residues between another essential surface antigenic glycoproteins hemagglutinin (HA) and host-cell, and is thus an attractive target for the prophylaxis and therapy of influenza.[7,8] Several neuraminidase inhibitors (NAIs), including oseltamivir (**1a**),[9] oseltamivir carboxylate (OSC, **1b**), zanamivir (ZA, **2**),[10] laninamivir octanoate (**3**),[11] and peramivir (**4**)[12] (**Figure 1**), have been approved for clinical use. Among them, oseltamivir (**1a**), the first orally available NAI, was marketed in 2000, and has been stockpiled by many countries as a precaution against a new pandemic, primarily because of its convenient oral availability.[13]

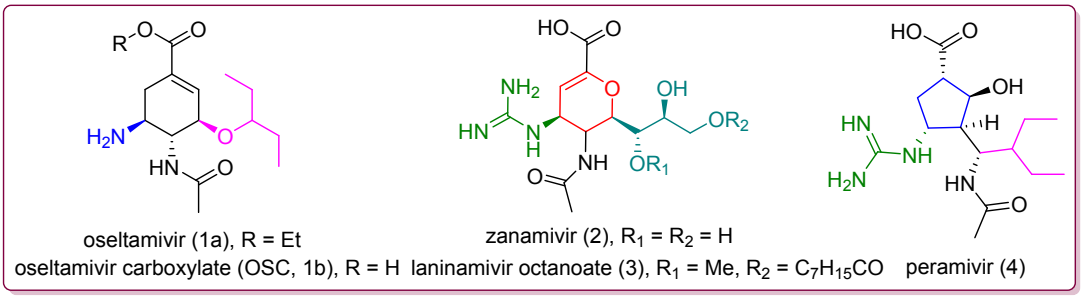

Figure 1. Chemical structures of clinically used neuraminidase inhibitors.

Despite the success of oseltamivir, resistance is a growing concern. Oseltamivir resistance is generally conferred via a single amino acid mutation (H274Y) in strains possessing the N1 subtype of NA (exemplified by H1N1pdm09-H274Y and H5N1-H274Y). Since 2007, viruses containing H274Y have rapidly become predominant among human seasonal H1N1 and avian influenza H5N1 isolates.[14-16] In NA inhibition assays, NAs with H274Y mutant were more resistant to oseltamivir than the wild-type NAs by a factor of more than 100,[17,18] leading to clinical failure of oral oseltamivir.[15,19,20] Therefore, discovery of new drugs active against oseltamivir-resistant strains, especially those with H274Y, is becoming increasingly urgent.

So far, based on phylogenetic relationships and X-ray crystallographic studies of NAs, the nine NAs of influenza A viruses have been well characterized and can be divided into two distinct families: group-1, containing N1, N4, N5 and N8 subtypes, and group-2, containing N2, N3, N6, N7 and N9 subtypes.[21,22] In group-1 NAs, a flexible 150-loop, consisting of residues 147-152, usually adopts an open conformation, whereas in group-2 NAs, this loop is always closed.[21] The open 150-loop can form in an open large cavity (150-cavity) adjacent to the active site in group-1 NAs, but this cavity is not present in group-2 NAs. Surprisingly, although the 2009 H1N1 neuraminidase (09N1) belongs to group-1 NAs, crystal structure studies showed it does not have the 150-cavity

(**Figure 2**).[23] Even so, recent computational studies of the 09N1 subtype suggest that the 150-loop has remarkable mobility and may open to a greater extent in solution than is observed in the crystal.[24,25]

Structure-based design is typically focused on the optimization of a chemical series to increase affinity for a mutable target protein, to probe biologically relevant chemical space, and to improve the potency against resistant mutations, as exemplified by our recent studies.[26,27] In this context, the flexibility of the 150-loop and also the opening of the 150-cavity near the active site of group-1 enzymes can be regarded as important targets for further drug modification studies. We speculated that modifications of oseltamivir that enable higher-affinity binding at the amino acids forming the 150-cavity could yield novel NA inhibitors that are not sensitive to common mutations of NA, including H274Y.

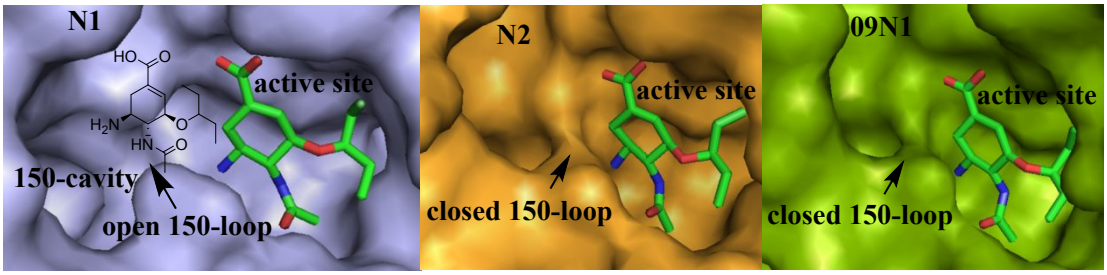

Figure 2. Comparison of the crystal structures of representative group-1 NAs (N1, PDB ID: 2HU0), group-2 NAs (N2, PDB ID: 4GZP), and 09N1 (PDB ID: 3TI6).

Close examination of the crystal structure of oseltamivir carboxylate bound to the N1 subtype indicated that the C-5 amino group of oseltamivir carboxylate could serve as a potential modification site in the design of group-1-specific inhibitors (**Figure 2**). On this basis, many investigators have attempted to chemically modify oseltamivir in order to overcome resistance-conferring mutations of NAs.[28] Our own previous research focused on exploiting the 150-cavity led to the identification of a series of N-substituted

oseltamivir derivatives with low nanomolar N1-selective inhibitory activity against NAs from three H5N1 viruses.[17] It is noteworthy that, compared with OSC, the two most potent compounds **5** and **6** (group-1-specific NA inhibitors in **Figure 3A**) showed about 3-9 times greater inhibitory potency against three H5N1 NA subtypes. However, compound **5** did not show improved activity against the H5N1-H274Y mutant as compared to OSC (**5**, IC_{50} = 1.16 μM; OSC, IC_{50} = 2.1 μM). But, interestingly, **6** showed a 12-fold increase in activity against this mutant relative to OSC (IC_{50} = 0.16 μM), supporting the idea that addition of substituents to the oseltamivir core could result in stronger interactions with the 150-cavity, restoring affinity for the H274Y mutant.[17]

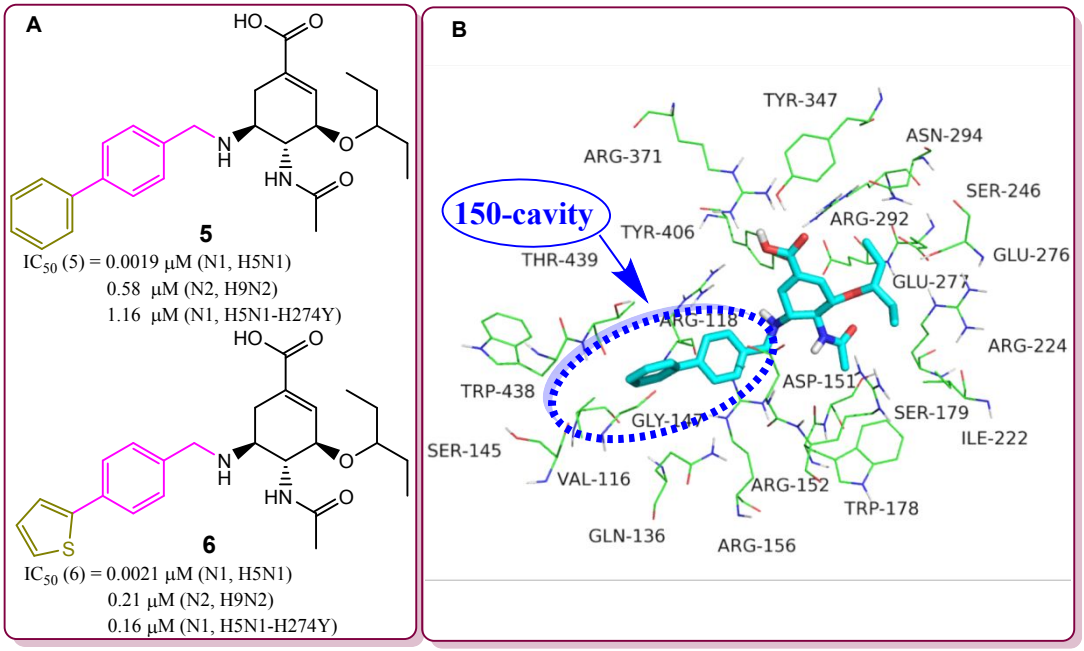

Figure 3. (A) Structures of our previously reported group-1-specific influenza NA inhibitors **5** and **6**; (B) Key residues that may interact with **5**.[17]

Our previous structure-activity relationships (SARs) study and molecular modeling indicated that some of the highest-affinity 150-cavity binders interact primarily through hydrophobic interactions.[17] As shown in **Figure 3B**, biphenyl or (thiophen-2-yl)phenyl

groups in compounds **5** and **6** might develop additional interactions with hydrophobic amino acid residues, such as W438, V116, G147, Q136, and R152 in N1 of H5N1. Thus, the SAR of the C5-NH_2-substituted benzyl group of compounds **5** and **6**, which occupy the 150-cavity of N1, needs to be further explored to improve the potency of these compounds against N1-H274Y mutants, while retaining their outstanding potency against other group-1 NAs.

In this work, therefore, we investigated a series of N-substituted benzenes incorporating various hydrophobic groups directly connected to the aromatic moiety, as well as some benzophenone and phenylsulfonyl derivatives (**Figure 4**). Specifically, we designed five new sub-series (**11**, **17**, **21**, **25** and **28**, and **32**) of C5-NH_2-substituted oseltamivir derivatives, synthesized them, and then biologically tested them in cell-based assays that address the cytopathic effect (CPE) of influenza virus infection, as well an in an enzymatic assay. Furthermore, we conducted preliminary evaluation of druggability, including oral bioavailability, acute toxicity in vivo and metabolic stability, as well as computational modeling studies, of some promising compounds.

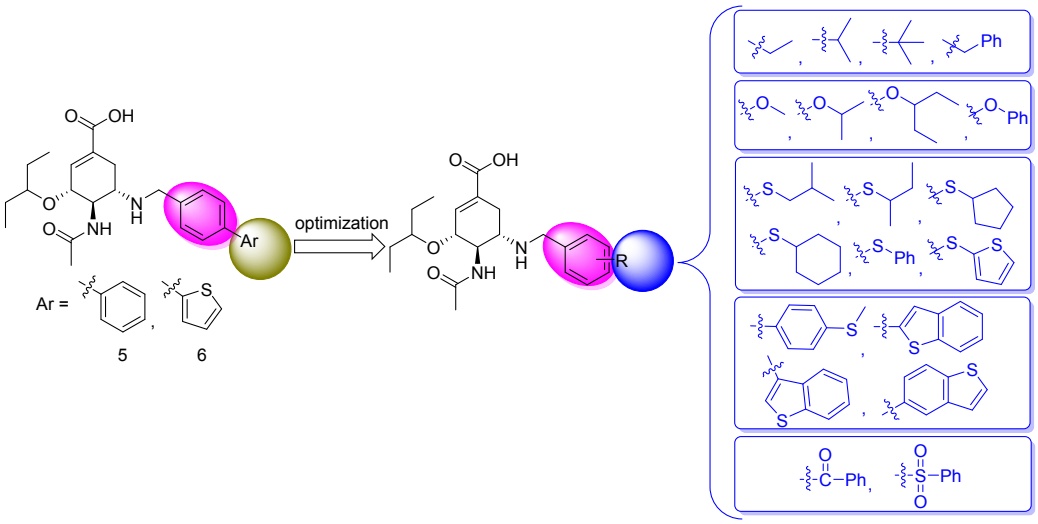

Figure 4. Previously discovered N-substituted oseltamivir derivatives **5** and **6** and design approach to

new derivatives. Pink benzene ring represents the privileged moiety; brown aromatic ring represents the active moiety of the lead compounds in our previous work; blue part represents our present structural optimization.

CHEMISTRY

The new N-substituted oseltamivir derivatives (**11a-d**, **17a-f**, **21a-h**, **25a-d**, **28**, and **32a-b)** were synthesized as illustrated in **Schemes 1-6**.

Scheme 1. Preparation of Compounds 11a-d[a]

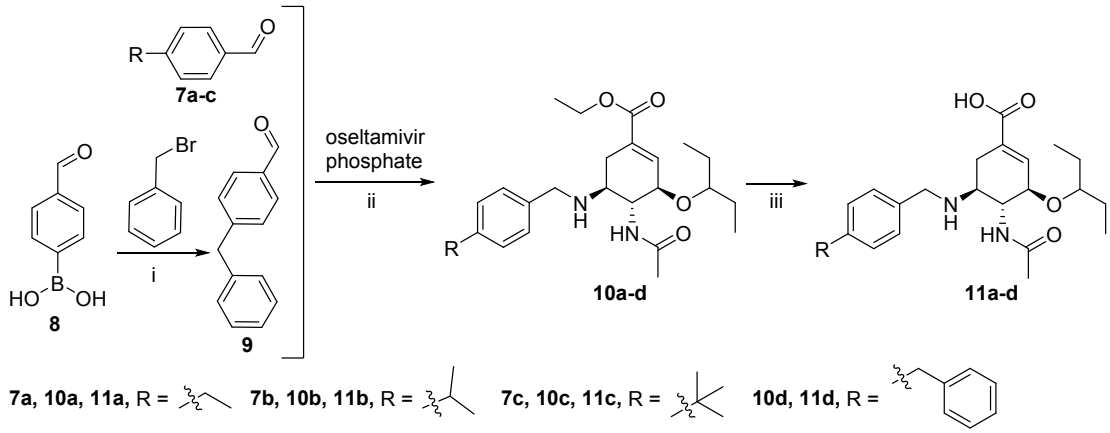

[a] (i) H_2O, THF, K_2CO_3, $Pd(PPh_3)_4$, N_2, 60℃; (ii) $NaBH_3CN$, EtOH, MeOH, r.t.; (iii) NaOH, MeOH, H_2O, r.t., then HCl (2 mol/L).

As shown in **Scheme 1**, 4-benzylbenzaldehyde (**9**) was synthesized from (4-formylphenyl)boronic acid (**8**) via Suzuki reaction.[29] Then, following a previously reported procedure,[17] the commercially available *para*-substituted benzaldehydes **7a-c** and newly prepared **9** were reacted with commercial oseltamivir phosphate in the presence of $NaBH_3CN$ to afford the key intermediates **10a-d**. Finally, target compounds **11a-d** were prepared by direct hydrolysis of the intermediates **10a-d**.

Scheme 2. Preparation of Compounds 17a-f[a]

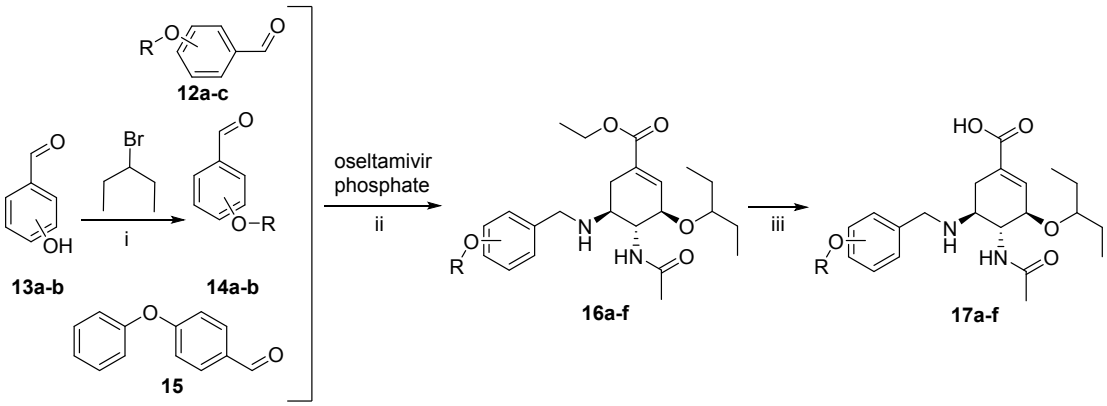

12a, 16a, 17a, (R = 4-methyl); **12b, 16b, 17b,** (R = 3-methyl); **12c, 16c, 17c,** (R = 4-isopropyl);
13a, *para*-position, **13b**, *meta*-position; **14a, 16d, 17d,** (R = 4-(pentan-3-yl));
14b, 16e, 17e, (R = 3-(pentan-3-yl)); **16f, 17f,** (R = 4-phenyl)

[a] (i) K_2CO_3, KI, DMF, 100℃. (ii) $NaBH_3CN$, EtOH, MeOH, r.t.; (iii) NaOH, MeOH, H_2O, r.t., then HCl (2 mol/L).

Scheme 2 illustrates the synthesis of compounds **17a-f**. Commercially available 3- or 4-hydroxybenzaldehydes (**13a,b**) were coupled with 3-bromopentane in DMF in the presence of K_2CO_3 and KI to obtain the aromatic aldehydes **14a-b.** Then, target compounds **17a-f** were prepared from **14a-b** and other commercially available arylaldehydes **12a-c** and **15** using a similar procedure to that described above.

Scheme 3. Preparation of Compounds 21a-h[a]

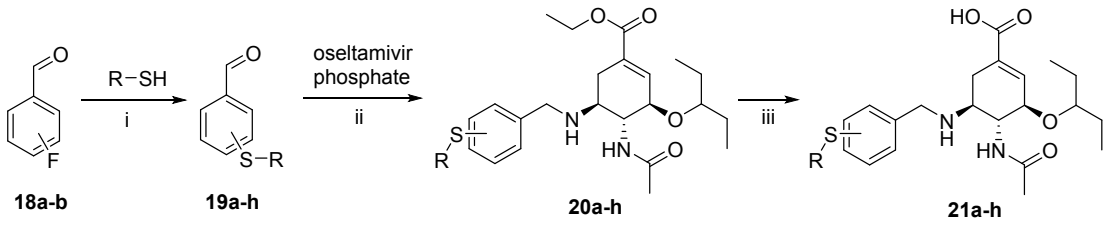

18a, *para*-position; **18b,** *meta*-position; **19a, 20a, 21a,** (R = 4-isobutyl); **19b, 20b, 21b,** (R = 4-*sec*-butyl);
19c, 20c, 21c, (R = 3-*sec*-butyl); **19d, 20d, 21d,** (R = 4-cyclopentyl); **19e, 20e, 21e,** (R = 3-cyclopentyl);
19f, 20f, 21f, (R = 4-cyclohexyl); **19g, 20g, 21g,** (R = 4-thiophen-2-yl); **19h, 20h, 21h,** (R = 4-phenyl)

[a] (i) DMF, K_2CO_3, 100℃. (ii) $NaBH_3CN$, EtOH, MeOH, r.t.; (iii) NaOH, MeOH, H_2O, r.t., then HCl (2 mol/L).

As shown in **Scheme 3**, treatment of fluorinated aromatic aldehydes **18a-b** with alkyl mercaptan, naphthenic mercaptan, thiophenol or thiophene-2-thiol gave

sulfur-containing aromatic aldehydes **19a-h,** which were used for the preparation of compounds **21a-h** in the same manner as described above.

Scheme 4. Preparation of Compounds 25a-d[a]

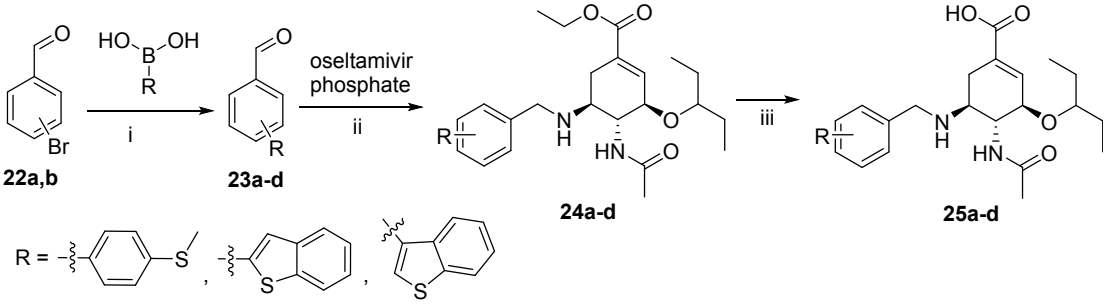

[a] (i) DMSO, K_2CO_3, $Pd(PPh_3)_4$, N_2, 100℃. (ii) $NaBH_3CN$, EtOH, MeOH, r.t.; (iii) NaOH, MeOH, H_2O, r.t., then HCl (2 mol/L).

Scheme 5. Preparation of Compound 28[a]

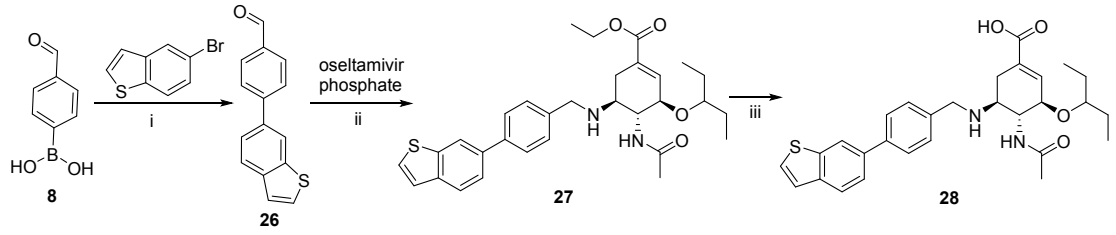

[a] (i) DMSO, K_2CO_3, $Pd(PPh_3)_4$, N_2, 100℃. (ii) $NaBH_3CN$, EtOH, MeOH, rt; (iii) NaOH, MeOH, H_2O, r.t., then HCl (2 mol/L).

As shown in **Scheme 4**, aromatic aldehydes **23a-d** were obtained *via* Suzuki reaction of the 3- or 4-bromobenzaldehyde (**22a** or **22b**) with the corresponding arylboronic acids, (4-(methylthio)phenyl)boronic acid, benzo[b]thiophen-2-ylboronic acid, and benzo[b]thiophen-3-ylboronic acid. As illustrated in **Scheme 5**, 4-(benzo[b]thiophen-6-yl)benzaldehyde (**26**) was synthesized from 4-formylphenyl)boronic acid (**8**) and 5-bromobenzo[b]thiophene. The target compounds **25a-d** and **28** were obtained from the aromatic aldehydes **23a-d** and **26** (**Schemes 4** and **5**) using a similar procedure to that described above.

Scheme 6 illustrates the conversion of methylarenes into bromobenzyls by treatment with N-bromosuccinimide (NBS) in the presence of a catalytic amount of benzoyl peroxide (BPO), followed by hydrocarbylation and saponification reactions to give the target compounds **32a-b**.

Scheme 6. Preparation of Compounds 32a-b[a]

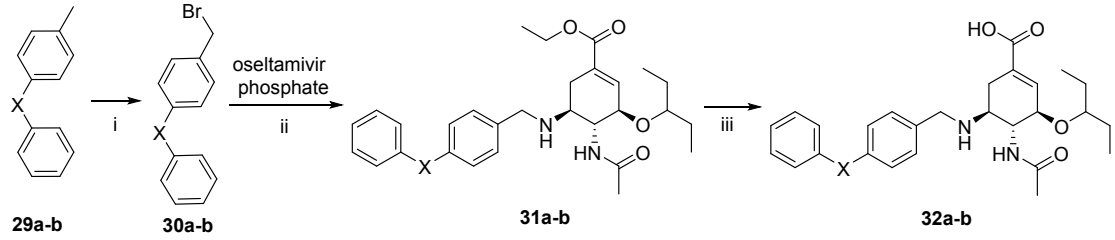

[a] X = CO or SO_2; (i) NBS, BPO, CCl_4, reflux; (ii) CH_3CN, K_2CO_3, reflux; (iii) NaOH, MeOH, H_2O, r.t., then HCl (2 mol/L).

RESULTS AND DISCUSSION

Anti-Influenza-Virus Activity in Cell Culture

In order to investigate the efficacy of the synthesized compounds against influenza virus infection, we employed cell-based assays (chicken embryo fibroblasts, CEFs) that address the CPE of AIV infection using A/goose/Guangdong/SH7/2013 (H5N1) and A/goose/Jiangsu/1306/2014 (H5N8) as representatives of group-1 NAs-containing influenza strains, and A/Chicken/Hebei/LZF/2014 (H5N2) and A/duck/Guangdong/674/2014 (H5N6) as representatives of group-2 NAs-containing influenza strains. OSC, ZA, and ribavirin (Rib) were run in parallel as control drugs. The assays were conducted in triplicate and repeated three times. The values of EC_{50} (anti-avian influenza A virus potency) and CC_{50} (cytotoxicity) of the synthesized compounds are summarized in **Table 1**. Notably, all the tested compounds exhibited

antiviral activity in CEFs. Furthermore, they showed no appreciable cytotoxicity at the highest tested concentration (CC_{50} > 200 μM) in CEFs.

Table 1. Anti-Influenza-Virus Activity and Cytotoxicity of Oseltamivir Derivatives in CEF Cells

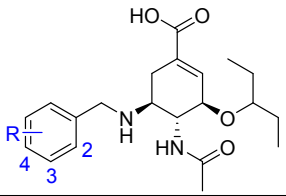

Compound[a]	R	EC_{50}[b] values (μM) against influenza virus				CC_{50}[c]
		H5N1[d]	H5N2[e]	H5N6[f]	H5N8[g]	
		Group-1	Group-2	Group-2	Group-1	
11a	4-Et	2.67±0.56	2.99±0.25	1.97±0.26	3.93±0.51	>200[h]
11b	4-$CH(Me)_2$	1.10±0.39	3.97±0.65	1.24±0.46	2.48±0.92	>200
11c	4-$CH(Me)_3$	5.39±1.48	6.71±0.1	3.39±0.62	6.79±1.24	>200
11d	4-CH_2Ph	5.83±1.79	0.25±0.08	1.13±0.32	0.59±0.09	>200
17a	4-OMe	1.27±0.35	0.78±0.07	5.65±0.85	4.73±1.04	>200
17b	3-OMe	31.88±6.23	1.33±0.06	3.42±0.79	>100	>200
17c	4-$OCH(Me)_2$	19.42±0.97	1.37±0.11	17.98±5.19	16.87±3.61	>200
17d	4-$OCH(Et)_2$	10.61±1.65	1.10±0.15	4.92±1.69	17.9±0.91	>200
17e	3-$OCH(Et)_2$	51.09±0.22	2.68±0.03	17.56±3.71	3.97±0.96	>200
17f	4-OPh	10.71±1.18	0.28±0.07	0.32±0.09	0.20±0.06	>200
21a	4-isobutylthio	18.09±2.53	0.74±0.14	12.96±3.80	2.59±0.94	>200
21b	4-*sec*-butylthio	6.37±2.35	1.15±0.11	1.83±0.85	80.13±15.88	>200
21c	3-*sec*-butylthio	31.08±4.66	1.29±0.23	4.72±1.76	10.78±4.46	>200
21d	4-cyclopentylthio	26.63±8.38	5.28±0.92	14.82±6.07	4.27±1.85	>200
21e	3-cyclopentylthio	24.16±9.12	0.87±0.37	6.50±1.36	5.75±1.78	>200
21f	4-cyclohexylthio	38.0±7.23	0.68±0.21	1.75±0.79	0.32±0.09	>200
21g	4-thiophen-2-ylthio	0.25±0.03	0.14±0.03	1.21±0.40	0.17±0.027	>200
21h	4-phenylthio	0.39±0.08	0.09±0.01	0.52±0.09	0.056±0.03	>200

25a	4-(methylthio)phenyl	4.10±0.87	0.51±0.13	2.57±1.09	0.64±0.21	>200
25b	3-(methylthio)phenyl	35.74±7.32	0.81±0.13	23.87±8.35	1.31±0.32	>200
25c	4-benzo[b]thiophen-2-yl	21.34±3.60	0.61±0.08	8.04±2.81	2.14±0.24	>200
25d	4-benzo[b]thiophen-3-yl	8.97±2.68	0.64±0.17	3.81±1.06	0.22±0.08	>200
28	4-benzo[b]thiophen-5-yl	16.40±6.48	0.68±0.21	2.47±0.69	0.31±0.09	>200
32a	4-PhCO	7.59±1.21	0.33±0.11	1.16±0.14	1.13±0.45	>200
32b	4-$PhSO_2$	>100	1.46±0.14	1.73±0.87	70.28±8.8	>200
OSC	---	0.53±0.06	0.10±0.01	0.44±0.22	1.99±0.36	>200
ZA	---	0.51±0.01	0.26±0.02	0.31±0.14	5.76±0.48	>200
Rib	---	11.27±2.56	15.81±1.71	5.06±1.11	11.33±0.58	>200

[a] Compounds **11a-32b** were checked against pan-assay interference compounds (PAINS), and none was flagged.[30,31]

[b] EC_{50}: concentration of a compound required to achieve 50% protection of CEF cultures against influenza virus-induced cytotoxicity, presented as the mean ± standard deviation (SD) and determined by the CCK-8 method.

[c] CC_{50}: concentration required to reduce the viability of mock-infected cell cultures by 50%, as determined by the CCK-8 method.

[d] A/goose/Guangdong/SH7/2013. [e]A/Chicken/Hebei/LZF/2014. [f]A/duck/Guangdong/674/2014. [g]A/goose/Jiangsu/1306/2014.

[h] Highest tested concentration.

First, we focused our attention on novel C5-NH_2-substituted oseltamivir derivatives (**11a-c**) in which the phenyl or thienyl group of the 4-benzyl moiety of **5** or **6** was replaced with relatively small alkyl groups containing 2 to 4 carbon atoms to explore the effect of steric bulk at this position. We also added a methylene bridge between the two benzenes of the lead compound **5** to give **11d**, aiming to introduce better flexibility to adapt to the cavity in NAs.

Among the synthesized compounds, **11b** (R = 4-$CH(Me)_2$) exhibited the highest potency against H5N1 (EC_{50} = 1.10 μM); it was less potent than OSC (EC_{50} = 0.53 μM) or ZA (EC_{50} = 0.51 μM), but its activity was about 10 times higher than that of Rib (EC_{50} = 11.27 μM). Replacing the isopropyl (**11b**) group with ethyl (**11a**), *tert*-butyl (**11c**) or benzyl (**11d**) slightly reduced the antiviral activity (**11a**, EC_{50} = 2.67 μM; **11c**, EC_{50} = 5.39 μM; **11d**, EC_{50} = 5.83 μM), but these compounds were still more potent than Rib. The order of potency against H5N1 of compounds with various substituents at the R-position in the benzene ring was: 4-$CH(Me)_2$ > 4-Et > 4-$CH(Me)_3$ > 4-CH_2Ph.

Interestingly, in contrast to H5N1, **11d** with the benzyl substituent turned out to be the most potent inhibitor in this sub-series against H5N2, H5N6 and H5N8 strains, with good EC_{50} values of 0.25, 1.13 and 0.59 μM, respectively. Although its activities against H5N2 and H5N6 were similar to those of OSC (H5N2, EC_{50} = 0.10 μM; H5N6, EC_{50} = 0.44 μM) and ZA (H5N2, EC_{50} = 0.26 μM; H5N6, EC_{50} = 0.31 μM), it showed higher potency against H5N8 as compared to OSC (EC_{50} = 1.99 μM) or ZA (EC_{50} = 5.76 μM). In contrast, **11a-c** exhibited weaker potency against the H5N2 and H5N6 strains compared to OSC and ZA. As for H5N8, **11a-c** showed weaker potency than OSC, but comparable efficacy to ZA. Thus, it appears that a moderately flexible aromatic group **(**4-CH_2Ph in **11d)** at the R position increases the potency toward H5N2, H5N6 and H5N8 strains.

To extend the SAR information, we inserted an oxygen atom between the alkyl group (or benzene) and benzyl group (compounds **17a-f**). However, **17b-f** displayed reduced anti-H5N1 activity (EC_{50} = 10.61-51.09 μM) compared to the above sub-series. Moreover, the *meta*-substituted compounds (**17b**, R = 3-OMe, EC_{50} =31.88 μM; **17e**, R =

3-OCH(Et)$_2$, EC_{50} = 51.09 μM) showed considerably decreased potency against H5N1 compared with their *para*-substituted counterparts (**17a**, R = 4-OMe, EC_{50} =1.27 μM; **17d**, R = 4-OCH(Et)$_2$, EC_{50} =10.61 μM).

Notably, **17f** (R = 4-OPh), bearing an aromatic phenoxy group, was the most potent compound among **17a-f** against H5N2, H5N6, and H5N8 strains (H5N2, EC_{50} = 0.28 μM; H5N6, EC_{50} =0.32 μM; H5N8, EC_{50} =0.20 μM). Moreover, **17f** displayed comparable activity to OSC and ZA against H5N2 and H5N6, and showed greater potency than OSC and ZA against H5N8. Compared to **11d**, the replacement of carbon by oxygen led to a marked increase of potency of **17f** against H5N6 and H5N8.

Inspired by those results, we next employed a bioisosterism strategy to design alkylsulfide and arylsulfide derivatives, with the aim of improving the antiviral potency, including against the N1-H274Y mutant. Specifically, we replaced the oxygen of **17f** with a sulfur atom, which has a larger radius and different bond angles, to afford compound **21h** as a derivative of lead **5**. Similarly, a sulfur atom was inserted between the two aryls of compound **6** to give **21g**. More diverse alkyl groups were also used in order to extend the SAR study.

However, compounds **21a-f** with alkyl sulfide or cycloalkyl sulfide groups were less potent than OSC and ZA against H5N1, with EC_{50} values from 6.37 to 38.0 μM. Among them, only **21b** (EC_{50} = 6.37 μM) with a 4-*sec*-butylthio group was more potent than Rib. But encouragingly, compounds **21g** and **21h** exhibited considerably enhanced anti-H5N1 activities (**21g**, EC_{50} = 0.25 μM; **21h**, EC_{50} = 0.39 μM), which were even higher than OSC and ZA. On the other hand, compounds **21d** and **21f** almost completely lost activity, although they have a hydrophobic 4-cycloalkyl moiety similar in size to the substituents

of **21g** and **21h**. This result confirms that the aromatic moieties play a critical role in the interaction with the binding pocket. It is also noteworthy that **21h** is about 13 or 27 times more potent than the C- and O- counterparts **11d** and **17f**, respectively. The order of potency seems to be in accordance with that of bond length: S-C (~180 pm) > C-C (~150 pm) > O-C (~140 pm). Thus, the larger size of 4-(phenylthio)benzyl, which may better occupy the 150-cavity in group-1 NAs, is essential for strong antiviral potency against H5N1.

As for inhibitory activity against H5N2 and H5N6, **21a-f** also showed lower activity than OSC and ZA, with EC_{50} values ranging from 0.68 to 5.28 μM and 1.75 to 14.82 μM, respectively. Importantly, **21g** and **21h** exhibited excellent potency against H5N2, with EC_{50} values of 0.14 and 0.09 μM, respectively, which are similar to those of OSC and ZA and more than 100 times higher than that of Rib. In addition, **21h** (EC_{50} = 0.52 μM) displayed comparable activity to OSC and ZA against H5N6, though **21g** was slightly less potent (EC_{50} = 1.21 μM) than OSC and ZA against H5N6.

Against H5N8, which is relatively insensitive to all three of the control drugs, **21a-e** showed only moderate to low activity (EC_{50} = 2.59-80.13 μM), while compound **21f** (EC_{50} = 0.32 μM) with the 4-cyclohexyl group was about five times more potent than OSC. Further, **21g** and **21h** displayed superior activity against H5N8, with EC_{50} values of 0.17 to 0.056 μM, being far more potent than OSC or ZA.

Inspired by the importance of the sulfur atom in this series, we designed five more sulfur-containing compounds based on the structures of **5** and **6**.

Introduction of a 4-methylthiophenyl group into R-position yielded **25a** (R = 4-(4-methylthiophenyl)) and **25b** (R = 3-(4-methylthiophenyl)), respectively. In addition,

we replaced the 4-phenyl group of compound **5** with three different fused 4-benzo[b]thiophenyls. Generally, the resulting five compounds (**25a-d** and **28**) were much less potent than OSC against H5N1, H5N2 and H5N6 strains. However, against H5N8, most of them (**25a**, EC_{50} = 0.64 μM; **25b**, EC_{50} = 1.31 μM; **25d**, EC_{50} = 0.22 μM; and **28**, EC_{50} = 0.31 μM) were more potent than all of the control drugs.

To further explore the SAR of the linker between the two aromatic rings, we also examined the use of carbonyl and sulfonyl (**32a-b**) to replace the sulfur atom in **21h**. However, both compounds, especially **32b**, showed greatly reduced antiviral activity toward all four strains.

In general, compounds bearing the aromatic phenyl group displayed greater activities towards H5N2, H5N6, and H5N8, as compared with the alkyl derivatives. However, the anti-H5N1 activities of the compounds were more structure-sensitive. Among all the compounds, **21h** showed excellent activity against the whole viral panel (H5N1, H5N2, H5N6, and H5N8). Its potency is comparable to or slightly better than that of the best control drug, OSC, against H5N1, H5N2 and H5N6. Even more remarkably, **21h** potently inhibited H5N8, being 35 and 103 times more active than OSC and ZA, respectively. Thus, we obtained a very promising candidate for further evaluation.

Then, we tested compounds **17a**, **17d**, **21f**, **21g**, **21h** and **25c** against influenza virus A/PR/8/34 (H1N1), A/Wisconsin/67/05 (H3N2), and B/Lee/40 strains by plaque reduction assays (PRA) in MDCK cells. OSC and ZA were used as positive controls for inhibition. We also tested the cytotoxicity of the compounds, as well as OSC and ZA as a reference, in MDCK cells by MTT assays. No cytotoxic effect was observed at the tested concentrations for any of the compounds. The values of EC_{50} (anti-influenza potency) of

the selected oseltamivir derivatives and the positive control drugs are summarized in **Table 2.**

In the anti-influenza activities evaluation against H1N1 and H3N2 strains, **17a**, **17d**, **21f**, **21g**, **21h** and **25c** turned out to be potent inhibitors against H1N1 with EC_{50} values from 0.041 to 17.07 μM. Among them, **21g** and **21h** (**21g**, EC_{50} = 0.04 μM; **21h**, EC_{50} = 0.06 μM) were the two most potent than other tested compounds, nearly equal to that of OSC and ZA. But all the tested compounds exhibited weaker potency against the H3N2 and FluB strains compared to OSC and ZA, which can be easily explained by the structural features of N2 and FluB NA. The closed 150-loop and the lack of 150-cavity in NA of H3N2 and FluB (**Figure 2**) indicate that the cavity would not well accommodate the selected oseltamivir derivatives bearing large groups at C-5-NH2 position. These results agreed with the data of the enzymatic assay against N1 and N2.

Table 2. Anti-Influenza-Virus Activity and Cytotoxicity of Oseltamivir Derivatives in MDCK Cells

Compound	R	EC_{50}[a] values (μM) against influenza virus			CC_{50}[b]
		H1N1[c]	H3N2[d]	FluB[e]	
		Group-1	Group-2		
17a	4-OMe	3.7 ± 0.8	>100	>100	>250[f]
17d	4-OCH(Et)$_2$	13.0 ± 0.5	>100	>100	>250
21f	4-cyclohexylthio	17.0 ± 3.0	>100	>100	>250

21g	4-thiophen-2-ylthio	0.04 ± 0.02	79 ± 5	8.5 ± 1.1	>250
21h	4-phenylthio	0.06 ± 0.02	71 ± 3	19.0 ± 2.0	>250
25c	4-benzo[b]thiophen-2-yl	7.2 ± 2.9	>100	>100	>250
OSC	---	0.041 ± 0.003	1.2 ± 0.1	2.9 ± 0.3	>250
ZA	---	0.038 ± 0.005	0.3 ± 0.1	0.9 ± 0.2	>250

[a] EC_{50}: concentration of compound required to achieve 50% protection of MDCK cell cultures against influenza virus-plaque formation, presented as the mean ± standard deviation (SD) and determined by the PRA method.

[b] CC_{50}: concentration required to reduce the viability of mock-infected cell cultures by 50%, as determined by the MTT method.

[c] A/PR/8/34. [d] A/Wisconsin/67/05. [e] B/Lee/40. [f] Highest tested concentration.

Inhibition of Influenza Neuraminidases

Eleven representative compounds were selected for enzymatic assay against influenza neuraminidases (H5N1, H5N2, H5N6, H5N8 and H5N1-H274Y) to validate their binding target. OSC and ZA were also run in parallel as control drugs. The results are shown in **Table 3**. OSC showed very good inhibitory activity against the four wild-type NAs, with IC_{50} values of 26.63, 4.85, 15.25 and 8.94 nM, respectively. ZA also displayed excellent potency against all the wild-type NAs; it still showed an IC_{50} of 22.8 nM even against the least sensitive NA, *i.e.*, H5N6. Of course, OSC and ZA did not equally inhibit these NA subtypes, but showed some selectivity, in accordance with the reported data [17,32-36] and these findings served to verify the reliability of our assay.

N1 (H5N1) and N8 (H5N8) belong to the group-1 NAs, and most of the inhibitors

showed relatively similar potency against both subtypes. In particular, **11a**, **11d**, **17a**, **17f**, **21g** and **21h** proved to be very potent inhibitors of N1 and N8 with most of the IC_{50}s at or below the two-digital nanomolar range. Notably, the best compound **21h** showed excellent inhibitory activity with IC_{50} values of 0.96 and 1.89 nM against N1 and N8, respectively, being 27 and 4 times more potent than OSC, and 7 and 3 times more potent than ZA, respectively.

We also performed enzymatic assay against N2 (H5N2) and N6 (H5N6). As expected, all of the compounds tested were significantly less active against the N2 and N6 subtypes compared to the N1 subtype, because of the closed 150-loop and absent 150-cavity in N2 and N6. The poor inhibitory activities suggested that N2 and N6 do not well accommodate compounds bearing a large group at the C5-NH_2 position. In other words, the conformations of these oseltamivir derivatives might be distorted in N2 and N6, resulting in unfavorable interactions with the binding pockets of these subtypes. These results further support our hypothesis and design strategy.

In agreement with previous reports,[17,28] OSC showed >100-fold weaker inhibitory activity against N1-H274Y (A/Anhui/1/2005 (H5N1-H274Y), IC_{50} = 2824 nM) compared to that against wild-type N1 (A/goose/Guangdong/SH7/2013 (H5N1), IC_{50} = 26.63 nM), whereas ZA was equally effective against N1-H274Y and wild-type N1 (A/Anhui/1/2005 (H5N1-H274Y), IC_{50} = 7.77 nM; A/goose/Guangdong/SH7/2013 (H5N1), IC_{50} = 7.67 nM).

Apart from **21g** and **21h**, all the tested compounds showed weak inhibitory activity against N1-H274Y mutation, with IC_{50} values of more than 363 nM. But, notably, compounds **21g** and **21h** showed outstanding inhibition of N1-H274Y (IC_{50} = 36.34 and

32.81 nM, respectively), being better than OSC and comparable to ZA in potency. Thus, we have successfully overcome a major disadvantage of OSC and the lead compounds **5** and **6**, i.e., their weak inhibitory activity against the most important clinical mutant.

Table 3. Neuraminidase (NA) Inhibition of Oseltamivir Derivatives in Chemiluminescence-based Assay

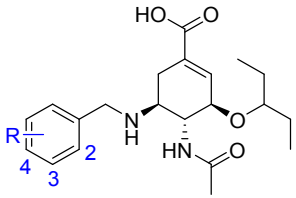

Compd	R	NA-Inhibitory Activity, IC_{50} (nM)[a]				
		H5N1[b]	H5N2[c]	H5N6[d]	H5N8[e]	H5N1-H274Y[f]
		Group-1	Group-2	Group-2	Group-1	Group-1
11a	4-Et	63.89±8.75	965.83±42.03	7250.67±563.99	41.78±8.37	727.23±86.95
11d	4-CH_2Ph	63.87±1.24	1046.03±78.97	6890.33±554.39	56.36±3.39	915.67±104.16
17a	4-OMe	20.45±1.61	1649±123.41	18105.33±1261.62	131.63±20.47	3147.33±193.75
17b	3-OMe	266.33±27.10	1112.87±184.79	10850±245.76	195.07±8.13	30026.67±3423.76
17d	4-OCH(Et)$_2$	1050.37±134.75	1243±120.58	3228±583.94	1143±124.21	>100000
17f	4-OPh	37.31±0.43	1595.67±104.04	4250.33±113.47	41.96±5.36	363.87±12.15
21f	4-cyclohexylthio	2023.67±232.73	398.5±66.39	2099.33±131.25	951.63±79.47	>100000

21g	4-thiophen-2-ylthio	3.83±0.38	1154.5±65.76	5681±494.14	3.47±0.34	36.34±5.62
21h	4-phenylthio	0.96±0.15	896.9±74.104	3065±217.73	1.89±0.23	32.81±2.11
25a	4-(methylthio)phenyl	1795.33±318.63	275±24.16	3045±59.174	592.6±61.31	82186.67±10941.01
25c	4-benzo[b]thiophen-2-yl	1179.33±188.99	541.27±51.06	4814.67±975.02	466.2±70.29	27003.33±1909.62
OSC	---	26.63±5.12	4.85±0.46	15.25±1.73	8.94±0.11	2824.67±56.05
ZA	---	7.77±0.5	10.04±0.74	22.80±1.08	7.43±0.62	7.67±1.0

[a] Concentration required to reduce NA activity to 50% of control NA activity (IC_{50}). Values are the mean of three experiments, presented as the mean ± standard deviation (SD). [b] A/goose/Guangdong/SH7/2013. [c] A/Chicken/Hebei/LZF/2014. [d] A/duck/Guangdong/674/2014. [e] A/goose/Jiangsu/1306/2014. [f] A/Anhui/1/2005.

We also tested compounds **21g** and **21h** in an enzymatic assay against NA of H1N1pdm09 (09N1), as shown in **Table 4**. OSC and ZA were quite effective against 09N1, with IC_{50} values of 5.20 and 5.28 nM, respectively, in accordance with reported data.[28,36] Surprisingly, **21g** and **21h** displayed robust activity against 09N1, with IC_{50} values of 7.05 and 5.57 nM, respectively, which were similar to those of the control drugs. The excellent inhibition to 09N1 by **21g** and **21h** can be easily explained on the basis of previous reports[24] showing that 09N1 exists preferentially with an open 150-cavity in solution, though it crystallizes without the 150-cavity that is characteristic of group-1 NAs.

Table 4. 09N1 (H1N1pdm09)-Inhibitory Activities of Compounds 21g and 21h[a]

Compounds	21g	21h	OSC	ZA
IC_{50} (nM): 09N1 (H1N1pdm09)[b]	7.05±0.51	5.57±0.22	5.20±0.26	5.28±0.79

[a] Values are the mean of three independent experiments. [b] A/California/04/2009.

In conclusion, like the lead compounds **5** and **6**, the representative derivatives synthesized in this work displayed high selectivity for N1 and N8 over N2 and N6. Notably, **21g** and **21h** were superior to OSC and ZA against N1 and N8. Furthermore, against the NA of H5N1-H274Y, they displayed comparable activity to ZA, exhibiting higher potency than leads **5** and **6**,[17] and were 77 and 86 times more potent than OSC. It is interesting that they also exhibited significant inhibitory activity toward 09N1.

It is noteworthy that, relative to the NAs (N2, N6, and N8)-inhibitory activities, some compounds showed unexpectedly improved anti-influenza activities in cell-based assay against H5N2, H5N6, and H5N8. In other words, although the enzyme-inhibitory (N2, N6, and N8) activities of some compounds were worse or slightly better than that of

OSC and ZA, the anti-influenza activities of them were comparable or far greater than that of OSC and ZA. Specifically, **11d**, **17f**, and **21g-h** showed remarkably elevated anti-influenza activities in comparison with their anti-NAs activities against H5N2 and H5N6 viruses (e.g. **21h** and OSC towards N2-NA/H5N2, mean IC_{50} values of 896.9 nM (**21h**) and 4.85 nM (OSC) in enzymatic assay versus EC_{50} values of 90 nM (**21h**) and 100 nM (OSC) in cell-based assay), A similar situation was found in the other two sets (for **17f**, and **21h** towards N6-NA/H5N6 strain; for **11d**, **17f**, **21f-h**, **25d** and **28** towards N8-NA/H5N8 strain).

These findings suggest that, in the cellular environment, some mechanism or effects (such as inhibition of other targets, protein-protein interactions, or asymmetric intracellular localization of compounds[33,37]) other than NA inhibition may be involved in the anti-influenza virus (H5N2, H5N6, and H5N8) action. There may also be other uncertainties, for example, host range restriction of influenza virus replication in CEFs.[38-41]

***In Vivo* Anti-influenza Virus Activity in Specific Pathogen Free (SPF) Chicken Embryonated Egg**

In further antiviral research, we tested anti-influenza virus activity of compound **21h** with an chicken embryonated eggs (10-11 days) model which was regarded to have no conflict with ethical and legal aspects of animal protection.[42] We infected the chicken embryonated eggs with H5N2 virus strain and treated them with injecting different concentrations of **21h**. Also, OSC was selected as control drug in parallel. At 48 h and 72 h post infection and treatment, we recorded the number of the survival and death to evaluate the anti-influenza virus activity of the compounds. As shown in **Table 5**

(Experiment and figure data were shown in Supporting Information), all embryos were survived within only infected normal saline (survived/dead = 5/0), and in other groups all were dead after infection without any treatment within 48 h (H5N2: survived/dead = 0/5), suggesting the test procedure was standard. After 48 h, all embryos were survived in curing with **21h** in concentration of 10 mM, while 3 embryos were survived in curing with OSC in the same concentration. By decreasing the concentration **of 21h** and OSC, the number of death was raised in both experiments, but the results clearly showed that the ability of **21h** to protect chicken embryos was stronger than that of OSC at the same concentration.

Table 5. Survival number of chicken embryos after inoculation of specific pathogen free (SPF) embryonated eggs with H5N2 and administration of 21h or OSC

Compounds	Therapeutic Concentration (mM) [a]	Chick Embryos Survived/Dead Number (survival rate)	
		48 h	72 h
21h	10	5/0 (100%)	3/2 (60%)
	2.5	4/1 (80%)	1/4 (20%)
	0.625	3/2 (60%)	0/5 (0%)
	0.156	1/4 (0%)	0/5 (0%)
	0.039	0/5 (0%)	0/5 (0%)
OSC	10	3/2 (60%)	0/5 (0%)
	2.5	1/4 (20%)	0/5 (0%)
	0.625	0/5 (0%)	0/5 (0%)
	0.156	1/4 (0%)	0/5 (0%)
	0.039	0/5 (0%)	0/5 (0%)
Normal aline control	---	5/0 (100%)	5/0 (100%)

virus (H5N2) control	---	0/5 (0%)	0/5 (0%)

[a] The virus solution was mixed with an equal volume of tested compounds and then incubated for 1h before inoculation.

Molecular Modeling

To further investigate the binding mode of the most promising compound **21h** with respect to that of the reference compound OSC in the 150-cavity of various NA structures, we built an open 150-loop conformation of the N8, 09N1, and N1-H247Y structures for molecular docking and MD-based free energy calculations.

Molecular dynamics analysis shows that all the protein-ligand complexes are stable at finite temperature and 1 atm pressure. The RMSD plots (see Supporting Information, Figure S1) for **21h** and OSC indicate that these ligands are localized in the binding site during the entire course of molecular dynamics (MD) simulation. The RMSF was also computed for each complex (see Supporting Information, Figure S2) and the general behavior seen for all neuraminidases is that RMSF was significantly reduced for **21h** as compared with OSC. Such overall low flexibility of **21h** is due to the fact that **21h** can bind effectively to both the 150-cavity and active site as compared to OSC, which binds only at the active site.

To further understand the key interactions between ligand and protein, we conducted MM-GBSA (Molecular Mechanics-Generalized Born combined with solvent accessible Surface Area) binding affinity calculations. A summary of the MM-GBSA output is provided in the Supporting Information ST1. As can be seen in the cases of subtypes N1, 09N1 and N8, compound **21h** showed lower binding free energy (-23.81 to -38.37 kcal/mol) than OSC (-16.05 to -26.48 kcal/mol).

When we examine the various contributing energy terms, it is evident that the increase in van der Waals (vdW) interaction between **21h** and NAs predominates over electrostatic interaction. As can be seen in **Figure 5**, compound **21h** shows key interactions in both the active site and the 150-cavity, as we expected (a schematic representation of the protein-ligand interaction of **21h** is provided in Supporting information, Figure S3). These key interactions include the formation of a salt-bridge between the carboxylate group of **21h** and Arg residue, as observed in the X-ray crystal structures of NAs bound to OSC. In addition, **21h** forms a strong hydrogen-bonding network between the amino-linker and anionic residues (Asp70 in N1 and N1-H247Y, Asp71 in 09N1, Glu38 in N8), which is not observed in OSC. Furthermore, the 4-(phenylthio)benzyl group of **21h** is well adapted to the 150-cavity of N1, N8, 09N1 and N1-H247Y, in which the 150-cavity is surrounded mostly by polar and non-polar residues. Overall, the increased binding affinity of **21h** is primarily due to the better shape complementarity with the 150-cavity, as reflected by the van der Waals interaction energies from MM-GBSA calculation. However, electrostatic interactions do play a role in binding of the common OSC fragment in the active site of NAs.

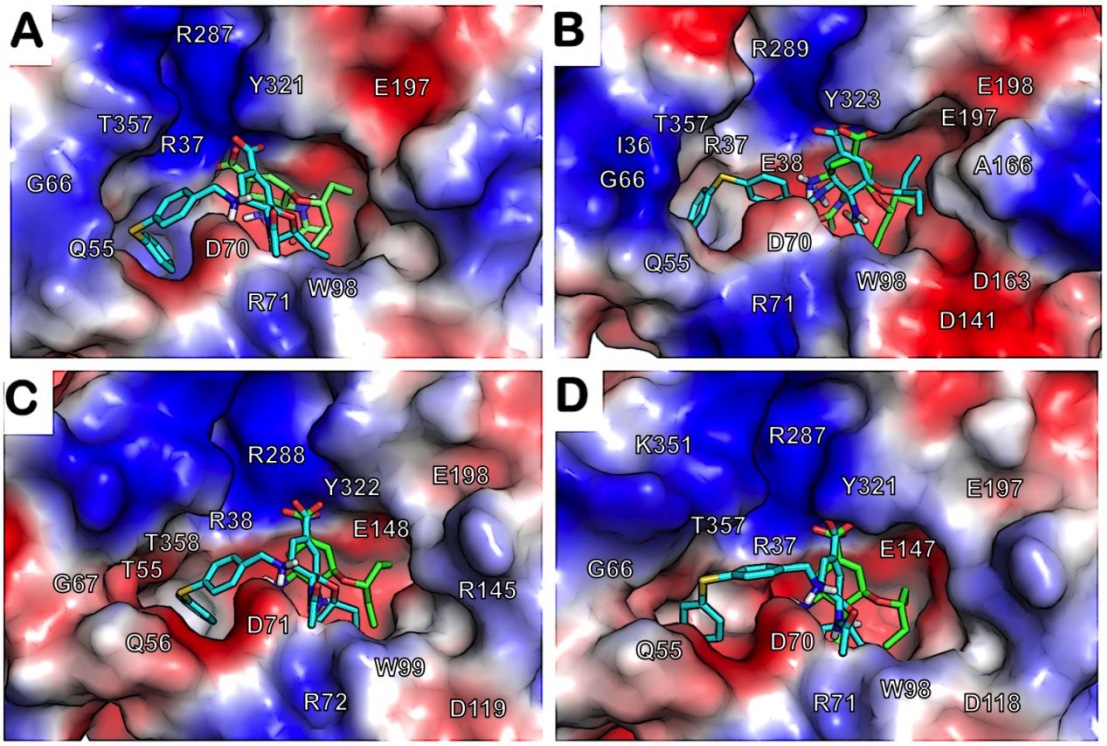

Figure 5. Comparison of binding modes of OSC (green) and compound **21h** (cyan) in the binding sites including the 150-cavity of various NAs (A: N1, B: N8, C:09N1, D: H5N1-H274Y). Electrostatic potential surface area with important residues is highlighted.

We also explored the importance of oxygen and sulphur linker in determining the binding affinity of **21h** and **17f** ligands towards neuraminidases. For this purpose, we carried out molecular docking studies of **21h** (having sulphur linker) and **17f** (with oxygen in the place of sulphur) towards different subtypes of neuraminidase, namely N1, N8, 09N1, N1-H274Y same as described in the method section. Prior to docking the molecular geometries of these two ligands were optimized at B3LYP/6-31+G* level of theory using the Gaussian09 software.

Although the binding pose of these compounds is quite similar (**Figure 6**), as one can see from the **Table 6** that compound **21h** showed stronger binding affinity as compared to compound **17f** and this mainly due to favorable non-polar interaction with all NA

subtypes in **21h**.

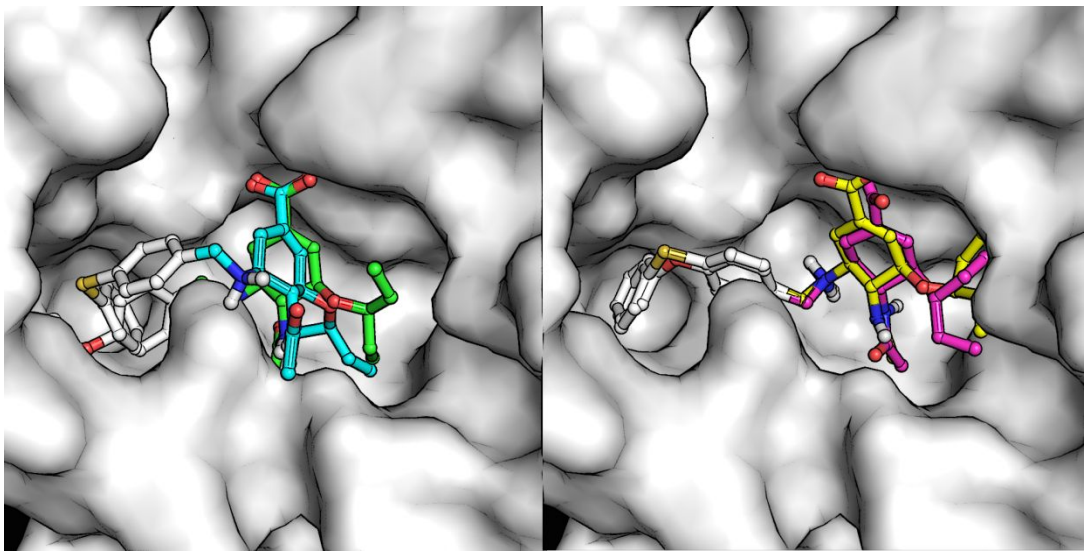

Figure 6. Binding mode of **17f** (green and pink) and **21h** (cyan and yellow) is shown in N1 (Left panel) and N8 (right) panel.

Table 6 The docking-based binding energies (in kcal/mol) of compounds 17f and 21h. Various energy contributions to binding energies are shown.

System	N1		N8		09N1		H274Y	
	21h	**17f**	**21h**	**17f**	**21h**	**17f**	**21h**	**17f**
ΔG	-10.75	-9.60	-11.90	-10.51	-11.65	-10.85	-10.12	-9.84
Ki	13.16	91.38	1.89	19.71	2.87	11.12	37.9	60.97
E_vdW	-9.86	-8.14	-10.44	-9.84	-9.86	-9.15	-9.15	-10.66
E_ele	-1.81	-2.56	-2.92	-3.12	-2.92	-2.86	-2.68	-0.57
E_Int	-2.36	-2.19	-1.83	-0.82	-2.16	-2.12	-1.58	-1.89

Moreover, sulfur atom not only is bigger enough to produce appropriate shape complementarity binding pose in the 150-cavity but also shows favorable vdW interactions. Its lower electronegativity and non-polar nature as compared to oxygen

are the factors possibly influence its overall interaction with relatively non-polar residues in the 150-cavity and contributes to larger binding affinity towards the neuraminidases (refer to ΔG and Ki given in Table) . Even though, overall the binding affinity of the two ligands in the nM range, the overall entropic contributions are also not favorable towards ligand association process towards neuraminidases (~3.28 kcal/mol) which has to be attributed to the presence of many flexible groups. Further, we compared the amino acid sequences of two NAs (A/goose/Guangdong/SH7/2013 (H5N1), and A/goose/Jiangsu/1306/2014 (H5N8)) with those of proteins of the same NA subtype (2HU0, 3NSS, and 2HT7) as used for the MD simulation studies. We found that NAs of the same subtypes showed a high degree of similarity (> 95% for N1 of H5N1 and 2HU0; > 93% for N8 of H5N8 and 2HT7; 3NSS and 3TI6 both originated from 09N1,[23,43] and data shown in the Supporting Information S5). No more than 50 of the nearly 400 residues are different in NAs of the same subtype, and this supports the credibility of the MD simulation studies. The MD simulation protocol is described in the MD simulation studies section.The results are fundamental for our understanding of ligand binding to NAs and should also serve to guide future inhibitor design.

Stability in Human Plasma

Early druggability studies during drug discovery are recognized as critical for reducing the attrition rate in late-stage drug development. Therefore, we initially examined the stability of compound **21h** in human plasma. Propantheline bromide was tested for comparison. We found that 91.58% of **21h** remained intact after incubation for 120 min at 37℃ (**Table 7**), and the half-life was longer than 289.1 min. As can be seen from **Table 6**, **21h** was considerably more stable than propantheline bromide (0.00%

intact after 120 min).

Metabolic Stability in Human Microsomes.

Because the liver is the major organ of drug metabolism, we examined the metabolic stability of **21h** in pooled human liver microsomes (HLM) (**Table 8**). Propranolol, diclofenac, and testosterone were used as control compounds with moderate metabolic stability. After 60 min, 100.6% of **21h** remained intact, and no significant levels of metabolites were detected by LC/MS/MS analysis. The intrinsic clearance (CL) of **21h** was very low (< 9.6 μL/min/mg), and the in vitro half-life was longer than 145 min. In contrast, the control compounds (propranolol, diclofenac, and testosterone) were readily metabolized (remaining amounts of 4.3-12.0% at 60 min and $t_{1/2}$ = 13.1-19.8 min).

Table 7. Results of Plasma Stability Assay (average value, n = 3)

Compounds	Batch	Time Point (min)	Remaining (%)[a]	$T_{1/2}$ (min)
			Human	
21h	/	0	100.00±0.00	>289.1
		10	101.91±1.47	
		30	100.10±9.75	
		60	99.96±10.76	
		120	91.58±8.43	
Propantheline bromide	110M1921V	0	100.0±0.00	10.8±0.00
		10	54.91±2.53	
		30	19.12±1.73	
		60	2.10±0.04	
		120	0.00±0.00	

[a] % Remaining = 100 × (PAR at appointed incubation time / PAR at time T0). PAR is the peak area ratio of test compound to internal standard. Accuracy should be within 80%~120% of the indicated value.

Table 8. Metabolic Stability of 21h in Human Liver Microsomes (average value, n = 3)

Compounds	HLM (final concentration of 0.5 mg protein/mL)					
	R^{2a}	$T_{1/2}$[b] (min)	$CL_{int(mic)}$[c] (μL/min/mg)	$CL_{int(liver)}$[d] (mL/min/kg)	Remaining[e] (60min, %)	Remaining (%) (*NCF[f]=60min)
21h	0.12±0.12	>145	<9.6	<8.6	100.6±0.081	114.9±0.045
Propafenone	0.94±0.0053	13.1±0.78	106.3±6.55	95.6±5.89	4.3±0.008	104.5±0.012
Diclofenac	0.99±0.0017	14.2±0.84	97.7±5.88	88.0±5.29	5.4±0.008	103.2±0.033
Testosterone	0.99±0.0019	19.8±0.65	70.1±2.29	63.1±2.06	12.0±0.004	102.6±0.062

[a] R^2 is the correlation coefficient of the linear regression for determination of the kinetic constant (see raw data worksheet in the Supporting Information).

[b] $T_{1/2}$ is half-life and CLint (mic) is the intrinsic clearance.

[c] $CL_{int\ (mic)}$ = 0.693/half-life/mg microsome protein per mL.

[d] $CL_{int(liver)} = CL_{int\ (mic)}$ × mg microsomal protein/g liver weight × g liver weight/kg body weight.

[e] Accuracy should be within 80%~120% of the indicated value.

[f] *NCF: no co-factor. No NADPH regenerating system was added to the NCF sample (replaced by buffer) during the 60 min incubation. If the remaining amount is less than 60%, then non-NADPH dependent reaction occurs.

In Vivo Pharmacokinetics Study and Safety Assessment

The *in vivo* pharmacokinetic profiles of compound **20h** (the ethyl ester prodrug of **21h**) and **21h** were examined in Sprague-Dawley rats (**Table 9** and **Figure 7**). Intravenous or oral administration resulted in measurable plasma concentrations of the active form (i.e., **21h)** over a period of 24 h. After intravenous administration of **21h**, the half-life was 1.76 h. Upon oral administration, compound **20h** was rapidly absorbed with a T_{max} of 0.57 h, a half-life of 8.68 h, and a mean residence time (MRT) of 17.12 h. Although the plasma concentration of **21h** was low after oral administration of the prodrug **20h** (F = 7.10%), the maximum concentration (C_{max} = 445.6 μg/L (0.92 μM)) was higher than the EC_{50} for all the tested viruses. Compound **21h** was also rapidly absorbed with a T_{max} of 0.83 h, a half-life of 3.82 h, and a mean residence time (MRT) of 4.05 h. The absolute oral bioavailability was 10.30%, which is appreciably higher than that of OSC (4.3%) in rats.[44] Meanwhile, the maximum concentration (C_{max}) of **21h** in plasma was 407 μg/L (0.84 μM), which is also much higher than that of OSC (30 μg/L, 0.15 μM), and is higher than the EC_{50} for all tested viruses.

A single-dose toxicity test of compound **21h** was carried out in Kunming mice. After intragastric administration of **21h** at a dose of 2000 mg/kg, no clinical signs of acute toxicity were observed and no gross lesions were observed upon necropsy after 1 week.

Table 9. Pharmacokinetic Parameters of Compounds 20h and 21h

Parameter	Unit	21h (iv)[a]	20h (po)[b]	21h (po)
		Mean±SD	Mean±SD	Mean±SD
rats (n)		5	5	3
dose	mg/kg	2	20	20
MW		482.63	510.69	482.63

AUC(0-t)	ug/L*h	1460.84±284.21	1036.63±981.39	1504.43±560.63
AUC(0-∞)	ug/L*h	1464.41±283.08	1594.62±1418.14	1558.63±582.37
MRT(0-∞)	h	2.03±0.63	17.12±13.87	4.05±0.89
$t_{1/2}$	h	1.76±0.54	8.68±6.79	3.82±1.52
T_{max}	h	0.083±0.0	0.57±0.42	0.83±0.29
CL	L/h/kg	1.41±0.27	NA	NA
V	L/kg	3.51±1.05	NA	NA
C_{max}	ug/L	1894±411.01	445.6±483.45	407±169.08
F	%	100	7.10	10.30

[a] Dosed intravenously at 2 mg/kg, [b] Dosed orally at 20 mg/kg.

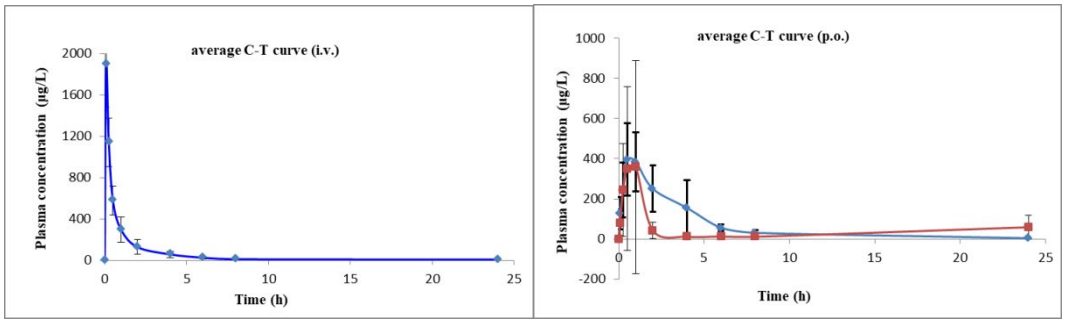

Figure 7 Plasma concentration-time profiles in rats following oral administration (**20h** (red), 20 mg/kg; **21h** (blue), 20 mg/kg) and intravenous administration (**21h**, 2 mg·kg-1).

CONCLUSIONS

Here, we report the results of further SAR studies on NA inhibitors belonging to the OSC chemotype, with the goal of improving the potency against N1-H274Y mutant.

In CEFs assays, compounds **21g** and **21h** exhibited the greatest potency against H5N1, being more potent than the control drugs. Against H5N2, compounds **11d**, **17f**, and **21g-h** displayed comparable antiviral activity to OSC and ZA, and were much more potent than Rib. Against H5N6, only **17f** and **21h** showed similar potency to OSC and ZA, and they were again more potent than Rib. Most of the new oseltamivir derivatives were more potent than Rib against H5N8; ten compounds bearing bulky hydrophobic

substituents at the R-position showed increased activity compared to OSC and ZA. Notably, **21g-h** were 11-103 times more potent than OSC and ZA toward H5N8.

In inhibitory assays, representative compounds were confirmed to be group-1-specific NAs inhibitors, and **21g-h** exhibited high potency against N1, N8 and N1-H274Y mutation, being more active than OSC and lead compounds **5** and **6**.[17] The high potency of **21g-h** against 09N1 again supports the idea that 09N1 favors an open form of the 150-loop.

The results of MD simulation combined with MM-GBSA-based free energy calculations show that **21h** has a higher binding affinity than OSC, and the main contributors to this are van der Waals interaction and shape complementarity. The diphenyl sulphide group of **21h** allows the molecule to interact efficiently with the 150-cavity in addition to the active site pocket.

Overall, **21h** proved to be an exceptionally potent compound with EC_{50} values of 0.39 μM (H5N1), 0.09 μM (H5N2), 0.52 μM (H5N6), and 0.056 μM (H5N8) in CEF; moreover, it was much more potent than OSC against the NAs of N1, N8, and N1-H274Y.

Compound **21h** also showed greater metabolic stability than all the reference compounds in HLM and human plasma assays and displayed drug-like in vivo pharmacokinetic properties and acceptable oral bioavailability in rats. Furthermore, it's remarkable that compound **21h** displayed better anti-influenza virus effect against H5N2 strain than OSC in the chicken embryonated egg model. On the basis of these excellent in vitro and in vivo results, we consider that **21h** is a promising new drug candidate for treatment of influenza virus infections, and should also be a useful lead for further

structural optimization to obtain increased activity against drug-resistant mutants.

EXPERIMENTAL SECTION

Chemistry. All reagents and solvents were obtained from commercial suppliers and were used as received. Reaction mixtures were magnetically stirred under an inert atmosphere. Oseltamivir phosphate was provided by Shandong Qidu Pharmaceutical Co., Ltd. Other chemicals and reagents were obtained commercially and were at least 97% pure. All melting points were measured with a micro melting point apparatus (RY-1G, Tianjin TianGuang Optical Instruments) without correction. The proton and carbon nuclear magnetic resonance (^{1}H-NMR and ^{13}C-NMR) spectra were measured on a Bruker AV-400 (400 MHz) spectrometer using tetramethylsilane (TMS) as an internal standard and DMSO-d_6, CD_3OD, or $CDCl_3$ as a solvent, unless otherwise indicated. When peak multiplicities are reported, the following abbreviations are used: s = singlet, d = doublet, t = triplet, m = multiplet, br = broadened, dd = doublet of doublets, dt = doublet of triplets. Coupling constants, when given, are reported in hertz, and chemical shifts are reported in δ values (ppm) from TMS. Mass spectra (MS) were obtained on an API 4000 LC/MS spectrometer (Applied Biosystems, USA). High-resolution mass spectra (HRMS) were measured using an Agilent 6520 Q-TOF LC/MS spectrometer (Agilent, Germany). Reaction progress was routinely monitored using thin-layer chromatography (TLC) analysis on Silica Gel GF254 for TLC, and spots were visualized by irradiation with UV light (λ = 254 nm). Silica Gel GF254 was from Qingdao Haiyang Chemical Company. Flash column chromatography was performed on columns packed with Silica Gel (200-300 mesh), purchased from Qingdao Haiyang Chemical Company. Solvents were

purified and dried by means of standard methods when necessary. Organic solutions were dried over anhydrous sodium sulfate and concentrated with a rotary evaporator under reduced pressure. Other reagents were obtained commercially and were used without further purification. The purity of the final compounds was verified using an HPLC system (Waers e2695) equipped and a Waters 2998a detector using a GOLD-C18 column (250 mm × 4.6 mm, 5 μm). HPLC solvent conditions: methanol/water with 0.1% acetic acid 15-85%; UV detection, from 200-400 nm; flow rate, 1.0 mL/min; temperature, 30℃; injection volume, 20 μL. All final compounds evaluated for biological effects were > 95% pure.

General Procedure for the Preparation of Compound 9.

The aromatic aldehyde **9** was prepared according to the reported method.[29]

Preparation of Compounds 10a-d.

To a solution of oseltamivir phosphate (0.82 g, 2.0 mmol) in 30 mL methanol and ethanol (V:V = 2:1), was added an aldehyde (2.4 mmol, 1.2 equiv) at room temperature. The reaction solution was stirred at this temperature for 0.5 h, and then $NaBH_3CN$ (0.31 g, 5.0 mmol, 2.5 equiv) was added. Stirring was continued at room temperature for 6 h. The solvent was evaporated under reduced pressure. The residue was taken up in water (30 mL) and extracted with ethyl acetate (3 × 30 mL). The combined organic phase was washed with saturated sodium chloride (2 × 30 mL), dried over anhydrous $MgSO_4$, and concentrated under reduced pressure. The residue was purified by flash column chromatography to afford the corresponding intermediates, **10a-d**.

Ethyl(3R,4R,5S)-4-acetamido-5-((4-ethylbenzyl)amino)-3-(pentan-3-yloxy)cyclohex-1-ene-1-carboxylate (10a). White solid, 62% yield, mp: 84.0–85.1°C. ^{1}H NMR (400

MHz, Methanol-d_4): δ 7.22 (d, J = 8.0 Hz, 2H, Ph-H), 7.15 (d, J = 7.9 Hz, 2H, Ph-H), 6.77 (s, 1H, CH), 4.21 (q, J = 7.1 Hz, $2H_2$), 4.05 (d, J = 8.5 Hz, 1H, CH), 3.96–3.87 (m, 1H, CH), 3.83 (d, J = 12.7 Hz, 1H, CH), 3.65 (d, J = 12.8 Hz, 1H, CH), 3.37 (p, J = 5.5 Hz, 1H, CH), 2.92–2.78 (m, 2H, 2CH), 2.61 (q, J = 7.6 Hz, 2H, CH_2), 2.29–2.17 (m, 1H, CH), 1.99 (s, 3H, CH_3), 1.57–1.44 (m, 4H, $2CH_2$), 1.29 (t, J = 7.1 Hz, 3H, CH_3), 1.20 (t, J = 7.6 Hz, 3H, CH_3), 0.89 (dt, J = 10.8, 7.4 Hz, 6H $2CH_3$). ^{13}C NMR (100 MHz, MeOD): δ 172.51, 166.39, 143.14, 137.45, 136.45, 128.84, 128.10, 127.63, 82.01, 75.65, 60.64, 54.44, 54.01, 49.25, 29.58, 28.14, 25.76, 25.30, 21.74, 14.86, 13.12, 8.54, 8.17. ESI-MS: m/z 431.6 $[M + H]^+$, $C_{25}H_{38}N_2O_4$ (430.5892).

Ethyl(3R,4R,5S)-4-acetamido-5-((4-isopropylbenzyl)amino)-3-(pentan-3-yloxy)cyclohex-1-ene-1-carboxylate (10b). White solid, 70% yield, mp: 101.8–104.1°C. ^{1}H NMR (400 MHz, DMSO-d_6): δ 7.82 (d, J = 9.1 Hz, 1H, NH), 7.21 (d, J = 8.2 Hz, 2H, Ph-H), 7.16 (d, J = 8.2 Hz, 2H, Ph-H), 6.64 (s, 1H, CH), 4.14 (q, J = 7.0 Hz, 2H, CH_2), 4.01 (d, J = 8.2 Hz, 1H, CH), 3.79–3.66 (m, 2H, CH_2), 3.61 (d, J = 13.1 Hz, 1H, CH), 3.41 – 3.35 (m, 1H, CH), 2.91 – 2.79 (m, 1H, CH), 2.78–2.69 (m, 1H, CH), 2.65 (dd, J = 17.5, 4.9 Hz, 1H, CH), 2.07 (ddt, J = 14.8, 9.2, 2.7 Hz, 1H, CH), 1.93–1.77 (overlapped, 4H, CH_3, CH), 1.50–1.35 (m, 4H, $2CH_2$), 1.22 (t, J = 7.1 Hz, 3H, CH_3), 1.18 (d, J = 6.9 Hz, 6H, $2CH_3$), 0.82 (dt, J = 14.6, 7.4 Hz, 6H, $2CH_3$). ^{13}C NMR (100 MHz, DMSO-d_6): δ 170.03, 166.30, 147.02, 138.83, 138.44, 129.14, 128.25, 126.46, 81.32, 75.73, 60.79, 54.86, 54.56, 49.98, 33.57, 30.92, 26.08, 25.64, 24.42, 23.48, 14.55, 9.91, 9.41. ESI-MS: m/z 445.6 $[M + H]^+$, $C_{26}H_{40}N_2O_4$ (444.6160).

Ethyl(3R,4R,5S)-4-acetamido-5-((4-(tert-butyl)benzyl)amino)-3-(pentan-3-yloxy)cyclohex-1-ene-1-carboxylate (10c). White solid, 71% yield, mp: 104.0–106.1°C. 1H

NMR (400 MHz, DMSO-d6): δ 7.78 (d, J = 9.0 Hz, 1H, NH), 7.31 (d, J = 8.3 Hz, 2H, Ph-H), 7.21 (d, *J* = 8.3 Hz, 2H, Ph-H), 6.64 (s, 1H, CH), 4.14 (q, *J* = 7.0 Hz, 2H, CH_2), 4.02 (d, *J* = 8.0 Hz, 1H, CH), 3.77–3.72 (m, 1H, CH), 3.70 (d, *J* = 10.2 Hz, 1H, CH), 3.62 (d, *J* = 13.3 Hz, 1H, CH), 3.36 (p, *J* = 5.6 Hz, 1H, CH), 2.75 (td, *J* = 9.7, 5.2 Hz, 1H, CH), 2.65 (dd, *J* = 17.5, 4.9 Hz, 1H, CH), 2.08 (ddt, *J* = 17.4, 9.2, 2.7 Hz, 1H, CH), 1.94–1.78 (overlapped, 4H, CH, CH3), 1.50–1.35 (m, 4H, $2CH_2$), 1.26 (s, 9H, $3CH_3$), 1.22 (t, *J* = 7.1 Hz, 3H, CH_3), 0.82 (dt, *J* = 13.4, 7.4 Hz, 6H, $2CH_3$). ^{13}C NMR (100 MHz, DMSO-d_6): δ 170.03, 166.33, 149.30, 138.37, 129.21, 127.97, 125.27, 81.34, 75.74, 60.77, 54.92, 54.62, 49.94, 34.57, 31.67, 30.94, 26.10, 25.70, 23.46, 14.55, 9.86, 9.42. ESI-MS: m/z 459.5 $[M + H]^+$, $C_{27}H_{42}N_2O_4$ (458.6430).

Ethyl(3R,4R,5S)-4-acetamido-5-((4-benzylbenzyl)amino)-3-(pentan-3-yloxy)cyclohex-1-ene-1-carboxylate (10d). White solid, 68% yield, mp: 110.4–112.5°C. ^{1}H NMR (400 MHz, Methanol-d_4): δ 7.27–7.19 (m, 4H, Ph-H), 7.19–7.09 (m, 5H, Ph-H), 6.76 (s, 1H, CH), 4.20 (q, *J* = 7.1 Hz, 2H, CH_2), 4.04 (d, *J* = 8.7 Hz, 1H, CH), 3.94–3.86 (overlapped, 3H, CH_2, CH), 3.81 (d, *J* = 12.8 Hz, 1H, CH), 3.65 (d, *J* = 12.8 Hz, 1H, CH), 3.36 (p, *J* = 5.6 Hz, 1H, CH), 2.91–2.84 (m, 1H, CH), 2.84–2.76 (m, 1H, CH), 2.21 (ddt, *J* = 17.3, 9.3, 2.9 Hz, 1H, CH), 1.97 (s, 3H, CH_3), 1.55–1.43 (m, 4H, $2CH_2$), 1.28 (t, *J* = 7.1 Hz, 3H, CH_3), 0.93–0.88 (m, 3H, CH_3), 0.88–0.83 (m, 3H, CH_3). ^{13}C NMR (100 MHz, CD_3OD): δ 180.90, 172.48, 166.42, 141.28, 140.39, 137.42, 137.09, 128.90, 128.66, 128.47, 128.13, 128.02, 125.63, 82.00, 75.64, 60.62, 54.50, 54.08, 49.26, 48.24, 41.08, 29.66, 25.77, 25.32, 21.73, 13.11, 8.51, 8.17. ESI-MS: m/z 493.4 $[M + H]^+$, $C_{30}H_{40}N_2O_4$ (492.6600).

Preparation of Compounds 11a-d.

Solution of intermediates **10a-d** (0.8 mmol) in a mixture of CH_3OH (30 mL) and 16% aqueous sodium hydroxide (10 mL) was stirred at room temperature for 6 hours. Mixture was concentrated to remove most CH_3OH. The residue was taken up in water (30 mL), resulting aqueous solution was acidified with HCl aqueous solution (2 mol/L), and the pH was adjusted to 4-5. Then extracted with ethyl acetate and tetrahydrofuran (V:V = 2:1, 4 × 30 mL), and the mixture of ethyl acetate and tetrahydrofuran was washed with saturated sodium chloride (2 × 30 mL), dried over anhydrous $MgSO_4$, and after removal of solvent *in vacuo* to afford the target compounds **11a-d**.

(3R,4R,5S)-4-Acetamido-5-((4-ethylbenzyl)amino)-3-(pentan-3-yloxy)cyclohex-1-ene-1-carboxylic acid (11a). White solid, 65% yield, mp: 186.7–190.2°C, melt and decompose at the same time. ^{1}H NMR (400 MHz, DMSO-d_6): δ 9.43 (s, 1H, OH), 8.17 (d, J = 9.1 Hz, 1H, NH), 7.45 (d, J = 8.0 Hz, 2H, Ph-H), 7.26 (d, J = 8.0 Hz, 2H, Ph-H), 6.64 (s, 1H, CH), 4.25 (d, J = 8.1 Hz, 1H, CH), 4.14 (q, J = 13.1 Hz, 2H, CH_2), 4.02 (q, J = 8.9 Hz, 1H, CH), 3.36–3.32 (m, 1H, CH), 2.91 (dd, J = 17.1, 4.8 Hz, 1H, CH), 2.73–2.64 (m, 1H, CH), 2.61 (q, J = 7.5 Hz, 2H, CH_2), 1.92 (s, 3H, CH_3), 1.51–1.35 (m, 4H, $2CH_2$), 1.17 (t, J = 7.6 Hz, 3H, CH_3), 0.82 (dt, J = 18.9, 7.3 Hz, 6H, $2CH_3$). ^{13}C NMR (100 MHz, DMSO-d_6): δ 171.20, 167.24, 145.01, 138.06, 130.62, 129.58, 128.47, 128.03, 81.56, 74.97, 54.28, 51.03, 45.79, 28.38, 26.02, 25.46, 23.96, 16.08, 9.86, 9.30. HRMS calcd for $C_{23}H_{34}N_2O_4$ $[M + H]^+$: 403.2591. Found: m/z 403.2592.

(3R,4R,5S)-4-Acetamido-5-((4-isopropylbenzyl)amino)-3-(pentan-3-yloxy)cyclo hex-1-ene-1-carboxylic acid (11b). White solid, 68% yield, mp: 170.9–176.0°C. melt and decompose at the same time. ^{1}H NMR (400 MHz, DMSO-d_6): δ 9.45 (s, 1H, OH), 8.17 (d, J = 9.1 Hz, 1H, NH), 7.46 (d, J = 8.0 Hz, 2H, Ph-H), 7.29 (d, J = 8.0 Hz, 2H,

Ph-H), 6.65 (s, 1H, CH), 4.26 (d, J = 8.0 Hz, 1H, CH), 4.19–4.08 (m, 2H, CH_2), 4.03 (q, J = 9.0 Hz, 1H, CH), 3.38–3.35 (m, 1H, CH), 2.96–2.85 (overlapped, 2H, 2CH), 2.74–2.60 (m, 1H, CH), 1.92 (s, 3H, CH_3), 1.50–1.34 (m, 4H, $2CH_2$), 1.20 (d, J = 6.9 Hz, 6H, $2CH_3$), 0.84 (t, J = 7.3 Hz, 3H, CH_3), 0.79 (t, J = 7.4 Hz, 3H, CH_3). ^{13}C NMR (100 MHz, DMSO-d_6): δ 171.18, 167.24, 149.60, 138.06, 130.66, 129.79, 128.05, 126.99, 81.56, 75.00, 54.38, 50.99, 45.74, 33.70, 26.03, 25.99, 25.47, 24.27, 23.97, 9.87, 9.31. HRMS calcd for $C_{24}H_{36}N_2O_4$ $[M + H]^+$: 417.2748. Found: m/z 417.2752.

(3R,4R,5S)-4-Acetamido-5-((4-(tert-butyl)benzyl)amino)-3-(pentan-3-yloxy)cyclohex-1-ene-1-carboxylic acid (11c). White solid, 68% yield, mp: 183.0–190.0°C, melt and decompose at the same time. ^{1}H NMR (400 MHz, DMSO-d_6): δ 8.16 (d, J = 9.1 Hz, 1H, NH), 7.47 (d, J = 8.5 Hz, 2H, Ph-H), 7.43 (d, J = 8.5 Hz, 2H, Ph-H), 6.65 (s, 1H, CH), 4.26 (d, J = 8.2 Hz, 1H, CH), 4.19–4.08 (m, 2H, CH_2), 4.07–3.98 (m, 1H, CH), 3.38–3.33 (m, 1H, CH), 2.91 (dd, J = 17.2, 4.9 Hz, 1H, CH), 2.71–2.58 (m, 1H, CH), 1.92 (s, 3H, CH_3), 1.42 (tq, J = 13.8, 6.9 Hz, 4H, $2CH_2$), 1.28 (s, 9H, $3CH_3$), 0.82 (dt, J = 18.5, 7.4 Hz, 6H, $2CH_3$). ^{13}C NMR (100 MHz, DMSO-d_6): δ 171.14, 167.27, 151.74, 138.03, 130.31, 129.73, 128.15, 125.83, 81.57, 75.06, 54.43, 51.14, 45.79, 34.84, 31.52, 26.15, 26.04, 25.49, 23.95, 9.85, 9.31. HRMS calcd for $C_{25}H_{38}N_2O_4$ $[M + H]^+$: 431.2904. Found: m/z 431.2903.

(3R,4R,5S)-4-Acetamido-5-((4-benzylbenzyl)amino)-3-(pentan-3-yloxy)cyclohex-1-ene-1-carboxylic acid (11d). White solid, 73% yield, mp: 148.2–154.0°C. ^{1}H NMR (400 MHz, Methanol-d_4): δ 7.40 (d, J = 8.1 Hz, 2H, Ph-H), 7.29 (d, J = 8.2 Hz, 2H, Ph-H), 7.25 (td, J = 7.3, 1.5 Hz, 2H, Ph-H), 7.20–7.11 (m, 3H, Ph-H), 6.81 (s, 1H, CH), 4.33 (d, J = 13.0 Hz, 1H, CH), 4.25–4.18 (m, 2H, CH_2), 4.18–4.13 (m, 1H, CH), 3.98 (s,

2H, CH_2), 3.56 (td, J = 10.1, 5.6 Hz, 1H, CH), 3.43 (p, J = 5.6 Hz, 1H, CH), 3.00 (dd, J = 17.4, 5.6 Hz, 1H, CH), 2.62 (ddt, J = 17.3, 9.9, 2.5 Hz, 1H, CH), 2.03 (s, 3H, CH_3), 1.59–1.44 (m, 4H, CH_2), 0.89 (q, J = 7.5 Hz, 6H, $2CH_3$). ^{13}C NMR (100 MHz, CD_3OD): δ 173.41, 168.02, 143.27, 140.75, 136.27, 129.64, 129.38, 128.76, 128.49, 128.29, 128.14, 125.84, 82.26, 74.65, 54.85, 51.59, 47.30, 41.07, 41.07, 26.17, 25.73, 25.22, 21.98, 8.41, 8.15. HRMS calcd for $C_{28}H_{36}N_2O_4$ $[M + H]^+$: 465.2748. Found: m/z 465.2749.

General procedure for the Preparation of Compounds 14a-b.

To a stirred solution of 4- or 3-hydroxybenzaldehyde (2 g, 16.39 mmol) in *N,N*-dimethylformamide (40 mL) at room temperature was added potassium carbonate (5 g, 36.18 mmol) and 3-bromopentane (2.47 g, 16.39 mmol). The reaction mixture was heated at 80°C for 12 h. The reaction mixture was cooled to room temperature, and then poured into cold water (160 mL). It was extracted in ethyl acetate (3 × 30 mL). The combined organic phase was washed with saturated sodium chloride (50 mL) and water (50 mL), dried over anhydrous $MgSO_4$ and concentrated reduced pressure to afford crude products. Purification by column chromatography gave the corresponding products, **14a-b**.

4-(Pentan-3-yloxy)benzaldehyde (14a). Pale yellow oil, 78% yield. ^{1}H NMR (400 MHz, Chloroform-*d*): δ 9.87 (s, 1H, CH), 7.82 (d, J = 8.7 Hz, 2H, Ph-H), 6.98 (d, J = 8.7 Hz, 2H, Ph-H), 4.25 (p, J = 5.8 Hz, 1H, CH), 1.83–1.64 (m, 4H, $2CH_2$), 0.96 (t, J = 7.4 Hz, 6H, $2CH_3$). ^{13}C NMR (100 MHz, $CDCl_3$): δ 190.78, 164.07, 132.07, 129.45, 115.65, 80.47, 26.01, 9.53. ESI-MS: m/z 193.3 $[M + H]^+$, $C_{12}H_{16}O_2$ (192.2580).

3-(Pentan-3-yloxy)benzaldehyde (14b). Pale yellow oil, 76% yield. ^{1}H NMR (400 MHz, Chloroform-*d*): δ 9.97 (s, 1H, CH), 7.46–7.35 (m, 3H, Ph-H), 7.21–7.12 (m, 1H, Ph-H), 4.22 (p, J = 5.7 Hz, 1H, CH), 1.75–1.66 (m, 4H, $2CH_2$), 0.96 (t, J = 7.5 Hz, 6H,

2CH_3). ^{13}C NMR (100 MHz, $CDCl_3$): δ 192.30, 159.35, 137.80, 130.10, 123.08, 121.96, 114.32, 80.43, 25.94, 9.54. ESI-MS: m/z 193.3 $[M + H]^+$, $C_{12}H_{16}O_2$ (192.2580).

Preparation of Compounds 16a-f.

The method of preparation was similar to that of **10a-d**, starting from **12a-c, 14a-b, and 15**.

Ethyl(3R,4R,5S)-4-acetamido-5-((4-methoxybenzyl)amino)-3-(pentan-3-yloxy)cyclohex-1-ene-1-carboxylate (16a). White solid, 69% yield. mp: 122.2–124.5°C. ^{1}H NMR (400 MHz, DMSO-d_6): δ 7.77 (d, J = 9.0 Hz, 1H, NH), 7.20 (d, J = 8.5 Hz, 2H, Ph-H), 6.86 (d, J = 8.5 Hz, 2H, Ph-H), 6.63 (s, 1H, CH), 4.14 (q, J = 7.0 Hz, 2H, CH_2), 4.00 (d, J = 7.7 Hz, 1H, CH), 3.76–3.70 (overlapped, 4H, CH, CH_3), 3.69 (d, J = 6.1 Hz, 1H, CH), 3.58 (d, J = 13.0 Hz, 1H, CH), 3.36 (p, J = 5.4 Hz, 1H, CH), 2.77–2.68 (m, 1H, CH), 2.64 (dd, J = 17.6, 4.7 Hz, 1H, CH), 2.11–2.01 (m, 1H, CH), 1.85 (s, 3H, CH_3), 1.79 (s, 1H, CH), 1.50–1.34 (m, 4H, 2CH_2), 1.22 (t, J = 7.1 Hz, 3H, CH_3), 0.82 (dt, J = 14.5, 7.4 Hz, 6H, 2CH_3). ^{13}C NMR (100 MHz, DMSO-d_6): δ 170.00, 166.32, 158.49, 138.37, 133.41, 129.42, 129.20, 114.01, 81.33, 75.72, 60.78, 55.46, 54.77, 54.57, 49.72, 30.95, 26.09, 25.68, 23.46, 14.55, 9.88, 9.42. ESI-MS: m/z 433.4–$[M + H]^+$, $C_{24}H_{36}N_2O_5$ (432.5610).

Ethyl(3R,4R,5S)-4-acetamido-5-((3-methoxybenzyl)amino)-3-(pentan-3-yloxy)cyclohex-1-ene-1-carboxylate (16b). white solid, 73% yield. mp: 82.7–84.2°C. ^{1}H NMR (400 MHz, Chloroform-*d*): δ 7.22 (t, J = 8.0 Hz, 1H, Ph-H), 6.93–6.84 (m, 2H Ph-H), 6.81–6.74 (overlapped, 2H Ph-H, CH), 5.45 (s, 1H, NH), 4.27–4.16 (overlapped, 3H, CH, CH_2), 3.89 (d, J = 13.3 Hz, 1H, CH), 3.80 (s, 3H, CH_3), 3.79 – 3.70 (m, 2H, CH_2), 3.36 (p, J = 5.6 Hz, 1H, CH), 3.15 (td, J = 9.0, 5.4 Hz, 1H, CH), 2.77 (dd, J = 17.8, 5.1 Hz,

1H, CH), 2.32–2.21 (m, 1H, CH), 2.00 (s, 3H, CH_3), 1.56–1.44 (m, 4H, $2CH_2$), 1.30 (t, *J* = 7.1 Hz, 3H, CH_3), 0.90 (t, *J* = 7.4 Hz, 6H, $2CH_3$). ^{13}C NMR (100 MHz, $CDCl_3$): δ 170.58, 166.51, 159.75, 142.00, 137.15, 129.38, 120.37, 113.55, 112.54, 81.75, 74.53, 60.86, 55.84, 55.20, 53.56, 50.59, 30.44, 26.17, 25.78, 23.72, 14.23, 9.51, 9.42. ESI-MS: m/z 433.6 $[M + H]^+$, $C_{24}H_{36}N_2O_5$ (432.5610).

Ethyl(3R,4R,5S)-4-acetamido-5-((4-isopropoxybenzyl)amino)-3-(pentan-3-yloxy)cyclohex-1-ene-1-carboxylate (16c). White solid, 70% yield. mp: 62.1–64.1°C. ^{1}H NMR (400 MHz, Chloroform-*d*): δ 7.20 (d, *J* = 8.5 Hz, 2H, Ph-H)), 6.83 (d, *J* = 8.5 Hz, 2H, Ph-H)), 6.79 (s, 1H, CH), 5.57 (d, *J* = 8.1 Hz, 1H, NH), 4.58–4.44 (m, 1H, CH), 4.21 (overlapped, 3H, NH, CH_2), 3.83 (d, *J* = 12.8 Hz, 1H, CH), 3.78 – 3.70 (m, 1H, CH), 3.67 (d, *J* = 12.8 Hz, 1H, CH), 3.35 (p, *J* = 5.6 Hz, 1H, CH), 3.21–3.09 (m, 1H, CH), 2.77 (dd, *J* = 17.7, 5.1 Hz, 1H, CH), 2.26 (ddt, *J* = 17.7, 8.6, 2.5 Hz, 1H, CH), 2.06 (s, 1H, CH), 2.00 (s, 3H, CH_3), 1.56–1.46 (m, 4H, $2CH_2$), 1.36–1.27 (overlapped, 9H, $3CH_3$), 0.89 (td, *J* = 7.4, 2.6 Hz, 6H, $2CH_3$). ^{13}C NMR (100 MHz, $CDCl_3$): δ 170.64, 166.52, 156.96, 137.23, 132.10, 129.38, 129.28, 115.86, 81.74, 74.60, 69.90, 60.84, 55.88, 53.53, 50.03, 30.46, 26.16, 25.75, 23.71, 22.07, 14.22, 9.51, 9.39. ESI-MS: m/z 461.5 $[M + H]^+$, $C_{26}H_{40}N_2O_5$ (460.6150).

Ethyl(3R,4R,5S)-4-acetamido-3-(pentan-3-yloxy)-5-((4-(pentan-3-yloxy)benzyl) amino)cyclohex-1-ene-1-carboxylate (16d). White solid, 75% yield, mp: 86.0–87.1°C. ^{1}H NMR (400 MHz, Chloroform-*d*): δ 7.20 (d, *J* = 8.5 Hz, 2H, Ph-H), 6.83 (d, *J* = 8.6 Hz, 2H, Ph-H), 6.79 (s, 1H, NH), 5.85–5.48 (m, 1H, CH), 4.21 (overlapped, 3H, NH, CH_2), 4.08 (p, *J* = 5.8 Hz, 1H, CH), 3.84 (d, *J* = 12.8 Hz, 1H, CH), 3.76 (q, *J* = 8.1 Hz, 1H, CH), 3.68 (d, *J* = 12.8 Hz, 1H, CH), 3.40–3.31 (m, 1H, CH), 3.27–3.12 (m, 1H, CH,

CH), 2.79 (dd, *J* = 17.7, 5.0 Hz, 1H, CH), 2.35 – 2.22 (m, 1H, CH), 1.99 (s, 3H, CH_3), 1.72–1.60 (m, 4H, $2CH_2$), 1.56–1.44 (m, 4H, $2CH_2$), 1.30 (t, *J* = 7.1 Hz, 3H, CH_3), 0.95 (t, *J* = 7.4 Hz, 6H, $2CH_3$), 0.89 (td, *J* = 7.4, 2.9 Hz, 6H, $2CH_3$). ^{13}C NMR (100 MHz, $CDCl_3$): δ 184.65, 179.84, 170.73, 166.46, 157.94, 137.30, 131.46, 129.37, 129.30, 115.97, 81.79, 80.29, 74.61, 60.87, 55.80, 53.47, 49.93, 30.30, 26.15, 26.07, 25.73, 23.69, 14.23, 9.60, 9.51, 9.38. ESI-MS: m/z 489.6 $[M + H]^+$, $C_{28}H_{44}N_2O_5$ (488.6690).

Ethyl(3R,4R,5S)-4-acetamido-3-(pentan-3-yloxy)-5-((3-(pentan-3-yloxy)benzyl) amino)cyclohex-1-ene-1-carboxylate (16e). Colorless sticky oil, 72% yield. ^{1}H NMR (400 MHz, Chloroform-*d*): δ 7.19 (t, *J* = 7.8 Hz, 1H, Ph-H), 6.89–6.81 (m, 2H, Ph-H), 6.80–6.73 (overlapped, 2H, Ph-H, CH), 5.55 (s, 1H, NH), 4.27–4.16 (overlapped, 3H, NH, CH_2), 4.12 (p, *J* = 5.8 Hz, 1H, CH), 3.86 (d, *J* = 13.2 Hz, 1H, CH), 3.81–3.73 (m, 1H, CH), 3.71 (d, *J* = 13.2 Hz, 1H, CH), 3.36 (p, *J* = 5.6 Hz, 1H, CH), 3.14 (td, *J* = 9.1, 5.4 Hz, 1H, CH), 2.78 (dd, *J* = 17.8, 5.2 Hz, 1H, CH), 2.32–2.22 (m, 1H, CH), 2.03–1.97 (overlapped, 4H, CH, CH_3), 1.72–1.62 (m, 4H, $2CH_2$), 1.56–1.45 (m, 4H, $2CH_2$), 1.30 (t, *J* = 7.1 Hz, 3H, CH_3), 0.95 (t, *J* = 7.4 Hz, 6H, $2CH_3$), 0.89 (td, *J* = 7.4, 1.8 Hz, 6H, $2CH_3$). ^{13}C NMR (100 MHz, $CDCl_3$): δ 170.62, 166.52, 158.90, 141.92, 137.21, 129.39, 129.34, 120.10, 115.87, 114.39, 81.75, 80.03, 74.65, 60.83, 55.78, 53.69, 50.61, 30.46, 26.16, 26.05, 26.03, 25.77, 23.68, 14.22, 9.57, 9.49, 9.39. ESI-MS: m/z 489.3 $[M + H]^+$, $C_{28}H_{44}N_2O_5$ (488.6690).

Ethyl(3R,4R,5S)-4-acetamido-3-(pentan-3-yloxy)-5-((4-phenoxybenzyl)amino)c yclohex-1-ene-1-carboxylate (16f). White solid, 76% yield. mp: 95.5–98.0°C. ^{1}H NMR (400 MHz, Methanol-d_4): δ 7.31 (dddd, *J* = 9.7, 7.7, 4.9, 2.4 Hz, 4H, Ph-H)), 7.12–7.04 (m, 1H, Ph-H)), 6.99 – 6.89 (m, 4H, Ph-H)), 6.77 (s, 1H, CH), 4.20 (q, *J* = 7.1 Hz, 2H,

CH_2), 4.10–4.03 (m, 1H, CH), 3.91 (dd, J = 10.5, 8.4 Hz, 1H, CH), 3.84 (d, J = 12.9 Hz, 1H, CH), 3.68 (d, J = 12.9 Hz, 1H, CH), 3.37 (p, J = 5.6 Hz, 1H, CH), 2.90 (td, J = 9.9, 5.4 Hz, 1H, CH), 2.81 (dd, J = 17.6, 5.3 Hz, 1H, CH), 2.22 (ddt, J = 17.5, 9.5, 2.9 Hz, 1H, CH), 1.99 (s, 3H, CH_3), 1.57–1.43 (m, 4H, $2CH_2$), 1.28 (t, J = 7.1 Hz, 3H, CH_3), 0.89 (dt, J = 9.6, 7.4 Hz, 6H, $2CH_3$). ^{13}C NMR (100 MHz, CD_3OD): δ 172.49, 166.44, 157.36, 156.48, 137.40, 134.56, 129.51, 128.94, 122.94, 118.44, 82.01, 75.64, 60.63, 54.55, 54.10, 48.98, 29.75, 25.78, 25.34, 21.75, 13.11, 8.52, 8.18. ESI-MS: m/z 495.4 $[M + H]^+$, $C_{29}H_{38}N_2O_5$ (494.6320).

Preparation of Compounds 17a-f.

The method of preparation was similar to that of **11a-d**, starting from **16a-f**.

(3R,4R,5S)-4-Acetamido-5-((4-methoxybenzyl)amino)-3-(pentan-3-yloxy)cycloh ex-1-ene-1-carboxylic acid (17a). White solid, 63% yield, mp: 176.0–178.0°C. ^{1}H NMR (400 MHz, DMSO-d_6): δ 9.37 (s, 1H, OH), 8.15 (d, J = 6.5 Hz, 1H, NH), 7.47 (d, J = 8.6 Hz, 2H, Ph-H), 6.97 (d, J = 8.4 Hz, 2H, Ph-H), 6.64 (s, 1H, CH), 4.24 (d, J = 7.8 Hz, 1H, CH), 4.12 (q, J = 13.0 Hz, 2H, CH_2), 4.01 (q, J = 9.0 Hz, 1H, CH), 3.76 (s, 3H, CH_3), 3.39–3.27 (overlapped, 3H, CH, CH_2), 2.90 (dd, J = 17.2, 4.8 Hz, 1H, CH), 2.74–2.58 (m, 1H, CH), 1.92 (s, 3H, CH_3), 1.51–1.33 (m, 4H, $2CH_2$), 0.84 (t, J = 7.4 Hz, 3H, CH_3), 0.79 (t, J = 7.4 Hz, 3H, CH_3). ^{13}C NMR (100 MHz, DMSO-d_6): δ 171.19, 167.24, 160.08, 138.07, 132.13, 128.04, 124.04, 114.43, 81.55, 74.95, 55.66, 54.06, 51.05, 45.51, 26.02, 25.46, 23.96, 9.86, 9.30. HRMS calcd for $C_{22}H_{32}N_2O_5$ $[M + H]^+$: 405.2384. Found: m/z 405.2380.

(3R,4R,5S)-4-Acetamido-5-((3-methoxybenzyl)amino)-3-(pentan-3-yloxy)cycloh ex-1-ene-1-carboxylic acid (17b). White solid, 64% yield, mp: 174.5–178.2°C. ^{1}H NMR

(400 MHz, DMSO-d_6): δ 8.04 (d, J = 8.6 Hz, 1H, NH), 7.27 (t, J = 7.8 Hz, 1H, Ph-H), 7.08 (s, 1H, Ph-H), 6.99 (d, J = 7.3 Hz, 1H, Ph-H), 6.88 (d, J = 6.7 Hz, 1H, Ph-H), 6.62 (s, 1H, CH), 4.22–4.07 (m, 1H, CH), 4.00 (d, J = 13.0 Hz, 1H, CH), 3.95–3.81 (m, 2H, CH_2), 3.76 (s, 3H, CH_3), 3.17–2.98 (m, 1H, CH), 2.79 (d, J = 15.0 Hz, 1H, CH), 2.47–2.28 (m, 1H, CH), 1.89 (s, 3H, CH_3), 1.53–1.29 (m, 4H, $2CH_2$), 0.93–0.70 (m, 6H, $2CH_3$). ^{13}C NMR (100 MHz, DMSO-d_6): δ 170.73, 167.69, 159.72, 137.85, 129.90, 128.94, 121.65, 114.89, 113.94, 81.43, 75.34, 55.49, 54.52, 52.71, 47.81, 28.14, 26.07, 25.54, 23.75, 9.89, 9.35. HRMS calcd for $C_{22}H_{32}N_2O_5$ $[M + H]^+$: 405.2384. Found: m/z 405.2280.

(3R,4R,5S)-4-Acetamido-5-((4-isopropoxybenzyl)amino)-3-(pentan-3-yloxy)cyclohex-1-ene-1-carboxylic acid (17c). White solid, 70% yield, mp: 174.5–178.2°C. ^{1}H NMR (400 MHz, DMSO-d_6): δ 8.12 (d, J = 7.9 Hz, 1H, NH), 7.37 (d, J = 7.9 Hz, 2H, Ph-H), 6.91 (d, J = 8.2 Hz, 2H, Ph-H), 6.61 (s, 1H, CH), 4.61 (dt, J = 11.7, 5.8 Hz, 1H, CH), 4.17 (s, 1H, CH), 4.04–3.84 (overlapped, 3H, CH, CH_2), 3.24–3.07 (m, 1H, CH), 2.82 (d, J = 15.5 Hz, 1H, CH), 2.49–2.29 (m, 1H, CH), 1.90 (s, 3H, CH_3), 1.54–1.31 (m, 4H, $2CH_2$), 1.26 (s, 3H, CH_3), 1.25 (s, 3H, CH_3), 0.82 (dt, J = 18.0, 7.2 Hz, 6H, $2CH_3$). ^{13}C NMR (100 MHz, DMSO-d_6): δ 170.82, 167.79, 157.77, 137.68, 131.37, 128.97, 115.86, 81.45, 75.34, 69.52, 54.36, 52.15, 46.76, 27.69, 26.05, 25.51, 23.82, 23.27, 22.26, 9.89, 9.33. HRMS calcd for $C_{24}H_{36}N_2O_5$ $[M + H]^+$: 433.2697. Found: m/z 433.2698.

(3R,4R,5S)-4-Acetamido-3-(pentan-3-yloxy)-5-((4-(pentan-3-yloxy)benzyl)amino)cyclohex-1-ene-1-carboxylic acid (17d). White solid, 70% yield, mp: 175.0–180.0°C. ^{1}H NMR (400 MHz, DMSO-d_6): δ 8.07 (d, J = 8.5 Hz, 1H, NH), 7.36 (d, J = 8.1 Hz, 2H, Ph-H), 6.93 (d, J = 8.3 Hz, 2H, Ph-H), 6.62 (s, 1H, CH), 4.23 (q, J = 5.6 Hz, 1H, CH),

4.20–4.13 (m, 1H, CH), 4.03–3.86 (overlapped, 3H, NH, CH_2), 3.81–3.42 (m, 2H, CH_2), 3.22–3.11 (m, 1H, CH), 2.82 (d, J = 15.3 Hz, 1H, CH), 2.49–2.34 (m, 1H, CH), 1.90 (s, 3H, CH_3), 1.66–1.53 (m, 4H, $2CH_2$), 1.42 (qt, J = 13.8, 7.0 Hz, 4H, $2CH_2$), 0.89 (d, J = 14.8 Hz, 6H, $2CH_3$), 0.82 (dt, J = 17.9, 7.3 Hz, 6H$2CH_3$). ^{13}C NMR (100 MHz, DMSO-d_6): δ 170.85, 158.69, 137.82, 131.38, 128.76, 115.94, 81.47, 79.44, 75.32, 73.12, 56.65, 54.38, 52.14, 46.74, 26.05, 25.98, 25.52, 23.82, 9.88, 9.82, 9.33. HRMS calcd for $C_{26}H_{40}N_2O_5$ $[M + H]^+$: 461.301. Found: m/z 461.3007.

(3R,4R,5S)-4-Acetamido-3-(pentan-3-yloxy)-5-((3-(pentan-3-yloxy)benzyl)amino)cyclohex-1-ene-1-carboxylic acid (17e). White solid, 70% yield, mp: 169.2–172.0°C. ^{1}H NMR (400 MHz, DMSO-d_6): δ 8.21–8.01 (m, 1H, NH), 7.26 (t, J = 7.6 Hz, 1H, Ph-H), 7.11 (s, 1H, Ph-H), 6.99 (d, J = 6.5 Hz, 1H, Ph-H), 6.88 (d, J = 7.3 Hz, 1H, Ph-H), 6.63 (s, 1H, CH), 4.32–4.11 (overlapped, 2H, 2CH), 4.09–3.81 (m, 3H, CH_2, NH), 3.30–3.12 (m, 1H, CH), 2.85 (d, J = 15.6 Hz, 1H, CH), 2.50–2.21 (m, 1H, CH), 1.90 (s, 3H, CH_3), 1.70–1.52 (m, 4H, $2CH_2$), 1.51–1.33 (m, 4H, $2CH_2$), 0.90 (t, J = 6.4 Hz, 6H, $2CH_3$), 0.86–0.68 (m, 6H, $2CH_3$). ^{13}C NMR (100 MHz, DMSO): δ 170.81, 167.64, 158.81, 137.80, 137.75, 129.99, 128.79, 121.78, 116.90, 116.03, 81.45, 79.45, 75.24, 54.60, 52.10, 47.15, 27.44, 26.06, 25.96, 25.91, 25.53, 23.79, 9.88, 9.85, 9.80, 9.33. HRMS calcd for $C_{26}H_{40}N_2O_5$ $[M + H]^+$: 461.301. Found: m/z 461.3009.

(3R,4R,5S)-4-Acetamido-3-(pentan-3-yloxy)-5-((4-phenoxybenzyl)amino)cyclohex-1-ene-1-carboxylic acid (17f). White solid, 77% yield, mp: 196.8–212.1°C, melt and decompose at the same time. ^{1}H NMR (400 MHz, Methanol-d_4): δ 7.47 (d, J = 8.6 Hz, 2H, Ph-H), 7.37 (tt, J = 7.6, 2.2 Hz, 2H, Ph-H), 7.19–7.12 (m, 1H, Ph-H), 7.06–6.97 (m, 4H, Ph-H), 6.85 (s, 1H, CH), 4.36 (d, J = 13.1 Hz, 1H, CH), 4.28–4.14 (overlapped, 3H,

CH, CH_2), 3.62 (td, *J* = 10.3, 5.6 Hz, 1H, CH), 3.45 (p, *J* = 5.6 Hz, 1H, CH), 3.01 (dd, *J* = 17.5, 5.6 Hz, 1H, CH), 2.64 (ddt, *J* = 17.2, 9.9, 2.6 Hz, 1H, CH), 2.05 (s, 3H, CH_3), 1.61–1.44 (m, 4H, $2CH_2$), 0.90 (q, *J* = 7.5 Hz, 6H, $2CH_3$). ^{13}C NMR (100 MHz, CD_3OD): δ 173.46, 167.61, 158.82, 156.38, 136.74, 131.42, 129.69, 127.82, 125.34, 123.79, 119.13, 118.41, 82.29, 74.59, 54.82, 51.61, 26.08, 25.74, 25.24, 22.03, 8.42, 8.16. HRMS calcd for $C_{27}H_{34}N_2O_5$ $[M + H]^+$: 467.254. Found: m/z 467.2538.

Preparation of Compounds 19a-h.

A solution of 4- or 3-fluorobenzaldehyde (2 g, 16.13 mmol, 1 equiv) in anhydrous DMF (30 mL) was treated with benzenethiol, thiophene-2-thiol, alkyl mercaptan or cycloalkyl mercaptan (16.13 mmol, 1 equiv) and K_2CO_3(5 g, 36.23 mmol). After stirring for 8 h at 120°C, the reaction mixture was cooled to room temperature, and then poured into cold water (120 ml). It was extracted with EtOAc (3 × 30 ml). The combined organic phase was washed with saturated sodium chloride (50 ml) and water (50 ml), then dried over anhydrous $MgSO_4$ and concentrated under reduced procure to afford crude product. Purification by column chromatography gave the corresponding products, **19a-h**.

4-(Isobutylthio)benzaldehyde (19a). Pale yellow oil, 69% yield. ^{1}H NMR (400 MHz, Chloroform-*d*): δ 9.92 (s, 1H, CH), 7.75 (d, *J* = 8.3 Hz, 2H, Ph-H), 7.35 (d, *J* = 8.3 Hz, 2H, Ph-H), 2.89 (d, *J* = 6.8 Hz, 2H, CH_2), 1.96 (dp, *J* = 13.4, 6.7 Hz, 1H, CH), 1.08 (s, 3H), 1.07 (s, 3H, $2CH_3$). ^{13}C NMR (100 MHz, $CDCl_3$): δ 191.25, 147.41, 133.04, 130.00, 126.33, 40.60, 28.09, 22.13. ESI-MS: m/z 195.3 $[M + H]^+$, $C_{11}H_{14}OS$ (194.2920).

4-(*Sec*-butylthio)benzaldehyde (19b). Pale yellow oil, 60% yield. ^{1}H NMR (400 MHz, Chloroform-*d*): δ 9.94 (s, 1H, CH), 7.78 (d, *J* = 8.3 Hz, 2H, Ph-H), 7.41 (d, *J* = 8.3 Hz, 2H, Ph-H), 3.42 (h, *J* = 6.7 Hz, 1H, CH), 1.69 (ddp, *J* = 35.7, 14.3, 6.9 Hz, 2H, CH_2),

1.38 (d, J = 6.7 Hz, 3H, CH_3), 1.06 (t, J = 7.4 Hz, 3H, CH_3). ^{13}C NMR (100 MHz, $CDCl_3$): δ 191.32, 146.28, 133.40, 130.01, 128.11, 42.97, 29.38, 20.33, 11.45. ESI-MS: m/z 195.3 $[M + H]^+$, $C_{11}H_{14}OS$ (194.2920).

3-(*Sec*-butylthio)benzaldehyde (19c). Pale yellow oil, 66% yield. ^{1}H NMR (400 MHz, Chloroform-*d*): δ 10.00 (s, 1H, CH), 7.88 (s, 1H, Ph-H), 7.72 (d, J = 7.6 Hz, 1H, Ph-H), 7.63 (d, J = 7.8 Hz, 1H, Ph-H), 7.47 (t, J = 7.7 Hz, 1H, Ph-H), 3.39–3.21 (m, 1H, CH), 1.74–1.55 (m, 2H, CH_2), 1.32 (d, J = 6.7 Hz, 3H, CH_3), 1.04 (t, J = 7.4 Hz, 3H, CH_3). ^{13}C NMR (100 MHz, $CDCl_3$): δ 191.89, 137.80, 136.86, 131.53, 129.37, 127.75, 44.61, 29.42, 20.48, 11.45.ESI-MS: m/z 195.3 $[M + H]^+$, $C_{11}H_{14}OS$ (194.2920).

4-(Cyclopentylthio)benzaldehyde (19d). Pale yellow oil, 63% yield. ^{1}H NMR (400 MHz, Chloroform-*d*): δ 9.92 (s, 1H, CH), 7.75 (d, J = 8.3 Hz, 2H, Ph-H), 7.37 (d, J = 8.3 Hz, 2H, Ph-H), 3.75 (p, J = 7.2 Hz, 1H, CH), 2.28–2.09 (m, 2H, CH_2), 1.88–1.75 (m, 2H, CH_2), 1.69 (dd, J = 10.7, 5.6 Hz, 4H, $2CH_2$). ^{13}C NMR (100 MHz, $CDCl_3$): δ 191.30, 147.80, 132.98, 129.97, 126.83, 43.89, 33.45, 24.99. ESI-MS: m/z 207.3 $[M + H]^+$, $C_{12}H_{14}OS$ (206.3030).

3-(Cyclopentylthio)benzaldehyde (19e). Pale yellow oil, 62% yield. ^{1}H NMR (400 MHz, Chloroform-*d*): δ 9.98 (s, 1H, CH), 7.82 (s, 1H, Ph-H), 7.65 (d, J = 7.5 Hz, 1H, Ph-H), 7.57 (d, J = 7.9 Hz, 1H, Ph-H), 7.44 (t, J = 7.7 Hz, 1H, Ph-H), 3.69 (p, J = 6.8 Hz, 1H, CH), 2.11 (td, J = 11.7, 10.9, 4.5 Hz, 2H, CH_2), 1.88–1.73 (m, 2H, CH_2), 1.72–1.58 (m, 4H, $2CH_2$). ^{13}C NMR (100 MHz, $CDCl_3$): δ 191.95, 139.55, 136.83, 134.89, 129.45, 129.30, 127.15, 45.35, 33.48, 24.85. ESI-MS: m/z 207.2 $[M + H]^+$, $C_{12}H_{14}OS$ (206.3030).

4-(Cyclohexylthio)benzaldehyde (19f). Pale yellow oil, 62% yield. ^{1}H NMR (400 MHz, Chloroform-*d*): δ 9.93 (s, 1H, CH), 7.76 (d, J = 8.3 Hz, 2H, Ph-H), 7.39 (d, J = 8.3

Hz, 2H, Ph-H), 3.45–3.26 (m, 1H, CH), 2.14–1.99 (m, 2H, CH_2), 1.81 (dd, *J* = 9.0, 3.6 Hz, 2H, CH_2), 1.72–1.61 (m, 1H, CH), 1.52–1.25 (m, 5H, CH $2CH_2$). ^{13}C NMR (100 MHz, $CDCl_3$): δ 191.30, 145.88, 133.40, 130.02, 128.04, 44.66, 33.01, 25.93, 25.66. ESI-MS: m/z 221.4 $[M + H]^+$, $C_{13}H_{16}OS$ (220.3300).

4-(Thiophen-2-ylthio)benzaldehyde (19g). Pale yellow oil, 62% yield. ^1H NMR (400 MHz, Chloroform-*d*): δ 9.91 (s, 1H, CH), 7.73 (d, *J* = 8.4 Hz, 2H, Ph-H), 7.60 (d, *J* = 5.4 Hz, 1H, thiophene-H), 7.39 (d, *J* = 8.3 Hz, 1H, thiophene-H), 7.36 (d, *J* = 3.5 Hz, 1H, thiophene-H), 7.20 (d, *J* = 8.3 Hz, 2H, Ph-H). ^{13}C NMR (100 MHz, $CDCl_3$): δ 191.20, 148.07, 137.64, 132.72, 130.16, 130.02, 128.44, 128.05, 125.56. ESI-MS: m/z 221.3 $[M + H]^+$, $C_{11}H_8OS_2$ (220.3040).

4-(Phenylthio)benzaldehyde (19h). Pale yellow power, 64% yield. ^1H NMR (400 MHz, DMSO-d_6): δ 9.93 (s, 1H, CH), 7.86–7.79 (m, 2H, 2H, Ph-H), 7.59–7.54 (m, 2H, 2H, Ph-H), 7.54–7.47 (m, 3H, 2H, Ph-H), 7.34–7.25 (m, 2H, 2H, Ph-H). ^{13}C NMR (100 MHz, DMSO-d_6): δ 192.49, 146.10, 134.41, 134.22, 131.09, 130.73, 130.62, 129.86, 127.67. ESI-MS: m/z 215.3 $[M + H]^+$, $C_{13}H_{10}OS$ (214.2820).

Preparation of Compounds 20a-h.

The method of preparation was similar to that of **10a-d**, starting from **19a-h**.

Ethyl(3R,4R,5S)-4-acetamido-5-((4-(isobutylthio)benzyl)amino)-3-(pentan-3-yloxy)cyclohex-1-ene-1-carboxylate (20a). White solid, 69% yield. mp: 99.2–101.9°C. ^1H NMR (400 MHz, Chloroform-*d*): δ 7.27 (d, *J* = 8.2 Hz, 2H, Ph-H), 7.22 (d, *J* = 8.2 Hz, 2H, Ph-H), 6.79 (s, 1H, CH), 5.45 (s, 1H, NH), 4.21 (q, *J* = 7.1 Hz, 3H, NH, CH_2), 3.85 (d, *J* = 13.2 Hz, 1H, CH), 3.76 (dd, *J* = 9.4, 8.0 Hz, 1H, CH), 3.70 (d, *J* = 13.2 Hz, 1H, CH), 3.36 (p, *J* = 5.7 Hz, 1H, CH), 3.12 (td, *J* = 8.9, 5.4 Hz, 1H, CH), 2.82 – 2.70

(overlapped, 3H, CH, CH_2), 2.26 (ddt, *J* = 17.8, 8.4, 2.4 Hz, 1H, CH), 2.00 (s, 3H, CH_3), 1.91–1.82 (m, 1H, CH), 1.81–1.75 (m, 1H, CH), 1.58–1.44 (m, 4H, $2CH_2$), 1.30 (t, *J* = 7.1 Hz, 3H, CH_3), 1.02 (d, *J* = 6.6 Hz, 6H, $2CH_3$), 0.89 (t, *J* = 7.4 Hz, 6H, $2CH_3$). ^{13}C NMR (100 MHz, $CDCl_3$) δ 170.57, 166.52, 138.04, 137.11, 135.70, 129.42, 129.14, 128.60, 81.74, 77.35, 74.52, 60.86, 55.77, 53.59, 50.20, 42.88, 30.45, 28.26, 26.16, 25.79, 23.72, 22.03, 14.24, 9.51, 9.42. ESI-MS: m/z 491.5-$[M + H]^+$, $C_{27}H_{42}N_2O_4S$ (490.7030).

Ethyl(3R,4R,5S)-4-acetamido-5-((4-(*sec*-butylthio)benzyl)amino)-3-(pentan-3-yl oxy)cyclohex-1-ene-1-carboxylate (20b). white solid, 75% yield. mp: 78.0–80.9°C. ^1H NMR (400 MHz, Chloroform-*d*): δ 7.34 (d, *J* = 8.0 Hz, 2H, Ph-H), 7.23 (d, *J* = 8.1 Hz, 2H, Ph-H), 6.79 (s, 1H, CH), 5.48 (s, 1H, NH), 4.21 (overlapped, *J* = 7.1 Hz, 3H, CH_2, NH), 3.87 (d, *J* = 13.2 Hz, 1H, CH), 3.82–3.74 (m, 1H, CH), 3.72 (d, *J* = 13.4 Hz, 1H, CH), 3.36 (p, *J* = 5.6 Hz, 1H, CH), 3.21–3.05 (m, 2H, CH_2), 2.76 (dd, *J* = 17.8, 5.1 Hz, 1H, CH), 2.27 (ddt, *J* = 17.8, 8.5, 2.4 Hz, 1H, CH), 2.00 (s, 3H, CH_3), 1.97–1.89 (m, 1H, CH), 1.65 (tt, *J* = 13.8, 7.4 Hz, 1H, CH), 1.57–1.44 (overlapped, 5H, $2CH_2$, CH), 1.30 (t, *J* = 7.1 Hz, 3H, CH_3), 1.26 (d, *J* = 6.7 Hz, 3H, CH_3), 1.00 (t, *J* = 7.4 Hz, 3H, CH_3), 0.89 (t, *J* = 7.4 Hz, 6H, $2CH_3$). ^{13}C NMR (100 MHz, $CDCl_3$): δ 170.58, 166.50, 139.03, 137.08, 133.78, 132.17, 129.41, 128.50, 81.74, 74.52, 60.86, 55.70, 53.69, 50.23, 45.04, 30.41, 29.47, 26.15, 25.78, 23.71, 20.52, 14.23, 11.45, 9.49, 9.40. ESI-MS: m/z 491.5 $[M + H]^+$, $C_{27}H_{42}N_2O_4S$ (490.7030).

Ethyl(3R,4R,5S)-4-acetamido-5-((3-(*sec*-butylthio)benzyl)amino)-3-(pentan-3-yl oxy)cyclohex-1-ene-1-carboxylate (20c). Colorless sticky oil, 70% yield. ^1H NMR (400 MHz, Chloroform-*d*): δ 7.35 (s, 1H, Ph-H), 7.27–7.19 (m, 2H, Ph-H), 7.15 (d, *J* = 7.3 Hz, 1H, Ph-H), 6.79 (s, 1H, CH), 5.56 (d, *J* = 7.8 Hz, 1H, NH), 4.27–4.14 (overlapped, 3H,

NH, CH_2), 3.88 (d, *J* = 13.3 Hz, 1H, CH), 3.78 (q, *J* = 8.3 Hz, 1H, CH), 3.72 (d, *J* = 13.3 Hz, 1H, CH), 3.42–3.31 (m, 1H, CH), 3.25–3.06 (m, 2H, CH_2), 2.77 (dd, *J* = 17.8, 5.2 Hz, 1H, CH), 2.39 (s, 1H, CH), 2.32–2.22 (m, 1H, CH), 2.01 (s, 3H, CH_3), 1.72–1.60 (m, 1H, CH), 1.59–1.45 (overlapped, 5H, CH, $2CH_2$), 1.30 (t, *J* = 7.1 Hz, 3H, CH_3), 1.27 (d, *J* = 6.7 Hz, 3H CH_3), 1.00 (t, *J* = 7.4 Hz, 3H CH_3), 0.89 (t, *J* = 7.4 Hz, 6H $2CH_3$). ^{13}C NMR (100 MHz, $CDCl_3$): δ 170.67, 166.47, 140.88, 137.17, 135.71, 131.30, 131.28, 130.23, 129.34, 128.78, 126.38, 81.78, 74.59, 60.87, 55.59, 53.70, 50.32, 44.73, 30.37, 29.50, 26.15, 25.77, 23.70, 20.57, 14.23, 11.45, 9.50, 9.40. ESI-MS: m/z 491.5–$[M + H]^+$, $C_{27}H_{42}N_2O_4S$ (490.7030).

Ethyl(3R,4R,5S)-4-acetamido-5-((4-(cyclopentylthio)benzyl)amino)-3-(pentan-3-yloxy)cyclohex-1-ene-1-carboxylate (20d). White solid, 73% yield. mp: 112.9–114.5°C. ^{1}H NMR (400 MHz, Chloroform-*d*): δ 7.30 (d, *J* = 7.9 Hz, 2H, Ph-H), 7.22 (d, *J* = 8.0 Hz, 2H, Ph-H), 6.79 (s, 1H, CH), 5.44 (s, 1H, NH), 4.29–4.11 (overlapped, 3H, NH, CH_2), 3.86 (d, J = 13.2 Hz, 1H, CH), 3.76 (dd, J = 9.4, 8.0 Hz, 1H, CH), 3.71 (d, J = 13.4 Hz, 1H, CH), 3.56 (p, J = 6.7 Hz, 1H, CH), 3.36 (p, J = 5.6 Hz, 1H, CH), 3.13 (q, J = 8.6 Hz, 1H, CH), 2.76 (dd, J = 17.8, 5.0 Hz, 1H, CH), 2.26 (dd, J = 17.8, 8.5 Hz, 1H, CH), 2.14–2.01 (m, 2H, CH_2), 2.00 (s, 3H, CH_3), 1.89–1.68 (m, 4H, $2CH_2$), 1.65–1.55 (m, 4H, $2CH_2$), 1.55–1.42 (m, 4H, $2CH_2$), 1.30 (t, J = 7.1 Hz, 3H, CH_3), 0.89 (t, J = 7.4 Hz, 6H, $2CH_3$). ^{13}C NMR (100 MHz, $CDCl_3$): δ 170.57, 166.52, 138.37, 137.11, 135.49, 130.28, 129.42, 128.52, 81.73, 74.52, 60.86, 55.77, 53.62, 50.23, 46.14, 33.55, 30.45, 26.16, 25.78, 24.78, 23.73, 14.23, 9.51, 9.41. ESI-MS: m/z 503.4 $[M + H]^+$, $C_{28}H_{42}N_2O_4S$ (502.7140).

Ethyl(3R,4R,5S)-4-acetamido-5-((3-(cyclopentylthio)benzyl)amino)-3-(pentan-3

-yloxy)cyclohex-1-ene-1-carboxylate (20e). White solid, 66% yield. mp: 83.7–86.0°C. ^{1}H NMR (400 MHz, Chloroform-*d*): δ 7.31 (s, 1H, Ph-H), 7.25–7.18 (m, 2H, Ph-H), 7.14–7.08 (m, 1H, Ph-H), 6.79 (s, 1H, CH), 5.44 (d, *J* = 8.1 Hz, 1H, NH), 4.27–4.15 (m, 3H, CH_2, NH), 3.87 (d, *J* = 13.3 Hz, 1H, CH), 3.81–3.73 (m, 1H, CH), 3.71 (d, *J* = 13.4 Hz, 1H, CH), 3.65–3.55 (m, 1H, CH), 3.36 (p, *J* = 5.7 Hz, 1H, CH), 3.12 (td, *J* = 8.7, 5.3 Hz, 1H, CH), 2.76 (dd, *J* = 17.8, 5.2 Hz, 1H, CH), 2.32–2.21 (m, 1H, CH), 2.07–2.03 (m, 1H, CH), 2.01 (s, 3H, CH_3), 1.92 (s, 2H, CH_2), 1.84–1.72 (m, 2H, CH_2), 1.66–1.56 (m, 4H, $2CH_2$), 1.55–1.44 (m, 4H, $2CH_2$), 1.30 (t, *J* = 7.2 Hz, 3H, CH_3), 0.95–0.85 (m, 6H, $2CH_3$). ^{13}C NMR (100 MHz, $CDCl_3$): δ 170.59, 166.50, 141.07, 137.39, 137.13, 129.44, 129.40, 128.75, 128.35, 125.67, 81.75, 77.34, 74.58, 55.74, 53.67, 50.44, 45.79, 33.57, 30.46, 26.17, 25.79, 24.81, 23.72, 14.23, 9.50, 9.41. ESI-MS: m/z 503.4 $[M + H]^+$, $C_{28}H_{42}N_2O_4S$ (502.7140).

Ethyl(3R,4R,5S)-4-acetamido-5-((4-(cyclohexylthio)benzyl)amino)-3-(pentan-3-yloxy)cyclohex-1-ene-1-carboxylate (20f). White solid, 70% yield. mp: 93.0–96.0°C. ^{1}H NMR (400 MHz, Chloroform-*d*): δ 7.34 (d, *J* = 8.2 Hz, 2H, Ph-H), 7.23 (d, *J* = 8.1 Hz, 2H, Ph-H), 6.79 (s, 1H, CH), 5.49 (d, *J* = 8.1 Hz, 1H, NH), 4.21 (q, *J* = 7.1 Hz, 3H, NH, CH_2), 3.86 (d, *J* = 13.2 Hz, 1H, CH), 3.82–3.74 (m, 1H, CH), 3.71 (d, *J* = 13.3 Hz, 1H, CH), 3.36 (p, *J* = 5.6 Hz, 1H, CH), 3.13 (td, *J* = 8.8, 5.3 Hz, 1H, CH), 3.06 (ddt, *J* = 10.4, 7.5, 3.6 Hz, 1H, CH), 2.76 (dd, *J* = 17.8, 5.2 Hz, 1H, CH), 2.33–2.21 (m, 1H, CH), 2.00 (s, 3H, CH_3), 1.99 – 1.91 (m, 2H, CH_2), 1.86–1.81 (m, 1H, CH), 1.80–1.73 (m, 2H, CH_2), 1.61 (dd, *J* = 10.7, 3.5 Hz, 1H, CH), 1.56–1.45 (m, 4H, $2CH_2$), 1.39–1.23 (overlapped, 8H, CH, 2CH2, CH_3), 0.95–0.84 (m, 6H, $2CH_3$). ^{13}C NMR (100 MHz, $CDCl_3$): δ 170.59, 166.51, 139.12, 137.10, 133.38, 132.18, 129.41, 128.48, 81.73, 74.53, 60.87, 55.70,

53.69, 50.24, 46.77, 33.36, 30.44, 26.15, 26.06, 25.76, 23.72, 14.23, 9.51, 9.41. ESI-MS: m/z 517.3-$[M + H]^+$, $C_{29}H_{44}N_2O_4S$ (516.7410).

Ethyl(3R,4R,5S)-4-acetamido-3-(pentan-3-yloxy)-5-((4-(thiophen-3-ylthio)benzyl)amino)cyclohex-1-ene-1-carboxylate (20g). Colorless sticky oil, 65% yield. ^{1}H NMR (400 MHz, Chloroform-*d*): δ 7.52–7.41 (m, 1H, thiophene-H), 7.34 (d, *J* = 8.0 Hz, 1H, Ph-H), 7.31–7.22 (m, 2H, Ph-H), 7.22–7.10 (m, 3H, Ph-H, thiophene-H), 7.06 (dd, *J* = 5.3, 3.6 Hz, 1H, thiophene-H), 6.78 (s, 1H, CH, CH), 5.57–5.34 (m, 1H, NH), 4.26–4.15 (overlapped, 3H, CH, CH_2), 3.84 (q, *J* = 11.0 Hz, 1H, CH), 3.79–3.73 (m, 1H, CH), 3.68 (d, *J* = 13.2 Hz, 1H, CH), 3.35 (p, *J* = 5.5, 4.9 Hz, 1H, CH), 3.16–3.04 (m, 1H, CH), 2.81–2.68 (m, 1H, CH), 2.25 (dddt, *J* = 17.5, 11.1, 8.5, 2.5 Hz, 1H, CH), 1.98 (s, 3H, CH_3), 1.56–1.44 (m, 4H, $2CH_2$), 1.29 (t, *J* = 7.1 Hz, 3H, CH_3), 0.95–0.84 (m, 6H, $2CH_3$). ^{13}C NMR (100 MHz, $CDCl_3$): δ 170.57, 166.49, 138.64, 137.09, 136.86, 135.75, 133.42, 132.19, 131.07, 129.39, 128.76, 128.49, 127.88, 127.55, 81.73, 74.49, 60.86, 55.74, 53.54, 50.09, 33.37, 26.16, 25.78, 23.71, 14.23, 9.50, 9.41. ESI-MS: m/z 517.5-$[M + H]^+$, $C_{27}H_{36}N_2O_4S_2$ (516.7150).

Ethyl(3R,4R,5S)-4-acetamido-3-(pentan-3-yloxy)-5-((4-(phenylthio)benzyl)amino)cyclohex-1-ene-1-carboxylate (20h). White solid, 78% yield. mp: 68.1–70.2°C. ^{1}H NMR (400 MHz, Chloroform-*d*): δ 7.35–7.26 (m, 7H, Ph-H), 7.26–7.19 (m, 2H, Ph-H), 6.80 (s, 1H, CH), 5.65–5.41 (m, 1H, NH), 4.21 (q, *J* = 7.1 Hz, 3H, CH, CH_2), 3.89 (d, *J* = 13.3 Hz, 1H, CH), 3.83–3.76 (m, 1H, CH), 3.74 (d, *J* = 13.3 Hz, 1H, CH), 3.36 (p, *J* = 5.7 Hz, 1H, CH), 3.17 (td, *J* = 8.8, 5.3 Hz, 1H, CH), 2.76 (dd, *J* = 17.8, 5.2 Hz, 1H, CH), 2.35–2.19 (overlapped, 2H, 2CH), 2.00 (s, 3H, CH_3), 1.58–1.42 (m, 4H, $2CH_2$), 1.30 (t, *J* = 7.1 Hz, 3H, CH_3), 0.89 (td, *J* = 7.4, 1.6 Hz, 6H, $2CH_3$). ^{13}C NMR (100 MHz, $CDCl_3$): δ

170.71, 166.45, 139.21, 137.10, 136.09, 134.02, 131.45, 130.68, 129.31, 129.14, 129.02, 126.88, 81.79, 74.49, 60.91, 55.58, 53.66, 50.09, 30.25, 26.15, 25.77, 23.71, 14.24, 9.51, 9.41. ESI-MS: m/z 511.5 $[M + H]^+$, $C_{29}H_{38}N_2O_4S$ (510.6930).

Preparation of Compounds 21a-h.

The method of preparation was similar to that of **10a-d**, starting from **20a-f**.

(3R,4R,5S)-4-Acetamido-5-((4-(isobutylthio)benzyl)amino)-3-(pentan-3-yloxy)cyclohex-1-ene-1-carboxylic acid (21a). White solid, 71% yield, mp: 161.2–164.7°C. ^{1}H NMR (400 MHz, DMSO-d_6) δ 8.12 (d, J = 8.5 Hz, 1H, NH), 7.43 (d, J = 7.9 Hz, 2H, Ph-H), 7.33 (d, J = 8.1 Hz, 2H, Ph-H), 6.63 (s, 1H, CH), 4.30–4.16 (m, 1H, NH), 4.07 (q, J = 11.5, 10.0 Hz, 2H, CH_2), 3.96 (q, J = 8.8, 8.2 Hz, 1H, CH), 3.68 – 3.44 (m, 1H, CH), 3.35–3.05 (m, 2H, CH_2), 2.90–2.67 (m, 3H, CH, CH_2), 2.65–2.52 (m, 1H, CH), 1.91 (s, 3H, CH_3), 1.84–1.69 (m, 1H, CH), 1.53–1.29 (m, 4H, $2CH_2$), 0.98 (d, J = 6.6 Hz, 6H, $2CH_3$), 0.81 (dt, J = 18.4, 7.3 Hz, 6H, $2CH_3$). ^{13}C NMR (100 MHz, DMSO-d_6): δ 171.05, 167.38, 137.99, 130.93, 130.69, 128.32, 127.98, 124.45, 81.51, 75.07, 65.73, 54.37, 51.54, 46.20, 28.09, 26.04, 25.48, 24.36, 23.90, 22.16, 9.88, 9.32. HRMS calcd for $C_{25}H_{38}N_2O_4S$ $[M + H]^+$: 463.2625. Found: m/z 463.2625.

(3R,4R,5S)-4-Acetamido-5-((4-(*sec*-butylthio)benzyl)amino)-3-(pentan-3-yloxy)cyclohex-1-ene-1-carboxylic acid (21b). White solid, 68% yield, mp: 173.2–176.0°C. ^{1}H NMR (400 MHz, DMSO-d_6) δ 9.49 (s, 1H, OH), 8.17 (d, J = 8.8 Hz, 1H, NH), 7.49 (d, J = 8.0 Hz, 2H, Ph-H), 7.39 (d, J = 8.0 Hz, 2H, Ph-H), 6.64 (s, 1H, CH), 4.25 (s, 1H, CH), 4.23–4.05 (m, 2H, CH_2), 4.01 (q, J = 8.9 Hz, 1H, CH), 3.36–3.02 (m, 2H, CH_2), 2.99–2.83 (m, 1H, CH), 2.74–2.59 (m, 1H, CH), 1.92 (s, 3H, CH_3), 1.55 (ddt, J = 26.6, 14.1, 6.8 Hz, 2H, CH_2), 1.48–1.33 (m, 4H, $2CH_2$), 1.23 (d, J = 6.6 Hz, 3H, CH_3), 0.96 (t, J =

7.3 Hz, 3H, CH_3), 0.81 (dt, J = 18.8, 7.2 Hz, 6H, $2CH_3$). ^{13}C NMR (100 MHz, DMSO-d_6): δ 171.22, 167.24, 138.04, 136.90, 131.28, 130.34, 128.06, 125.09, 81.55, 74.95, 59.89, 54.39, 51.05, 45.58, 43.38, 29.27, 26.03, 25.47, 23.97, 20.63, 11.55, 9.87, 9.31. HRMS calcd for $C_{25}H_{38}N_2O_4S$ $[M + H]^+$: 463.2625. Found: m/z 463.2626.

(3R,4R,5S)-4-Acetamido-5-((3-(*sec*-butylthio)benzyl)amino)-3-(pentan-3-yloxy) cyclohex-1-ene-1-carboxylic acid (21c). White solid, 73% yield, mp: 180.2-188.5°C, melt and decompose at the same time. ^{1}H NMR (400 MHz, Methanol-d_4): δ 7.85–7.67 (m, 2H, Ph-H), 7.67–7.37 (m, 1H, Ph-H), 7.37–7.14 (m, 1H, Ph-H), 6.87 (s, 1H, CH, CH), 4.55–4.15 (overlaped, 4H, CH, CH, CH_2), 3.73–3.58 (m, 1H, CH), 3.50–3.42 (m, 1H, CH), 3.11–2.96 (m, 1H, CH), 2.95–2.74 (m, 1H, CH), 2.74–2.60 (m, 1H, CH), 2.06 (s, 3H, CH_3), 1.99–1.38 (overlapped, 6H, $3CH_2$), 1.38–1.10 (m, 3H, CH_3), 1.01 (q, J = 8.2, 7.0 Hz, 3H, CH_3), 0.91 (q, J = 7.7 Hz, 6H, $2CH_3$). ^{13}C NMR (100 MHz, MeOD): δ 173.52, 167.22, 137.17, 132.78, 132.28, 130.95, 129.80, 127.30, 126.51, 125.48, 116.25, 82.32, 74.51, 60.63, 55.24, 51.66, 51.57, 25.97, 25.74, 25.24, 22.07, 21.36, 10.38, 9.68, 8.42, 8.17. HRMS calcd for $C_{25}H_{38}N_2O_4S$ $[M + H]^+$: 463.2625. Found: m/z 463.2707.

(3R,4R,5S)-4-Acetamido-5-((4-(cyclopentylthio)benzyl)amino)-3-(pentan-3-yloxy)cyclohex-1-ene-1-carboxylic acid (21d). White solid, 73% yield, mp: 166.6–168.9°C. ^{1}H NMR (400 MHz, Methanol-d_4): δ 7.48 (s, 1H, Ph-H), 7.39 (q, J = 8.2 Hz, 2H, Ph-H), 7.29 (d, J = 6.8 Hz, 1H, Ph-H), 6.87 (s, 1H, CH), 4.37 (d, J = 13.0 Hz, 1H, CH), 4.32–4.10 (m, 3H, CH, CH_2), 3.73 (p, J = 6.6 Hz, 1H, CH), 3.69–3.55 (m, 1H, CH), 3.53–3.40 (m, 1H, CH), 3.12–2.95 (m, 1H, CH), 2.67 (dd, J = 16.3, 7.8 Hz, 1H, CH), 2.19–2.07 (m, 2H), 2.06 (s, 3H, CH_3), 1.84–1.71 (m, 2H, CH_2), 1.71–1.62 (m, 2H, CH_2), 1.62–1.45 (m, 6H, $3CH_2$), 0.91 (q, J = 7.5 Hz, 6H, $2CH_3$). ^{13}C NMR (100 MHz, MeOD): δ 173.39,

168.54, 139.34, 137.28, 131.62, 129.96, 129.75, 129.37, 126.54, 105.08, 82.32, 74.54, 61.20, 55.09, 51.47, 44.89, 33.11, 33.05, 25.88, 25.73, 25.23, 24.36, 22.06, 8.43, 8.17. HRMS calcd for $C_{26}H_{38}N_2O_4S$ $[M + H]^+$: 475.2625. Found: m/z 475.2626.

(3R,4R,5S)-4-Acetamido-5-((3-(cyclopentylthio)benzyl)amino)-3-(pentan-3-yloxy)cyclohex-1-ene-1-carboxylic acid (21e). White solid, 73% yield, mp: 184.0–188.2°C. ^{1}H NMR (400 MHz, DMSO-d_6): δ 9.47 (s, 1H, OH), 8.16 (d, J = 9.0 Hz, 1H, NH), 7.71 (q, J = 8.0 Hz, 1H, Ph-H), 7.41 (dd, J = 48.7, 8.0 Hz, 3H, Ph-H), 6.64 (s, 1H, CH), 4.31–4.07 (overlapped, 3H, NH, CH_2), 4.00 (q, J = 9.0 Hz, 1H, CH), 3.75 (p, J = 6.6 Hz, 1H, CH), 3.36 – 3.14 (overlapped, 2H, 2CH), 2.96–2.84 (m, 1H, CH), 2.75–2.58 (m, 1H, CH), 2.20–1.98 (m, 2H, CH_2), 1.92 (s, 3H, CH_3), 1.88–1.76 (m, 1H, CH), 1.76–1.62 (m, 2H, CH_2), 1.62–1.53 (m, 2H, CH_2), 1.53–1.46 (m, 2H, CH_2), 1.46–1.31 (overlapped, 4H, $2CH_2$), 0.81 (dt, J = 18.9, 7.2 Hz, 6H, $2CH_3$). ^{13}C NMR (100 MHz, DMSO-d_6): δ 171.22, 167.24, 138.58, 138.02, 131.24, 129.34, 128.64, 128.04, 125.02, 67.75, 62.90, 54.33, 51.06, 45.60, 44.41, 33.42, 27.95, 26.32, 26.03, 25.83, 25.47, 24.88, 23.97, 23.27, 9.87, 9.31. HRMS calcd for $C_{26}H_{38}N_2O_4S$ $[M + H]^+$: 475.2625. Found: m/z 475.2627.

(3R,4R,5S)-4-Acetamido-5-((4-(cyclohexylthio)benzyl)amino)-3-(pentan-3-yloxy)cyclohex-1-ene-1-carboxylic acid (21f). White solid, 73% yield, mp: 175.9–178.2°C. ^{1}H NMR (400 MHz, Methanol-d_4): δ 7.77–7.35 (m, 4H, Ph-H), 6.87 (s, 1H, CH), 4.37 (d, J = 12.9 Hz, 1H, CH), 4.33–4.10 (m, 3H, CH, CH_2), 3.74–3.55 (m, 1H, CH), 3.52–3.40 (m, 1H, CH), 3.29–3.18 (m, 1H, CH), 3.12–2.94 (m, 1H, CH), 2.74–2.55 (m, 1H, CH), 2.06 (s, 3H, CH_3), 2.03–1.87 (m, 2H, CH_2), 1.86–1.70 (m, 2H, CH_2), 1.65 (t, J = 11.5 Hz, 1H, CH), 1.60–1.46 (m, 4H, $2CH_2$), 1.45–1.22 (m, 5H, CH, $2CH_2$), 0.91 (q, J = 7.5 Hz, 6H, $2CH_3$). ^{13}C NMR (100 MHz, MeOD): δ 138.07, 137.22, 134.72, 130.70, 130.40,

130.07, 128.48, 125.59, 82.32, 74.53, 54.97, 51.51, 47.84, 47.08, 45.32, 32.94, 26.22, 25.98, 25.73, 25.52, 25.46, 25.23, 24.84, 22.02, 8.42, 8.16. HRMS calcd for $C_{27}H_{40}N_2O_4S$ $[M + H]^+$: 489.2782. Found: m/z 489.2782.

(3R,4R,5S)-4-Acetamido-3-(pentan-3-yloxy)-5-((4-(thiophen-2-ylthio)benzyl)amino)cyclohex-1-ene-1-carboxylic acid (21g). White solid, 73% yield, mp: 196.6–199.3°C. ^{1}H NMR (400 MHz, Methanol-d_4): δ 7.76–7.10 (m, 7H, thiophene-H, Ph-H), 6.86 (s, 1H), 4.36 (dd, J = 12.8, 8.1 Hz, 1H), 4.19 (dt, J = 17.5, 9.0 Hz, 3H), 3.67–3.54 (m, 1H), 3.49–3.41 (m, 1H), 3.09–2.95 (m, 1H), 2.71–2.57 (m, 1H), 2.04 (s, 3H), 2.01–1.88 (m, 1H), 1.58–1.49 (m, 4H), 0.94–0.86 (m, 6H). ^{13}C NMR (100 MHz, MeOD): δ 141.16, 138.09, 136.84, 132.12, 130.70, 130.30, 130.07, 129.24, 128.46, 128.40, 128.02, 126.75, 82.31, 74.51, 54.93, 51.51, 48.26, 45.32, 32.93, 25.72, 25.22, 22.00, 8.41, 8.15. HRMS calcd for $C_{25}H_{32}N_2O_4S_2$ $[M + H]^+$: 489.1876. Found: m/z 489.1877.

(3R,4R,5S)-4-Acetamido-3-(pentan-3-yloxy)-5-((4-(phenylthio)benzyl)amino)cyclohex-1-ene-1-carboxylic acid (21h). White solid, 73% yield, mp: 141.1–147.5°C, melt and decompose at the same time. ^{1}H NMR (400 MHz, DMSO-d_6): δ 7.93 (d, J = 8.1 Hz, 1H, NH), 7.37 (t, J = 7.5 Hz, 4H, Ph-H), 7.31 (d, J = 7.5 Hz, 5H, Ph-H), 6.61 (s, 1H, CH), 4.14–3.99 (1H, CH), 3.89 (d, J = 13.2 Hz, 1H, NH), 3.84–3.70 (m, 2H, CH_2), 3.67–3.43 (1H, CH), 3.30–3.05 (1H, CH), 2.99–2.80 (1H, CH), 2.76–2.62 (1H, CH), 2.29–2.06 (1H, CH), 1.86 (s, 3H, CH_3), 1.53–1.31 (m, 4H, $2CH_2$), 0.81 (dt, J = 15.0, 7.2 Hz, 6H, $2CH_3$). ^{13}C NMR (100 MHz, DMSO-d_6); δ 170.81, 167.55, 137.95, 134.90, 131.42, 131.36, 130.95, 130.84, 130.81, 130.09, 128.67, 128.07, 81.45, 75.26, 54.61, 52.39, 47.06, 31.80, 26.11, 25.52, 23.79, 9.89, 9.35. HRMS calcd for $C_{27}H_{34}N_2O_4S$ $[M + H]^+$: 483.2313. Found: m/z 483.2317.

Preparation of Compounds 23a-d.

To a solution of arylbromide (1 equiv.), **22a-d** in DMSO is added the boronic acid (1.1 equiv.), tetrakis (triphenylphosphine) palladium (0.05 equiv.) and potassium carbonate (5 equiv.). The mixture is purged with nitrogen for 10 min. After heating under 120℃ for 12 h, the reaction mixture was cooled to room temperature, and then poured into cold water (120 ml). It was extracted with EtOAc (3 × 30 ml). The organic phase is washed with saturated sodium chloride (50 ml) and water (50 ml), and dried over $MgSO_4$. The solvent is evaporated under vacuo to afford crude product. The crude aldehyde, which is purified by flash chromatography gave the corresponding product, **23a-d**.

4'-(Methylthio)-[1,1'-biphenyl]-4-carbaldehyde (23a). White crystalline solid, 66% yield, mp: 100.1–102.2°C. 1H NMR (400 MHz, DMSO-d6): δ 10.04 (s, 1H, CH), 8.01–7.95 (m, 2H, Ph-H), 7.90 (d, *J* = 8.3 Hz, 2H, Ph-H), 7.76–7.70 (m, 2H, Ph-H), 7.41–7.36 (m, 2H, Ph-H), 2.53 (s, 3H, CH_3). ^{13}C NMR (100 MHz, DMSO-d_6): δ 193.07, 145.65, 139.76, 135.45, 135.38, 130.65, 127.95, 127.34, 126.70, 14.92. ESI-MS: m/z 229.3 $[M + H]^+$, $C_{14}H_{12}OS$ (228.3090).

4'-(Methylthio)-[1,1'-biphenyl]-3-carbaldehyde (23b). White crystalline solid, 69% yield, mp: 53.5–55.5°C. ^1H NMR (400 MHz, Chloroform-*d*): δ 10.08 (s, 1H, CH), 8.07 (t, *J* = 1.6 Hz, 1H, Ph-H), 7.86–7.80 (m, 2H, Ph-H), 7.59 (t, *J* = 7.7 Hz, 1H, Ph-H), 7.57–7.53 (m, 2H, Ph-H), 7.37–7.32 (m, 2H, Ph-H), 2.53 (s, 3H, CH_3). ^{13}C NMR (100 MHz, $CDCl_3$): δ 192.27, 138.79, 136.97, 136.31, 132.67, 129.54, 128.60, 127.72, 127.43, 126.88, 15.71. ESI-MS: m/z 229.3 $[M + H]^+$, $C_{14}H_{12}OS$ (228.3090).

4-(Benzo[b]thiophen-2-yl)benzaldehyde (23c). White crystalline solid, 62% yield, mp: 182.9–188.0°C ^1H NMR (400 MHz, DMSO-d_6): δ 10.05 (s, 1H, CH), 8.08 (s, 1H,

thiophene-H), 8.03–7.99 (m, 5H, Ph-H), 7.92–7.89 (m, 1H, Ph-H), 7.45–7.40 (m, 2H, Ph-H). ^{13}C NMR (100 MHz, DMSO-d_6): δ 192.76, 142.11, 140.73, 139.70, 139.46, 136.09, 130.83, 126.99, 125.87, 125.52, 124.75, 123.05, 122.97. ESI-MS: m/z 239.3 [M + H]$^+$, $C_{15}H_{10}OS$ (238.3040).

4-(Benzo[b]thiophen-3-yl)benzaldehyde (23d). White crystalline solid, 62% yield, mp: 60.1–62.2°C ^{1}H NMR (400 MHz, Methanol-d_4): δ 10.02 (s, 1H, CH), 8.01 (d, J = 1.8 Hz, 1H, Ph-H), 7.99 (d, J = 1.9 Hz, 1H, Ph-H), 7.96–7.91 (m, 1H, Ph-H), 7.91–7.87 (m, 1H, Ph-H), 7.78 (d, J = 1.6 Hz, 1H, Ph-H), 7.76 (d, J = 1.6 Hz, 1H, Ph-H), 7.69 (s, 1H, thiophene-H), 7.43–7.36 (m, 2H, Ph-H). ^{13}C NMR (100 MHz, CD_3OD): δ 192.28, 142.07, 140.87, 137.09, 136.44, 135.53, 129.81, 128.83, 125.28, 124.42, 124.39, 122.67, 122.09, 47.82. ESI-MS: m/z 239.3 [M + H]$^+$, $C_{15}H_{10}OS$ (238.3040).

Preparation of Compounds 24a-d.

The method of preparation was similar to that of **10a-d**, starting from **23a-d**.

Ethyl(3R,4R,5S)-4-acetamido-5-(((4'-(methylthio)-[1,1'-biphenyl]-4-yl)methyl)amino)-3-(pentan-3-yloxy)cyclohex-1-ene-1-carboxylate (24a). White solid, 75% yield, mp: 202.1–204.2°C. 1H NMR (400 MHz, DMSO-d6): δ 7.81 (d, J = 9.1 Hz, 1H, NH), 7.60 (t, J = 8.0 Hz, 4H, Ph-H), 7.36 (dd, J = 16.7, 8.3 Hz, 4H, Ph-H), 6.65 (s, 1H, CH), 4.15 (q, J = 7.0 Hz, 2H, CH_2), 4.02 (d, J = 8.1 Hz, 1H, CH), 3.81 (d, J = 13.7 Hz, 1H, CH), 3.78–3.65 (m, 2H, CH_2), 3.37 (q, J = 5.5 Hz, 1H, CH), 2.81–2.72 (m, 1H, CH), 2.68 (dd, J = 17.5, 4.9 Hz, 1H, CH), 2.51 (s, 3H, CH_3), 2.10 (ddt, J = 17.4, 9.2, 2.5 Hz, 1H, CH), 2.03–1.91 (m, 1H, CH), 1.87 (s, 3H, CH_3), 1.54 – 1.33 (m, 4H, $2CH_2$), 1.22 (t, J = 7.1 Hz, 3H, CH_3), 0.82 (dt, J = 13.4, 7.4 Hz, 6H, $2CH_3$). ^{13}C NMR (100 MHz, DMSO-d_6): δ 170.05, 166.32, 140.76, 138.43, 138.21, 137.65, 137.03, 129.17, 128.91,

127.38, 126.89, 126.53, 81.34, 75.73, 60.80, 54.86, 54.62, 49.88, 30.97, 26.09, 25.67, 23.50, 15.20, 14.56, 9.90, 9.43. ESI-MS: m/z 525.4 $[M + H]^+$, $C_{30}H_{40}N_2O_4S$ (524.7200).

Ethyl(3R,4R,5S)-4-acetamido-5-(((4'-(methylthio)-[1,1'-biphenyl]-3-yl)methyl)amino)-3-(pentan-3-yloxy)cyclohex-1-ene-1-carboxylate (24b). White solid, 70% yield, mp: 126.0–128.7°C. ^{1}H NMR (400 MHz, DMSO-d_6): δ 7.83 (d, J = 9.0 Hz, 1H, NH), 7.67–7.57 (m, 3H, 3H, Ph-H), 7.52 (d, J = 7.6 Hz, 1H, 3H, Ph-H), 7.40 (t, J = 7.6 Hz, 1H, 3H, Ph-H), 7.35 (d, J = 8.5 Hz, 2H, 3H, Ph-H), 7.30 (d, J = 7.5 Hz, 1H, 3H, Ph-H), 6.65 (s, 1H, CH), 4.15 (q, J = 7.1 Hz, 2H, CH_2), 4.06 (d, J = 7.6 Hz, 1H, CH), 3.91 (d, J = 13.1 Hz, 1H, CH), 3.86 – 3.72 (m, 2H, CH_2), 3.34–3.18 (m, 1H, CH), 2.98–2.78 (m, 1H, CH), 2.71 (dd, J = 16.9, 3.7 Hz, 1H, CH), 2.51 (s, 3H, CH_3), 2.27–2.11 (m, 1H, CH), 1.86 (s, 3H, CH_3), 1.52–1.33 (m, 4H, $2CH_2$), 1.22 (t, J = 7.1 Hz, 3H, CH_3), 0.82 (dt, J = 13.4, 7.4 Hz, 6H, $2CH_3$). ^{13}C NMR (100 MHz, DMSO-d_6): δ 170.23, 166.21, 151.52, 139.86, 138.43, 138.05, 137.95, 137.12, 129.29, 128.92, 127.53, 126.79, 126.60, 125.33, 81.38, 75.56, 60.86, 54.94, 54.17, 49.76, 30.31, 26.08, 25.65, 23.56, 15.13, 14.56, 9.89, 9.43. ESI-MS: m/z 525.5 $[M + H]^+$, $C_{30}H_{40}N_2O_4S$ (524.7200).

Ethyl(3R,4R,5S)-4-acetamido-5-((4-(benzo[b]thiophen-2-yl)benzyl)amino)-3-(pentan-3-yloxy)cyclohex-1-ene-1-carboxylate (24c). White solid, 77% yield, mp: 211.1–213.1°C. 1H NMR (400 MHz, Chloroform-d): δ 7.81 (d, J = 7.8 Hz, 1H, Ph-H), 7.75 (d, J = 7.2 Hz, 1H, Ph-H), 7.66 (d, J = 8.2 Hz, 2H, Ph-H), 7.52 (s, 1H, thiophene-H), 7.39 (d, J = 8.1 Hz, 2H, Ph-H), 7.36–7.28 (m, 2H, Ph-H), 6.80 (s, 1H, CH), 5.85–5.50 (m, 1H, NH), 4.27–4.12 (overlapped, 3H, CH, CH_2), 3.96 (d, J = 13.4 Hz, 1H, CH), 3.88–3.74 (m, 2H, CH_2), 3.36 (p, J = 5.7 Hz, 1H, CH), 3.18 (td, J = 9.0, 5.5 Hz, 1H, CH), 2.80 (dd, J = 17.7, 5.1 Hz, 1H, CH), 2.32 (dd, J = 17.7, 8.6 Hz, 1H, CH), 2.02 (s, 3H, CH_3), 1.59–1.43 (m,

4H, $2CH_2$), 1.30 (t, J = 7.1 Hz, 3H, CH_3), 0.89 (t, J = 7.4 Hz, 6H, $2CH_3$). ^{13}C NMR (100 MHz, $CDCl_3$): δ 170.78, 166.42, 143.99, 140.70, 139.41, 137.22, 133.19, 129.22, 128.84, 126.66, 126.52, 124.51, 124.29, 123.52, 122.24, 119.30, 81.84, 77.24, 74.63, 60.91, 55.46, 53.63, 30.14, 26.15, 25.77, 23.73, 14.23, 9.50, 9.40. ESI-MS: m/z 535.4 $[M + H]^+$, $C_{28}H_{38}N_2O_4S$ (534.7150).

Ethyl(3R,4R,5S)-4-acetamido-5-((4-(benzo[b]thiophen-3-yl)benzyl)amino)-3-(pentan-3-yloxy)cyclohex-1-ene-1-carboxylate (24d). White solid, 72% yield, mp: 61.1–65.2°C. ^{1}H NMR (400 MHz, Methanol-d_4): δ 7.96–7.89 (m, 1H, Ph-H), 7.89–7.83 (m, 1H, Ph-H), 7.56 (d, J = 8.2 Hz, 2H, Ph-H), 7.52 (s, 1H, thiophene-H), 7.47 (d, J = 8.1 Hz, 2H, Ph-H), 7.41–7.34 (m, 2H, Ph-H), 6.79 (s, 1H, CH), 4.21 (q, J = 7.1 Hz, 2H, CH_2), 4.12–4.06 (m, 1H, CH), 4.03–3.93 (overlapped, 2H, 2CH), 3.84 (d, J = 13.1 Hz, 1H, CH), 3.38 (p, J = 5.6 Hz, 1H, CH), 3.02 (td, J = 9.9, 5.4 Hz, 1H, CH), 2.89 (dd, J = 17.6, 5.3 Hz, 1H, CH), 2.31 (ddt, J = 17.6, 9.6, 2.9 Hz, 1H, CH), 2.02 (s, 3H, CH_3), 1.58–1.44 (m, 4H, $2CH_2$), 1.29 (t, J = 7.1 Hz, 3H, CH_3), 0.90 (q, J = 7.5 Hz, 6H, $2CH_3$). ^{13}C NMR (100 MHz, CD_3OD): δ 172.67, 166.32, 140.79, 137.90, 137.64, 137.42, 135.18, 128.68, 128.66, 128.49, 124.14, 124.03, 123.28, 122.55, 122.26, 82.07, 75.50, 60.70, 54.26, 54.20, 49.12, 29.33, 25.78, 25.32, 21.81, 13.12, 8.52, 8.19. ESI-MS: m/z 535.3 $[M + H]^+$, $C_{28}H_{38}N_2O_4S$ (534.7150).

Preparation of Compounds 25a-d.

The method of preparation was similar to that of **11a-d**, starting from **24a-d**.

(3R,4R,5S)-4-Acetamido-5-(((4'-(methylthio)-[1,1'-biphenyl]-4-yl)methyl)amino)-3-(pentan-3-yloxy)cyclohex-1-ene-1-carboxylic acid (25a). White solid, 73% yield, mp: 172.7–180.0°C, melt and decompose at the same time. ^{1}H NMR (400 MHz,

Methanol-d_4) δ 7.73 (d, J = 7.7 Hz, 2H, Ph-H), 7.59 (t, J = 8.3 Hz, 4H, Ph-H), 7.36 (d, J = 8.0 Hz, 2H, Ph-H), 6.88 (s, 1H, CH), 4.45 (d, J = 13.0 Hz, 1H, CH), 4.37–4.15 (overlapped, 3H, CH, CH_2), 3.64 (s, 1H, CH), 3.53–3.41 (m, 1H, CH), 3.16 – 3.02 (m, 1H, CH), 2.77–2.62 (m, 1H, CH), 2.53 (s, 3H, CH_3), 2.09 (s, 3H, CH_3), 1.66–1.47 (m, 4H, $2CH_2$), 0.93 (q, J = 7.4 Hz, 6H, $2CH_3$). ^{13}C NMR (100 MHz, MeOD): δ 141.70, 138.86, 136.33, 130.12, 129.60, 127.01, 126.93, 126.41, 82.30, 74.57, 54.90, 51.64, 50.02, 26.08, 25.73, 25.23, 22.02, 14.11, 8.42, 8.17. HRMS calcd for $C_{28}H_{36}N_2O_4S$ [M + H]$^+$: 467.2469. Found: m/z 497.2563.

(3R,4R,5S)-4-Acetamido-5-(((4'-(methylthio)-[1,1'-biphenyl]-3-yl)methyl)amino)-3-(pentan-3-yloxy)cyclohex-1-ene-1-carboxylic acid (25b). White solid, 73% yield, mp: 195.9–202.0°C, melt and decompose at the same time. ^{1}H NMR (400 MHz, DMSO-d_6): δ 8.16 (d, J = 8.6 Hz, 1H, NH), 7.93 (s, 1H, Ph-H), 7.69 (d, J = 8.3 Hz, 3H, Ph-H), 7.49 (d, J = 4.5 Hz, 2H, Ph-H), 7.37 (d, J = 8.3 Hz, 2H, Ph-H), 6.66 (s, 1H, CH), 4.38–4.14 (overlapped, 3H, CH, CH_3), 4.05 (q, J = 8.8 Hz, 1H, CH), 3.59–3.45 (m, 1H, CH), 3.37–3.24 (m, 1H, CH), 2.97 (dd, J = 16.2, 2.9 Hz, 1H, CH), 2.71 (dt, J = 15.3, 7.1 Hz, 1H, CH), 2.52 (s, 3H, CH_3), 1.93 (s, 3H, CH_3), 1.54–1.34 (m, 4H, $2CH_2$), 0.83 (dt, J = 16.8, 7.3 Hz, 6H, $2CH_3$). ^{13}C NMR (100 MHz, DMSO): δ 171.23, 167.26, 138.39, 138.00, 136.53, 133.26, 129.66, 129.42, 128.77, 128.18, 127.00, 126.84, 81.59, 74.98, 54.54, 51.18, 46.13, 26.06, 25.53, 23.98, 15.13, 9.84, 9.33. HRMS calcd for $C_{28}H_{36}N_2O_4S$ [M + H]$^+$: 497.2469. Found: m/z 497.2464.

(3R,4R,5S)-4-Acetamido-5-((4-(benzo[b]thiophen-2-yl)benzyl)amino)-3-(pentan-3-yloxy)cyclohex-1-ene-1-carboxylic acid (25c). White solid, 73% yield, mp: 166.7–172.0°C, melt and decompose at the same time. ^{1}H NMR (400 MHz, DMSO-d_6): δ 8.21

(d, J = 1.5 Hz, 1H, NH), 8.16 (d, J = 8.9 Hz, 1H, Ph-H), 8.10 (d, J = 8.4 Hz, 1H, Ph-H), 7.86–7.79 (m, 2H, Ph-H), 7.78 (s, 1H, thiophene-H), 7.70 (dd, J = 8.5, 1.6 Hz, 1H, Ph-H), 7.65 (d, J = 8.1 Hz, 2H, Ph-H), 7.53 (d, J = 5.4 Hz, 1H, Ph-H), 6.66 (s, 1H, CH), 4.32–4.12 (overlapped, 3H, CH, CH_2), 4.03 (q, J = 9.0 Hz, 1H, CH), 3.39–3.14 (overlapped, 2H, 2CH), 2.94 (dd, J = 17.2, 4.7 Hz, 1H, CH), 2.72–2.59 (m, 1H, CH), 1.95 (s, 3H, CH_3), 1.52–1.37 (m, 4H, $2CH_2$), 0.83 (dt, J = 15.2, 7.4 Hz, 6H, $2CH_3$). ^{13}C NMR (100 MHz, DMSO-d_6): δ 171.10, 167.33, 140.92, 140.67, 139.01, 138.02, 136.44, 131.01, 128.74, 128.34, 127.42, 124.71, 123.73, 123.55, 122.05, 81.57, 75.13, 54.51, 51.57, 46.27, 26.71, 26.07, 25.54, 23.93, 9.84, 9.33. HRMS calcd for $C_{29}H_{34}N_2O_4S$ $[M + H]^+$: 507.2312. Found: m/z 507.2307.

(3R,4R,5S)-4-Acetamido-5-((4-(benzo[b]thiophen-3-yl)benzyl)amino)-3-(pentan-3-yloxy)cyclohex-1-ene-1-carboxylic acid (25d). White solid, 73% yield, mp: 165.2–162.7°C. ^{1}H NMR (400 MHz, Methanol-d_4): δ 7.98–7.90 (m, 1H, Ph-H), 7.90–7.82 (m, 1H, Ph-H), 7.68 (d, J = 8.2 Hz, 2H, Ph-H), 7.65–7.57 (overlapped,, 3H, Ph-H, thiophene-H), 7.43–7.35 (m, 2H, Ph-H), 6.84 (s, 1H, CH), 4.44 (d, J = 13.1 Hz, 1H, CH), 4.30 (d, J = 13.1 Hz, 1H, CH), 4.27–4.15 (overlapped, 2H, 2CH), 3.61 (td, J = 9.6, 5.2 Hz, 1H, CH), 3.45 (p, J = 5.6 Hz, 1H, CH), 3.15–2.98 (m, 1H, CH), 2.75–2.58 (m, 1H, CH), 2.07 (s, 3H, CH_3), 1.60–1.46 (m, 4H, $2CH_2$), 0.90 (q, J = 7.3 Hz, 6H, $2CH_3$). ^{13}C NMR (100 MHz, CD_3OD): δ 178.50, 173.46, 140.83, 137.38, 137.21, 136.70, 136.27, 130.55, 129.98, 129.03, 129.03, 124.30, 124.20, 124.13, 122.65, 122.05, 82.26, 74.67, 54.95, 51.84, 48.25, 26.40, 25.75, 25.23, 22.01, 8.43, 8.17. HRMS calcd for $C_{29}H_{34}N_2O_4S$ $[M + H]^+$: 507.2312. Found: m/z 507.2312.

Preparation of Compound 26.

The method of preparation was similar to that of **23a-d**, starting from **8** and 5-bromobenzo[b]thiophene.

4-(Benzo[b]thiophen-5-yl)benzaldehyde (26). White solid, 63% yield. mp: 150.0–152.0°C. 1H NMR (400 MHz, Chloroform-d): δ 10.07 (s, 1H, CH), 8.08 (d, J = 1.5 Hz, 1H, Ph-H), 7.97 (d, *J* = 8.4 Hz, 3H, Ph-H), 7.82 (d, *J* = 8.2 Hz, 2H, Ph-H), 7.62 (dd, *J* = 8.4, 1.7 Hz, 1H, thiophene-H), 7.52 (d, *J* = 5.4 Hz, 1H, thiophene-H), 7.41 (d, *J* = 5.4 Hz, 1H, Ph-H). ^{13}C NMR (100 MHz, $CDCl_3$): δ 191.91, 147.39, 140.26, 139.94, 136.13, 135.10, 130.34, 127.90, 127.59, 124.09, 123.67, 123.05, 122.39. ESI-MS: m/z 239.3 $[M + H]^+$, $C_{15}H_{10}OS$ (238.3040).

Preparation of Compound 27.

The method of preparation was similar to that of **10a-d**, starting from **26**.

Ethyl(3R,4R,5S)-4-acetamido-5-((4-(benzo[b]thiophen-5-yl)benzyl)amino)-3-(pentan-3-yloxy)cyclohex-1-ene-1-carboxylate (27). White solid, 74% yield. mp: 185.0–186.5°C. ^{1}H NMR (400 MHz, Chloroform-*d*): δ 8.01 (d, *J* = 1.4 Hz, 1H, Ph-H), 7.92 (d, *J* = 8.4 Hz, 1H, Ph-H), 7.61 (d, *J* = 8.2 Hz, 2H, Ph-H), 7.58 (dd, *J* = 8.4, 1.7 Hz, 1H, Ph-H), 7.47 (d, *J* = 5.4 Hz, 1H, Ph-H), 7.40 (overlapped, 6.8 Hz, 3H, Ph-H, thiophene-H), 6.81 (s, 1H, CH), 4.22 (overlapped, 3H, CH, CH_2), 3.96 (d, *J* = 13.2 Hz, 1H), 3.84–3.72 (m, 2H), 3.41–3.33 (m, 1H), 3.26 – 3.13 (m, 1H), 2.81 (dd, *J* = 17.8, 5.2 Hz, 1H, CH), 2.37–2.23 (m, 1H, CH), 2.02 (s, 3H, CH_3), 1.59–1.44 (m, 4H, $2CH_2$), 1.30 (t, *J* = 7.1 Hz, 3H, CH_3), 0.90 (t, *J* = 7.4 Hz, 6H, $2CH_3$). ^{13}C NMR (100 MHz, $CDCl_3$): δ 170.62, 166.54, 140.21, 140.03, 139.34, 138.70, 137.42, 137.17, 129.42, 128.62, 127.40, 127.03, 124.07, 123.81, 122.70, 121.85, 81.77, 74.54, 60.88, 55.86, 53.63, 50.31, 30.47, 26.18, 25.80, 23.77, 14.25, 9.53, 9.44. ESI-MS: m/z 535.3 $[M + H]^+$, $C_{31}H_{38}N_2O_4S$ (534.7150).

Preparation of Compound 28.

The method of preparation was similar to that of **11a-d**, starting from **27.**

(3R,4R,5S)-4-Acetamido-5-((4-(benzo[b]thiophen-5-yl)benzyl)amino)-3-(pentan-3-yloxy)cyclohex-1-ene-1-carboxylic acid (28). White solid, 67% yield, mp: 200.2–204.5°C. 1H NMR (400 MHz, Methanol-d4): δ 7.89–7.77 (m, 4H, Ph-H), 7.73 (s, 1H, Ph-H), 7.56 (d, *J* = 8.1 Hz, 2H, Ph-H), 7.39–7.29 (m, 2H, thiophene-H), 6.81 (s, 1H, CH), 4.40 (d, *J* = 13.1 Hz, 1H, CH), 4.25 (d, *J* = 12.6 Hz, 2H, CH_2), 4.21–4.13 (m, 1H, CH), 3.59 (s, 1H, CH), 3.44 (p, *J* = 5.4 Hz, 1H, CH), 3.13–2.95 (m, 1H, CH), 2.71–2.54 (m, 1H, CH), 2.07 (s, 3H, CH_3), 1.62–1.42 (m, 4H, $2CH_2$), 0.90 (q, *J* = 7.3 Hz, 6H, $2CH_3$). ^{13}C NMR (100 MHz, CD_3OD): δ 142.52, 140.72, 139.47, 135.37, 131.21, 130.23, 126.56, 124.53, 124.44, 123.54, 121.83, 120.30, 82.26, 74.80, 55.10, 51.94, 26.57, 25.76, 25.25, 22.04, 8.43, 8.18. HRMS calcd for $C_{29}H_{34}N_2O_4S$ $[M + H]^+$: 507.2312. Found: m/z 507.2309.

Preparation of Compounds 30a-b.

The reaction of phenyl(p-tolyl)methanone or 1-methyl-4-(phenylsulfonyl)benzene (30 mmol, 1 equiv.) and N-bromosucinimide (NBS) (2.66 g, 15 mmol) was carried out in the presence of benzoic peroxide (BPO) (0.36 g, 1.5 mmol) in carbon tetrachloride (50 mL) under the reflux condition for 6 h. After that, the resulting mixture was washed with $FeSO_4$ aqueous solution (0.1 mol/L) and water twice, respectively. The organic phase was dried over anhydrous $MgSO_4$ and concentrated under reduced pressure. The residue was purified by the recrystalization from isopropyl ether to afford the corresponding substituted benzyl bromides **30a-b**.

(4-(Bromomethyl)phenyl)(phenyl)methanone (30a). White solid, 81% yield, mp:

85.7–87.9°C. ^{1}H NMR (400 MHz, Chloroform-*d*) δ 7.79 (dd, *J* = 7.5, 4.7 Hz, 4H, Ph-H), 7.70–7.46 (m, 5H, Ph-H), 4.54 (s, 2H, CH_2). ^{13}C NMR (100 MHz, $CDCl_3$): δ 196.02, 142.11, 137.36, 132.61, 130.58, 130.04, 128.97, 128.37, 126.57, 32.33. ESI-MS: m/z 275.2 and 277.2 $[M + H]^+$, $C_{14}H_{10}O_2$ (275.1450).

1-(Bromomethyl)-4-(phenylsulfonyl)benzene (30b). White solid, 84% yield, mp: 111.0–113.8°C. ^{1}H NMR (400 MHz, Chloroform-*d*): δ 7.98–7.90 (m, 4H, Ph-H), 7.71–7.48 (m, 5H, Ph-H), 4.46 (s, 2H, CH_2). ^{13}C NMR (100 MHz, $CDCl_3$): δ 143.14, 141.46, 141.27, 133.39, 129.89, 129.39, 128.21, 127.73, 31.41. ESI-MS: m/z 311.3 and 313.3 $[M + H]^+$, $C_{13}H_{10}O_3S$ (311.1930).

Preparation of Compounds 31a-b.

A mixture of **30a** or **30b** (2.2 mmol) and oseltamivir phosphate (0.82 g, 2.0 mmol) in the presence of potassium carbonate (2 g, 14.5 mmol) in acetonitrile (30 mL), at 60-70 °C for 8 h. After completion of the reaction, the solvent was evaporated under reduced pressure, and then water (30 mL) was added. This mixture was extracted with ethyl acetate and tetrahydrofuran (V:V = 2:1, 3 × 30 mL), and the organic phase was washed with saturated sodium chloride (2 × 30 mL), dried over anhydrous $MgSO_4$, and concentrated under reduced pressure to give the crude product, which was purified by flash column chromatography to afford the corresponding intermediates, **31a-b**.

Ethyl(3R,4R,5S)-4-acetamido-5-((4-benzoylbenzyl)amino)-3-(pentan-3-yloxy)cyclohex-1-ene-1-carboxylate (31a). White solid, 63% yield, mp: 92.5–95.1°C. ^{1}H NMR (400 MHz, Chloroform-*d*): δ 7.83–7.71 (m, 4H, Ph-H), 7.59 (tt, *J* = 6.8, 1.3 Hz, 1H, Ph-H), 7.52–7.41 (m, 4H, Ph-H), 6.81 (s, 1H, CH), 5.59 (d, *J* = 6.7 Hz, 1H, NH), 4.27–4.15 (overlapped, 3H, CH_2, NH), 3.99 (d, *J* = 13.8 Hz, 1H, CH), 3.86 (d, *J* = 10.3 Hz, 1H,

CH), 3.84–3.76 (m, 1H, CH), 3.38 (p, *J* = 5.7 Hz, 1H, CH), 3.15 (td, *J* = 8.7, 5.4 Hz, 1H, CH), 2.77 (dd, *J* = 17.8, 5.2 Hz, 1H, CH), 2.31 (ddt, *J* = 17.9, 8.3, 2.5 Hz, 1H, CH), 2.12–2.04 (m, 1H, CH), 2.02 (s, 3H, CH_3), 1.58–1.45 (m, 4H, $2CH_2$), 1.30 (t, *J* = 7.1 Hz, 3H, CH_3), 0.90 (t, *J* = 7.4 Hz, 6H, $2CH_3$). ^{13}C NMR (100 MHz, $CDCl_3$): δ 196.51, 170.70, 166.47, 145.31, 137.72, 137.05, 136.34, 132.34, 130.32, 129.99, 129.34, 128.26, 127.89, 81.80, 77.24, 74.50, 60.92, 55.43, 53.80, 50.30, 30.28, 26.15, 25.79, 23.70, 14.24, 9.50, 9.42. ESI-MS: m/z 507.4 $[M + H]^+$, $C_{30}H_{38}N_2O_5$ (506.6430).

Ethyl(3R,4R,5S)-4-acetamido-3-(pentan-3-yloxy)-5-((4-(phenylsulfonyl)benzyl)amino)cyclohex-1-ene-1-carboxylate (31b). White solid, 71% yield, mp: 101.7–103.5°C. 1H NMR (400 MHz, Chloroform-d): δ 7.93 (dd, J = 7.1, 1.5 Hz, 2H, Ph-H), 7.86 (d, *J* = 8.4 Hz, 2H, Ph-H), 7.59–7.53 (m, 1H, Ph-H), 7.53–7.41 (m, 4H, Ph-H), 6.79 (s, 1H, CH), 5.54 (d, *J* = 8.2 Hz, 1H, NH), 4.20 (q, *J* = 7.1 Hz, 2H, CH_2), 4.16–4.09 (m, 1H, CH), 3.92 (d, *J* = 14.2 Hz, 1H, CH), 3.87–3.74 (m, 2H, 2CH), 3.36 (p, *J* = 5.6 Hz, 1H, CH), 3.06 (td, *J* = 8.5, 5.3 Hz, 1H, CH), 2.70 (dd, *J* = 17.8, 5.2 Hz, 1H, CH), 2.26 (ddt, *J* = 17.9, 8.2, 2.5 Hz, 1H, CH), 1.99 (s, 3H, CH_3), 1.88 (s, 1H, CH), 1.55–1.43 (m, 4H, $2CH_2$), 1.29 (t, *J* = 7.1 Hz, 3H, CH_3), 0.88 (t, *J* = 7.4 Hz, 6H, $2CH_3$). ^{13}C NMR (100 MHz, $CDCl_3$): δ 170.66, 166.42, 146.70, 141.73, 139.95, 136.93, 133.11, 129.30, 129.26, 128.75, 127.77, 127.57, 81.80, 74.49, 60.92, 55.14, 53.94, 50.00, 30.21, 26.13, 25.79, 23.65, 14.22, 9.47, 9.41. ESI-MS: m/z 543.4 $[M + H]^+$, $C_{29}H_{38}N_2O_6S$ (542.6910).

Preparation of Compounds 32a-b.

The method of preparation was similar to that of **11a-d**, starting from **31a-b.**

(3R,4R,5S)-4-Acetamido-5-((4-benzoylbenzyl)amino)-3-(pentan-3-yloxy)cyclohex-1-ene-1-carboxylic acid (32a). White solid, 74% yield, mp: 210–218.4°C, melt and

decompose at the same time. ^{1}H NMR (400 MHz, DMSO-d_6): δ 7.89 (d, J = 8.9 Hz, 1H, NH), 7.79–7.64 (m, 5H, Ph-H), 7.61–7.49 (m, 4H, Ph-H), 6.63 (s, 1H, CH), 4.06 (d, J = 7.2 Hz, 1H, CH), 4.02–3.84 (m, 2H, CH_2), 3.79 (q, J = 9.1 Hz, 1H, CH), 2.98–2.80 (m, 1H, CH), 2.76–2.65 (m, 1H, CH), 2.27–2.07 (m, 1H, CH), 1.88 (s, 3H, CH_3), 1.51–1.34 (m, 4H, $2CH_2$), 0.82 (dt, J = 14.5, 7.3 Hz, 6H, $2CH_3$). ^{13}C NMR (100 MHz, DMSO-d_6): δ 195.95, 170.34, 167.88, 137.93, 137.67, 136.18, 133.03, 130.18, 129.97, 129.45, 129.01, 128.74, 81.36, 75.70, 54.98, 54.07, 49.08, 30.12, 26.10, 25.62, 23.60, 9.91, 9.40. HRMS calcd for $C_{28}H_{34}N_2O_5$ $[M + H]^+$: 479.254. Found: m/z 479.2540.

(3R,4R,5S)-4-Acetamido-3-(pentan-3-yloxy)-5-((4-(phenylsulfonyl)benzyl)amino)cyclohex-1-ene-1-carboxylic acid (32b). White solid, 72% yield, mp: 162.1–164.3°C. ^{1}H NMR (400 MHz, Methanol-d_4): δ 8.01 (d, J = 8.4 Hz, 2H, Ph-H), 7.96 (dd, J = 7.2, 1.5 Hz, 2H, Ph-H), 7.66 (d, J = 8.4 Hz, 2H, Ph-H), 7.65–7.60 (m, 1H, Ph-H), 7.60–7.53 (m, 2H, Ph-H), 6.81 (s, 1H, NH), 4.35 (d, J = 13.5 Hz, 1H, CH), 4.25–4.15 (m, 2H, 2CH), 4.10 (dd, J = 10.8, 8.2 Hz, 1H, CH), 3.44 (dp, J = 16.9, 5.6 Hz, 2H, CH_2), 2.97 (dd, J = 17.4, 5.3 Hz, 1H, CH), 2.53 (ddt, J = 17.1, 9.8, 2.4 Hz, 1H, CH), 2.00 (s, 3H, CH_3), 1.51 (th, J = 13.8, 6.6 Hz, 4H, $2CH_2$), 0.88 (q, J = 7.5 Hz, 6H, $2CH_3$). ^{13}C NMR (100 MHz, CD_3OD): δ 173.33, 167.80, 142.15, 141.28, 139.03, 136.76, 133.41, 130.27, 129.29, 128.15, 127.95, 127.39, 82.23, 74.82, 55.30, 52.34, 47.22, 26.88, 25.75, 25.25, 21.93, 8.42, 8.17. HRMS calcd for $C_{27}H_{34}N_2O_6S$ $[M + H]^+$: 515.221. Found: m/z 515.2214.

Biological Assays

Cells and Viruses

Chicken embryo fibroblasts (CEFs) were provided by Institute of Poultry Science, Shandong Academy of Agricultural Sciences, and maintained in Dulbecco's modified

Eagle's medium (DMEM, Thermo Fisher Scientific) supplemented with 5% (vol/vol) fetal bovine serum (FBS, Thermo Fisher Scientific) at 37°C in a humidified atmosphere supplemented with 5% CO_2. Madin-Darby Canine Kidney (MDCK) cells were grown in Dulbecco's modified Eagle's medium (DMEM, Life Biotechnologies) supplemented with 10% (vol/vol) fetal bovine serum (FBS, Life Biotechnologies) and antibiotics (100 U/mL penicillin and 100 μg/mL streptomycin, Life Technologies). Cells were maintained at 37°C in a humidified atmosphere supplemented with 5% CO_2.

The diluted suspensions of avian influenza viruses [A/goose/Guangdong/SH7/2013 (H5N1), A/Chicken/Hebei/LZF/2014 (H5N2), A/duck/Guangdong/674/2014 (H5N6), and A/goose/Jiangsu/1306/2014 (H5N8)] were harvested from the allantoic fluid of avian influenza viruses-infected embryonated chicken eggs (Institute of Poultry Science, Shandong Academy of Agricultural Sciences). Influenza A/PR/8/34 (PR8) (H1N1, Cambridge lineage) was obtained from P. Digard (Roslin Institute, University of Edinburgh, United Kingdom). The H3N2 virus A/Wisconsin/67/05 (WSN) was provided by R. Cusinato (Clinical Microbiology and Virology Unit, Padua University Hospital, Padua, Italy). The influenza B/Lee/40 virus was obtained from W. S. Barclay (Imperial College, London, United Kingdom).

Determination of EC_{50} and CC_{50} of NA Inhibitors in CEFs

The anti-influenza activity and cytotoxicity of the newly synthesized compounds were evaluated as described by Shie *et al*.[45] with minor modifications. Results were expressed as EC_{50} values, which are the concentrations affording 50% protection against H5N1, H5N2, H5N6, and H5N8 virus infection-mediated CPE. Aliquots of 50 μL of diluted H5N1, H5N2, H5N6, and H5N8 at 50 $TCID_{50}$ were mixed with equal volumes of

solutions of the newly synthesized compounds in serial two-fold dilutions in assay media (DMEM). The mixtures were used to infect 100 μL of CEF at 1×10^5 cells/mL in 96-well plates. The plates were incubated for 48 h at 37°C under 5.0% CO_2 in air, then 100 μL per well of Cell Counting Kit-8 (CCK-8) reagent solution (10 μL CCK-8 and 90 μL media) was added. After incubation at 37°C for 90 min, the absorbance at 450 nm was read on a microplate reader. Inhibitor EC_{50} values were determined by fitting the curve of percent CPE *versus* NA inhibitor concentration. OSC, ZA and ribavirin were used as control drugs at the same time. The CC_{50} value was employed as a measure of the cytotoxicity of newly synthesized compounds to CEF and was determined in the same manner as EC_{50}, but without virus infection.

Plaque Reduction Assay (PRA) in MDCK Cells

The antiviral activities of selected compounds against the influenza A PR8 and WSN viruses and against influenza B/Lee/40 virus were tested by PRA as previously described,[46,47,48] with some modifications. MDCK cells were seeded at a density of 7×10^5 cells per well in 12-well plates. The next day, the culture medium was removed and the monolayers were first washed with serum-free DMEM, and then infected with influenza A virus (PR8 or WSN strain) or influenza B virus (Lee strain) at 30-40 PFU/well in DMEM supplemented with 0.14% BSA and 2 μg/mL TPCK-treated trypsin (Worthington Biochemical Corporation) for 1 h at 37°C. Cells were then incubated with medium containing 1.2% (wt/vol) Avicel cellulose, 0.14% BSA, 2 μg/mL TPCK-treated trypsin, and different concentrations of each test compound. After 2 days of incubation for influenza A viruses[46,47] or 3 days of incubation for influenza B virus,[48] cell monolayers were fixed with 4% (vol/vol) formaldehyde and stained with 0.1% toluidine

blue, and viral plaques were counted. OSC and ZA were included in each experiment as reference compounds. Values obtained from the wells treated with only DMSO were set as 100% of plaque formation.

Citotoxicity Assay in MDCK Cells

Cytotoxicity of selected compounds was assessed in MDCK cells by the 3-(4,5-dimethylthiazol-2-yl)-2,5-diphenyltetrazolium bromide (MTT) method, as previously described.[49,50] MDCK cells (seeded at a density of 2×10^4 cells per well) were grown in 96-well plates for 24 hours and then treated with serial dilutions of test compounds, or DMSO as a control, in DMEM supplemented with 10% FBS. After incubation at 37°C for 48 hours, 5 mg/ml of MTT (Sigma) in PBS was added into each well and incubated at 37°C for further 4 hours. Successively, a solubilizing solution (10% SDS, 0.01 N HCl) was added to dissolve the formazan salt and lyse the cells, and incubated O/N at 37°C. Finally, absorbance was read at the wavelength of 620 nm using an ELISA microplate reader (Tecan Sunrise). Values obtained from the wells treated with only DMSO were set as 100% of viable cells.

Influenza Virus NA-Inhibitory Assay

Neuraminidase activity was measured using either a fluorogenic or a luminogenic substrate according to the standard method.[51] N1-H24Y (A/Anhui/1/2005 (H5N1-H274Y mutation) and 09N1 (A/California/04/2009) were obtained from Sino Biological Inc. Diluted suspensions of influenza viruses (H5N1, H5N2, H5N6, and H5N8) were harvested from the allantoic fluid of influenza virus-infected embryonated chicken eggs. The fluorogenic substrate 2′-(4-methylumbelliferyl)-α-D-acetylneuraminic acid sodium salt hydrate (MUNANA; Sigma) was cleaved by NA to afford a quantifiable fluorescent

product. Test compounds were dissolved in DMSO, and then diluted to the required concentrations in MES buffer (3.54 g 2-(N-morpholino)ethanesulfonic acid and 0.185 g $CaCl_2$ in 400 mL Milli-Q water). To a 96-well fluorescent plate, 10 μL of the diluted virus supernatant or NA assay diluent, 70 μL of MES buffer, and 10 μL of test compound at different concentrations were added successively, and the plate was incubated for 10 min at 37°C. The reaction was started by the addition of 10 μL of fluorogenic substrate. After incubation for 40-60 min, the reaction was terminated by adding 150 μL of termination solution (6.01 g glycine and 3.20 g NaOH in 400 mL Milli-Q water). The fluorescence of the released 4-methylumbelliferone was measured with an Envision plate reader (Perkin-Elmer, Wellesley, MA) using excitation and emission wavelengths of 365 and 460 nm, respectively. Substrate blanks were subtracted from the sample readings. The inhibitor IC_{50} values were determined from the dose-response curves by plotting the percent inhibition of NA activity *versus* inhibitor concentration.

Computational Modeling

Preparation of Ligand and Neuraminidases Structures

The initial structures for molecular docking were prepared as we previously described.[52] To understand the binding modes of **21h** and OSC in the 150-cavity of the N1, N8, 09N1 and N1-H247Y (PDB ID: 3CL0)[53] structures, the X-ray crystal structures were preprocessed, including modeling of the closed-form of the 150-cavity and open-form for N8, 09N1 and N1-H247Y NAs, as previously described.[45] All modeled NA structures were energy-minimized using the FF99SB force field as implemented in Amber12.[54] The energy-minimized structures for all three subtypes and the crystal structure of subtype N1 were used as targets for subsequent molecular docking studies.

Generation of Ligand Binding Conformation

The ligands **21h** and OSC were geometry-optimized using Gaussian09[55] software at the B3LYP/6-31G* level of theory, and molecular docking was carried out using Autodock 4 software.[56] The center of mass of OSC in the N1 subtype was used as the grid center for all the docking studies (the number of grid points was set as 70, 70, 70 with a default grid size of 0.375 Å). The Lamarckian genetic algorithm was employed to find the most stable binding pose. The top 50 low-energy docking poses were stored for further manual inspection and the best protein-ligand complexes for all four NA subtypes were considered for the MD-based free energy calculations.

Molecular Dynamics Simulations

Molecular dynamics (MD) simulations for all four subtypes of neuraminidases (N1, N8, 09N1 and N1-H247Y) complex with OSC and **21h** were carried using Amber12 software.[54] Initially, the charges for the ligands were generated using the CHELPG protocol[57] as implemented in Gaussian09 software[55] by employing the B3LYP/6-31G* level of theory.

All MD simulations were performed and analyzed using Amber12 software.[53] The general Amber force field was used to describe the dispersion interactions.[58] For protein structures and water, the FF99SB force-field and TIP3P force-field were adopted, respectively. The protein-ligand complex was solvated (~20000 water molecules) and a sufficient number of counter ions was added to neutralize the overall system. The simulation involves a minimization run followed by constant-temperature and constant-pressure simulation at finite temperature and 1 atm pressure. The temperature was maintained by connecting the system to a Langevin thermostat[59] while the pressure

was maintained using a Berendsen barostat[60] with a collision frequency of 1ps^{-1}. The time scale for the equilibration run was 5 ns. The total time scale for the production run was approximately 15 ns. The convergence was checked using various properties, e.g. density and energies, to make sure that the time scale for the production run was sufficient. We also carried out various analysis such as root-mean-square displacement (RMSD) and root-mean-square fluctuation (RMSF) for all the residues using only the trajectory corresponding to the last 5 ns. Finally, 2000 configurations were saved at equal intervals from the trajectory for the subsequent free energy calculations.

MM-GBSA Calculations

Molecular docking serves as a quick approach for estimating the binding affinity of protein-ligand complexes. However, it does not account for protein flexibility in the ligand binding, and thus the MM-GBSA approach[61] was used to estimate binding free energy from the MD simulations. The theory and methodology have been described in detail elsewhere.[61-65] The binding free energies (ΔG_{bind}) for all protein−ligand complexes were calculated using the MMPBSA.py script[66] in Amber12.

Pharmacokinetics Assays.

Oral bioavailability of **20h** and **21h** was examined in male Sprague-Dawley rats, which were randomly divided into three groups to receive intravenous (**21h,** 2 mg·kg^{-1}) or oral administration (**20h**, 20 mg·kg^{-1} or **21h**, 20 mg·kg^{-1}). The animals were kept in an air-conditioned rat room, and used to determine the kinetic profiles. Solutions of **20h** and **21h** were prepared in a mixture of polyethylene glycol (PEG) 400/normal saline (70/30, V/V) before the experiment. Blood samples (200 μL each time) from the intravenous or oral administration group were collected from the sinus jugularis into heparinized

centrifugation tubes at 5 min, 15 min, 30 min, 1 h, 2 h, 4 h, 6 h, 8 h, and 24 h after dosing. Plasma samples were obtained by centrifugation at 8000 rpm, 4ºC for 5 min and immediately frozen (-80°C). LC-MS analysis was used to determine the concentration of **21h** in plasma. Standard curves for **21h** in blood were generated by the addition of various concentrations together with an internal standard to blank plasma. Details of the analytical method are given in the supporting information. Pharmacokinetic parameters were calculated using DAS2.0 software. The research protocol complied strictly with the institutional guidelines of Animal Care and Use Committee at New Drug Evaluation Center of Shandong Academy of Pharmaceutical Sciences

Acute Toxicity Experiment

Kunming mice (18-22 g and 4-5 weeks old) were purchased from the animal experimental center of Shandong University. The research protocol complied strictly with the institutional guidelines of Animal Care and Use Committee at Shandong University. **21h** was suspended in a mixture of polyethylene glycol (PEG) 400/normal saline (70/30, V/V) up to 200 mg/mL, and administered intragastrically by gavage to mice that had been fasted for 12 h. Dosages of 2000 mg·kg-1 were administered to 10 mice per group (5 males, 5 females). Death, body weight, tremor, convulsion, body jerks, hypoactivity, hunched posture, and piloerection were monitored.

ASSOCIATED CONTENT

The Supporting Information is available free of charge via the Internet at http://pubs.acs.org.

MD simulation figures, amino acid sequences of the NAs (A/goose/Guangdong/SH7/2013 (H5N1), 2HU0 (H5N1), A/goose/Jiangsu/1306/2014

(H5N8), 2HT7 (H5N8), A/Chicken/Hebei/LZF/2014 (H5N2), A/duck/Guangdong/674/2014 (H5N6), determination of influenza virus $TCID_{50}$ and the $TCID_{50}$ in CEFs and MDCK cells, analytical method for pharmacokinetics assays of compound **21h**, stability in human plasma and metabolic stability in human liver microsomes, *in vivo* anti-influenza virus activity in specific pathogen free (SPF) chicken embryonated egg, figures of body weight of male and female mice (g)-time(day) and clinical behaviors after administration of **21h** in mice, ^{1}H NMR and ^{13}C NMR spectra for the new compounds

Molecular formula strings.

AUTHOR INFORMATION

Corresponding Authors

*B.H.: e-mail, hbind@163.com; phone, 086-531-85999436;

*P.Z.: e-mail, zhanpeng1982@sdu.edu.cn; phone, 086-531-88382005;

*X.L.: e-mail, xinyongl@sdu.edu.cn; phone, 086-531-88380270.

ORCID

Peng Zhan: 0000-0002-9675-6026

Notes

The authors declare that all experimental work complied with the institutional guidelines on animal studies (care and use of laboratory animals).

The authors declare no competing financial interest.

ACKNOWLEDGMENTS

Financial support from the National Natural Science Foundation of China (NSFC no. 81773574), the Science and Technology Development Project of Shandong Province (no.

2014GSF118175), Young Scholars Program of Shandong University (YSPSDU No. 2016WLJH32), Key research and development project of Shandong Province (no. 2017CXGC1401), from the University of Padua, Progetto di Ricerca di Ateneo 2014 Grant CPDA141311 (to A.Loregian.), and from Associazione Italiana per la Ricerca sul Cancro (AIRC), Investigator Grant 18855 (to A.Loregian.). We are very grateful to Dr. Xiuli Ma and Min Shang at Shandong Academy of Agricultural Sciences for their work in the biological activity assays.

ABBREVIATIONS USED

AIV, avian influenza virus; BPO, benzoyl peroxide; CC_{50}, 50% cytotoxicity concentration; CCK-8, cell counting kit-8; CEF, chicken embryo fibroblasts; CPE, cytopathic effect; DMF, N,N-Dimethylformamide; DMSO, dimethyl sulphoxide; EC_{50}, the concentration causing 50% inhibition of antiviral activity; HA, hemagglutinin; HPAI, highly pathogenic avian influenza; HLM, human liver microsome; CL, clearance; HRMS, high resolution mass spectra; SAR, structure-activity relationship; MD, molecular dynamics; MDCK, Madin-Darby Canine Kidney cells; MM-GBSA, Molecular Mechanics-Generalized Born combined with solvent accessible Surface Area; MRT, mean residence time; MS, Mass spectra; NA, neuraminidase; NAIs, neuraminidase inhibitors; 09N1, NA of 2009 pandemic H1N1; NBS, N-Bromobutanimide; OSC, oseltamivir carboxylate; PAINS, pan-assay interference compounds; PEG, polyethylene glycol; PRA, plaque reduction assay; MUNANA, 2′-(4-methyl-umbelliferyl)-α-D-N-acetylneuraminic acid; Rib, ribavirin; RMSD, root mean square displacement; RMSF, root mean square fluctuations; SPF, specific pathogen free; $TCID_{50}$, 50% tissue culture infectious dose; TMS, tetramethylsilane; TLC, thin-layer

chromatography; ZA, zanamivir.

REFERENCES

(1) Mohan, S.; Kerry, P. S.; Bance, N.; Niikura, M.; Pinto, B. M. Serendipitous discovery of a potent influenza virus a neuraminidase inhibitor. *Angew. Chem. Int. Ed. Engl.* **2014**, *53*, 1076–1080.

(2) Neumann, G.; Noda T.; Kawaoka, Y. Emergence and pandemic potential of swine-origin H1N1 influenza virus. *Nature* **2009**. *459*, 931–939.

(3) Kaplan, B. S.; Webby, R. J. The avian and mammalian host range of highly pathogenic avian H5N1 influenza. *Virus Res*. **2013**. *178*, 3–11.

(4) García-Sosa, A. T.; Sild, S.; Maran, U. Design of multi-binding-site inhibitors, ligand efficiency, and consensus screening of avian influenza H5N1 wild-type neuraminidase and of the oseltamivir-resistant H274Yvariant. *J. Chem. Inf. Model*. **2008**, *48*, 2074–2080.

(5) D'Ursi, P.; Chiappori, F.; Merelli, I.; Cozzi, P.; Rovida, E.; Milanesi, L. Virtual screening pipeline and ligand modelling for H5N1 neuraminidase. *Biochem. Biophys Res. Commun.* **2009**, *383*, 445–449.

(6) Wang, S. Q.; Cheng, X. C.; Dong, W. L.; Wang, R. L.; Chou, K. C. Three new powerful oseltamivir derivatives for inhibiting the neuraminidase of influenzavirus. *Biochem Biophys Res. Commun*. **2010** *401*, 188–1891.

(7) Das, K.; Aramini, J. M.; Ma, L. C.; Krug, R. M.; Arnold, E. Structures of influenza A proteins and insights into antiviral drug targets. *Nat. Struct. Mol. Biol*. **2010**, *17*, 530–538.

(8) Loregian, A; Mercorelli, B; Nannetti, G; Compagnin, C; Palù, G. Antiviral Strategies

Against Influenza Virus: Towards New Therapeutic Approaches. *Cell. Mol. Life. Sci*. **2014**, *71*, 3659–3683.

(9) McClellan, K.; Perry, C. M. Oseltamivir: a review of its use in influenza. *Drugs* **2001**, *61*, 263–283.

(10) (a) von Itzstein, M.; Wu, W. Y.; Kok, G. B.; Pegg, M. S.; Dyason, J. C.; Jin, B.; Van Phan, T.; Smythe, M. L.; White, H. F.; Oliver, S. W. Rational design of potent sialidase-based inhibitors of influenza virus replication. *Nature* **1993**, *363*, 418-423. (b) Dunn, C. J.; Goa, K. L. Zanamivir: a review of its use in influenza. *Drugs* **1999**, *58*, 761–784.

(11) Kubo, S.; Tomozawa, T.; Kakuta, M.; Tokumitsu, A.; Yamashita, M. Laninamivir prodrug CS-8958, a long-acting neuraminidase inhibitor, shows superior anti-influenza virus activity after a single administration. *Antimicrob. Agents Chemother.* **2010**, *54*, 1256–1264.

(12) Chand, P.; Kotian, P. L.; Dehghani, A.; El-Kattan, Y.; Lin, T. H.; Hutchison, T. L.; Babu, Y. S.; Bantia, S.; Elliott, A. J.; Montgomery, J. A. Systematic structure-based design and stereoselective synthesis of novel multisubstituted cyclopentane derivatives with potent antiinfluenza activity. *J. Med. Chem*. **2001**, *44*, 4379–4392.

(13) Anuwongcharoen, N.; Shoombuatong, W.; Tantimongcolwat, T.; Prachayasittikul, V.; Nantasenamat, C. Exploring the chemical space of influenza neuraminidase inhibitors. *PeerJ*. **2016**, *19*, e1958.

(14) Bloom J. D.; Gong, L. I.; Baltimore, D. Permissive secondary mutations enable the evolution of influenza oseltamivir resistance. *Science* **2010**, *328*, 1272−1275.

(15) Collins, P. J.; Haire, L. F.; Lin, Y. P.; Liu, J.; Russell, R. J.; Walker, P. A.; Skehel J.

J.; Martin, S. R.; Hay, A. J.; Gamblin, S. J. Crystal structures of oseltamivir-resistant influenza virus neuraminidase mutants. *Nature* **2008,** *453*, 1258−1261.

(16) Singh, A.; Soliman, M. E. Understanding the cross-resistance of oseltamivir to H1N1 and H5N1 influenza A neuraminidase mutations using multidimensional computational analyses. *Drug. Des. Devel. Ther*. **2015**, *9*, 4137–4154.

(17) Xie, Y.; Xu, D.; Huang, B.; Ma, X.; Qi, W.; Shi, F.; Liu, X.; Zhang, Y.; Xu, W. Discovery of N-substituted oseltamivir derivatives as potent and selective inhibitors of H5N1 influenza neuraminidase. *J. Med. Chem.* **2014**, *57*, 8445–8458.

(18) Samson, M.; Pizzorno, A.; Abed, Y.; Boivin, G. Influenza virus resistance to neuraminidase inhibitors. *Antiviral Res.* **2013**, *98*, 174–185.

(19) Memoli, M. J.; Hrabal, R. J.; Hassantoufighi, A.; Eichelberger, M. C.; Taubenberger, J. K. Rapid selection of oseltamivir-and peramivir resistant pandemic H1N1 virus during therapy in 2 immunocompromised hosts. *Clin. Infect. Dis.* **2010**, *50*, 1252–1255.

(20 Dapat, C.; Kondo, H.; Dapat, I. C.; Baranovich, T.; Suzuki, Y.; Shobugawa, Y.; Saito, K.; Saito, R.; Suzuki, H. Neuraminidase inhibitor susceptibility profile of pandemic and seasonal influenza viruses during the 2009-2010 and 2010-2011 influenza seasons in Japan. *Antiviral Res.* **2013**, *99*, 261–269.

(21) Wu, Y.; Wu, Y.; Tefsen, B.; Shi, Y.; Gao, G. F.. Bat-derived influenza-like viruses H17N10 and H18N11. *Trends Microbiol.* **2014**, *22*, 183–191.

(22) Russell, R. J.; Haire, L. F.; Stevens, D. J.; Collins, P. J.; Lin, Y. P.; Blackburn, G. M.; Hay, A. J.; Gamblin, S. J.; Skehel, J. J. The structure of H5N1 avian influenza neuraminidase suggests new opportunities for drug design. *Nature* **2006**, *443*, 45–49.

(23) Li, Q.; Qi, J; Zhang W.; Vavricka, C. J.; Shi Y.; Wei, J.; Feng, E.; Shen, J.; Chen, J.;

Liu, D.; He, J.; Yan, J.; Liu, H.; Jiang, H.; Teng, M.; Li, X.; Gao, G. F. The 2009 pandemic H1N1 neuraminidase N1 lacks the 150-cavity in its active site. *Nat. Struct. Mol. Biol.* **2010**, *17*, 1266–1268.

(24) (a) Amaro, R. E.; Swift, R. V.; Votapka, L.; Li W. W.; Walker, R. C.; Bush, R. M. Mechanism of 150-cavity formation in influenza neuraminidase. *Nat. Commun.* **2011**, *2*, 388. (b) Han, N.; Mu, Y. Plasticity of 150-loop in influenza neuraminidase explored by Hamiltonian replica exchange molecular dynamics simulations. *PLoS. One.* **2013**, *8*, e60995.

(25) Amaro, R. E.; Cheng, X.; Ivanov, I.; Xu, D.; McCammon, J. A. Characterizing loop dynamics and ligand recognition in human-and avian-type influenza neuraminidases via generalized born molecular dynamics and end-point free energy calculations. *J. Am. Chem. Soc*. **2009**, *131*, 4702–4709.

(26) Kang, D.; Fang, Z.; Huang, B.; Lu, X.; Zhang, H.; Xu, H.; Huo, Z.; Zhou, Z.; Yu, Z.; Meng, Q.; Wu, G.; Ding, X.; Tian, Y.; Daelemans, D.: De Clercq, E.; Pannecouque, C.; Zhan, P.; Liu, X. Structure-based optimization of thiophene[3,2-d]pyrimidine derivatives as potent HIV-1 non-nucleoside reverse transcriptase inhibitors with improved potency against resistance-associated variants. *J. Med. Chem.* **2017**, *60*, 4424–4443.

(27) Kang, D.; Fang, Z.; Li, Z.; Huang, B.; Zhang, H.; Lu, X.; Xu, H.; Zhou, Z.; Ding, X.; Daelemans, D.; De Clercq, E.; Pannecouque, C.; Zhan, P.; Liu, X. Design, synthesis, and evaluation of thiophene[3,2-d]pyrimidine derivatives as HIV-1 non-nucleoside reverse transcriptase inhibitors with significantly improved drug resistance profiles. *J. Med. Chem.* **2016**, *59*, 7991–8007.

(28) Mooney, C. A.; Johnson, S. A.; 't Hart, P.; Quarles van Ufford, L.; de Haan, C. A.;

Moret, E. E.; Martin, N. I. Oseltamivir analogues bearing N-substituted guanidines as potent neuraminidase inhibitors. *J. Med. Chem.* **2014**, *57*, 3154–3160.

(29) Pidathala, C.; Amewu, R.; Pacorel, B.; Nixon, G. L.; Gibbons, P.; Hong, W. D.; Leung, S. C.; Berry, N. G.; Sharma, R.; Stocks, P. A.; Srivastava, A.; Shone, A, E.; Charoensutthivarakul, S.; Taylor, L.; Berger, O.; Mbekeani, A.; Hill, A.; Fisher, N. E.; Warman, A. J.; Biagini, G. A.; Ward, S. A.; O'Neill, P. M. Identification, design and biological evaluation of bisarylquinolones targeting Plasmodium falciparum type IINADH:quinone oxidoreductase (PfNDH2). *J. Med. Chem*. 2012, *55*, 1831–1843.

(30). ZINC PAINS patterns search http://zinc15.docking.org/patterns/home/ (accessed February 25, 2018).

(31). Baell, J. B.; Holloway, G. A. New substructure filters for removal of pan assay interference compounds (PAINS) from screening libraries and for their exclusion in bioassays. *J. Med. Chem.* **2010,** *53*, 2719–2740.

(32) Govorkova, E. A.; Leneva, I. A.; Goloubeva, O. G.; Bush, K.; Webster, R. G. Comparison of efficacies of RWJ-270201, zanamivir, and oseltamivir against H5N1, H9N2, and other avian influenza viruses. *Antimicrob. Agents Chemother*. **2001**, *45*, 2723–2732.

(33) Sriwilaijaroen, N.; Magesh, S.; Imamura, A.; Ando, H.; Ishida, H.; Sakai, M.; Ishitsubo, E.; Hori, T.; Moriya, S.; Ishikawa, T.; Kuwata, K.; Odagiri, T.; Tashiro, M.; Hiramatsu, H.; Tsukamoto, K.; Miyagi, T.; Tokiwa, H.; Kiso, M.; Suzuki, Y. A novel potent and highly specific inhibitor against influenza viral N1-N9 neuraminidases: insight into neuraminidase-inhibitor interactions. *J. Med. Chem.* **2016**, *59*, 4563–4577.

(34) McKimm-Breschkin, J. L. Influenza neuraminidase inhibitors: antiviral action and

mechanisms of resistance. *Influenza Other Respir Viruses* **2013,** *7 Suppl 1*, 25–36.

(35) Monto, A. S.; McKimm-Breschkin, J. L.; Macken, C.; Hampson, A. W.; Hay, A.; Klimov, A.; Tashiro, M.; Webster, R. G.; Aymard, M.; Hayden, F. G.; Zambon, M. Detection of influenza viruses resistant to neuraminidase inhibitors in global surveillance during the first 3 years of their use. *Antimicrob. Agents Chemother.* **2006,** *50*, 2395–2402.

(36) Shie, J. J.; Fang, J. M.; Lai, P. T.; Wen, W. H.; Wang, S. Y.; Cheng, Y. S.; Tsai, K. C.; Yang, A. S.; Wong, C. H. A practical synthesis of zanamivir phosphonate congeners with potent anti-influenza activity. *J. Med. Chem.* **2011**, *133*, 17959–17968.

(37) Schwaid, A. G.; Cornella-Taracido, I. Causes and significance of increased compound potency in cellular or physiological contexts. *J. Med. Chem.* **2018**, *61*, 1767–1773.

(38) Asaoka, N.; Tanaka, Y.; Sakai, T.; Fujii, Y.; Ohuchi, R.; Ohuchi, M. Low growth ability of recent influenza clinical isolates in MDCK cells is due to their low receptor binding affinities. *Microbes Infect* **2006**, *8*, 511–519.

(39) McKimm-Breschkin, J. L.; Barrett, S.; Pilling, P. A.; Hader, S.; Watts, A. G.; Streltsov, V. A. Structural and functional analysis of anti-Influenza activity of 4-, 7-, 8- and 9-deoxygenated 2,3-difluoro- N-acetylneuraminic acid derivatives. *J. Med. Chem.* **2018**, *61*, 1921–1933.

(40) Richard, M.; Erny, A.; Caré B.; Traversier, A.; Barthélémy, M.; Hay, A.; Lin Y. P.; Ferraris, O.; Lina, B. Rescue of a H3N2 influenza virus containing a deficient neuraminidase protein by ahemagglutinin with a low receptor-binding affinity. *PLoS. One*. **2012**, *7*, e33880.

(41) Ayora-Talavera, G.; Cetina-Montejo, L.; Matos-Patrón, A.; Romero-Beltrán, L.

Hemagglutinin variants of influenza A(H1N1)pdm09 virus with reduced affinity for sialic acid receptors. *Arch. Virol*. **2014**, *159,* 1207–1211.

(42) Sauerbrei, A.; Haertl, A.; Brandstaedt, A.; Schmidtke, M.; Wutzler, P. Utilization of the embryonated egg for in vivo evaluation of the anti-influenza virus activity of neuraminidase inhibitors. *Med. Microbiol. Immunol.* **2006**, *195*, 65–71.

(43) Vavricka, C. J.; Li, Q.; Wu, Y.; Qi, J.; Wang, M.; Liu, Y.; Gao, F.; Liu, J.; Feng, E.; He J.; Wang, J.; Liu, H.; Jiang, H. Gao, G. F. Structural and functional analysis of laninamivir and its octanoate prodrug reveals group specific mechanisms for influenza NA inhibition. *PLoS. Pathog*. **2011**, *7*, e1002249.

(44) Li, W.; Escarpe, P. A.; Eisenberg, E. J.; Cundy, K. C.; Sweet, C.; Jakeman, K. J.; Merson, J.; Lew, W.; Williams, M.; Zhang, L.; Kim, C. U.; Bischofberger, N.; Chen, M. S.; Mendel, D. B. Identification of GS 4104 as an orally bioavailable prodrug of the influenza virus neuraminidase inhibitor GS 4071. Antimicrob. *Agents Chemother*. **1998**, *42*, 647–653.

(45) Shie, J. J.; Fang, J. M.; Wang, S. Y; Tsai, K. C.; Cheng, Y. S.; Yang, A. S.; Hsiao, S. C; Su, C. Y; Wong, C. H.. Synthesis of tamiflu and its phosphonate congeners possessing potent anti-influenza activity. *J. Am. Chem. Soc.* **2007**, *129*, 11892–11893.

(46) Muratore, G; Goracci, L; Mercorelli, B; Foeglein, Á; Digard, P; Cruciani, G; Palù, G; Loregian, A. Small Molecule Inhibitors Of Influenza A and B Viruses that Act by Disrupting Subunit Interactions of the Viral Polymerase. *Proc. Natl. Acad. Sci. USA.* **2012**, *109*, 6247–6252.

(47) Massari, S; Nannetti, G; Goracci, L; Sancineto, L; Muratore, G; Sabatini, S; Manfroni, G; Mercorelli, B; Cecchetti, V; Facchini, M; Palù, G; Cruciani, G; Loregian,

A; Tabarrini, O. Structural Investigation of Cycloheptathiophene-3-carboxamide Derivatives Targeting Influenza Virus Polymerase Assembly. *J. Med. Chem*. **2013**, *56*, 10118–10131.

(48) Muratore, G.; Mercorelli, B.; Goracci, L.; Cruciani, G.; Digard, P.; Palù, G.; Loregian, A. Human Cytomegalovirus Inhibitor AL18 Also Possesses Activity against Influenza A and B Viruses. *Antimicrob. Agents Chemother*. **2012**, *56*, 6009–6013.

(49) Massari, S; Nannetti, G; Desantis, J; Muratore, G; Sabatini, S; Manfroni, G; Mercorelli, B; Cecchetti, V; Palù, G; Cruciani, G; Loregian, A; Goracci, L; Tabarrini, O. A Broad Anti-influenza Hybrid Small Molecule That Potently Disrupts the Interaction of Polymerase Acidic Protein-Basic Protein 1 (PA-PB1) Subunits. *J. Med. Chem*. **2015**, *58*, 3830–3842.

(50) Lepri, S.; Nannetti, G.; Muratore, G.; Cruciani, G.; Ruzziconi, Mercorelli, B.; Palù, G.; Cruciani, G.; Loregian, A.; Goracci, L. Optimization of Small-Molecule Inhibitors of Influenza Virus Polymerase: From Thiophene-3-Carboxamide to Polyamido Scaffolds. *J. Med. Chem.* **2014**, *57*, 4337–4350.

(51) Liu, A. L.; Wang, H. D.; Lee, S. M.; Wang, Y. T.; Du, G. H. Structure-activity relationship of flavonoids as influenza virus neuraminidase inhibitors and their in vitro anti-viral activities. *Bioorg. Med. Chem.* **2008**, *16*, 7141–7147.

(52) Zhang, J.; Poongavanam, V.; Kang, D.; Bertagnin, C.; Lu, H.; Kong, X.; Ju, H.; Lu, X.; Gao, P.; Tian, Y.; Jia, H.; Desta, S.; Ding, X.; Sun, L.; Fang, Z.; Huang, B.; Liang, X.; Jia, R.; Ma, X.; Xu, W.; Murugan, N. A.; Loregian, A.; Huang, B.; Zhan, P.; Liu, X. Optimization of N-Substituted Oseltamivir Derivatives as Potent Inhibitors of Group-1 and -2 Influenza A Neuraminidases, Including a Drug-Resistant Variant. *J. Med. Chem*.

2018, *61*, 6379−6397.

(53) Collins, P. J.; Haire, L. F.; Lin, Y. P.; Liu, J.; Russell, R. J.;Walker, P. A.;Skehel, J. J.; Martin, S. R.;Hay, A. J.; Gamblin, S. J. Crystal structures of oseltamivir-resistant influenza virus neuraminidase mutants. *Nature* **2008**, *453*, 1258−1261.

(54) Case, D.A.; Darden, T.A.; Cheatham, T.E.; Simmerling, C.L.; Wang, J.; Duke, R.E.; Luo, R.; Walker, R.C.; Zhang, W.; Merz, K.M.; Roberts, B.; Hayik, S.; Roitberg, R.; Seabra, G.; Swails, J.; Götz, A.W.; Kolossváry, I.; Wong, K.F.; Paesani, F.; Vanicek, J.; Wolf, R.M.; Liu, J.; Wu, X.; Brozell, S.R.; Steinbrecher, T.; Gohlke, H.; Cai, Q.; Ye, X.; Wang, J.; Hsieh, M.-J.; Cui, G.; Roe, D.R.; Mathews, D.H.; Seetin, M.G.; Salomon-Ferrer, R.; Sagui, C.; Babin, V.; Luchko, T.; Gusarov, S.; Kovalenko, A.; Kollman, P.A.; (2012), AMBER 12, University of California, San Francisco.

(55) Frisch, M.J.; Trucks, G.W.; Schlegel, H.B.; Scuseria, G.E.; Robb, M.A.; Cheeseman, J.R.; Scalmani, G.; Barone, V.; Petersson, G.A.; Nakatsuji, H.; Li, X.; Caricato, M.; Marenich, A.; Bloino, J.; Janesko, B.G.; Gomperts, R.; Mennucci, B.; Hratchian, H.P.; Ortiz, J.V.; Izmaylov, A.F.; Sonnenberg, J.L.; Williams-Young, D.; Ding, F.; Lipparini, F.; Egidi, F.; Goings, J.; Peng, B.; A. Petrone, A.; Henderson, T.; Ranasinghe, D.; Zakrzewski, V.G.; Gao, J.; Rega, N.; Zheng, G.; Liang, W.; Hada, M.; Ehara, M.; Toyota, K.; Fukuda, R.; Hasegawa, J.; Ishida, M.; Nakajima, T.: Honda, Y.; Kitao, O.; Nakai, H.; Vreven, T.; Throssell, K.; Montgomery, Jr., J. A.; Peralta, J.E.; Ogliaro, F.; Bearpark, M.; Heyd, J.J.; Brothers, E.; Kudin, K. N.; Staroverov, V.N.; Keith, T.; Kobayashi, R.; Normand, J.; Raghavachari, K.; Rendell, A.; Burant, J. C.; Iyengar, S.S.; Tomasi, J.; Cossi, M.; Millam, J.M.; Klene, M.; Adamo, C.; Cammi, R.; Ochterski, J. W.; Martin, R.L.; Morokuma, K.; Farkas, O.; Foresman, J.B.; Fox, D.J. ; Gaussian 09, RevisionA.02,

Gaussian, Inc., Wallingford CT, 2009.

(56) Morris, G. M.; Huey, R.; Lindstrom, W.; Sanner, M. F.; Belew, R. K.; Goodsell, D. S.; Olson, A. J. Autodock4 and AutoDockTools4: automated docking with selective receptor flexiblity. *J. Computational Chemistry* **2009**, *16*, 2785−2791.

(57) Breneman, C.; Wiberg, K. Determining AtomCentered Monopoles from molecular electrostatic potentials. The need for high sampling density in formamide conformational analysis. *J. Comput. Chem.* **1990**,*11*, 361−373

(58) Wang, J.; Wolf, R.; Caldwell, J.; Kollman, P.; Case, D. Development and testing of a general AMBER force field. *J. Comput. Chem.* **2004**, *25*, 1157−1174.

(59) Ryckaert, J. P.; Ciccotti, G.; Berendsen, H. J. C. Numerical integration of the cartesian equations of motion of a system with constraints: molecular dynamics of n-alkanes. *J. Comput. Phys.* **1977,** *23*, 327−341.

(60) Berendsen, H. J.C.; Postma, J. P. M.; Gunsteren, W. F. V.; DiNola, A.; Haak, J. R. Molecular dynamics with coupling to an external bath. *J. Chem. Phys.* **1984**, *81*, 3684−3690.

(61) Kollman, P. A.; Massova, I.; Reyes, C.; Kuhn, B.; Huo, S.; Chong, L.; Lee, M.; Lee, T.; Duan, Y.; Wang, W.; Donini, O.; Cieplak, P.; Srinivasan, J.; Case, D. A.; Cheatham TE 3rd. Calculating structures and free energies of complex molecules: combining molecular mechanics and continuum models. *Acc. Chem. Res.* **2000**, *33*, 889−897.

(62) Genheden, S.; Ryde, U. The MM/PBSA and MM/GBSA methods to estimate ligand-binding affinities. *Expert Opin. Drug Discov.* **2015**, *10*, 449−461.

(63) Murugan, N. A.; Nordberg, A.; Ågren, H. Different positron emission tomography tau tracers bind to multiple binding sites on the tau fibril: insight from computational

modeling. *ACS Chem. Neurosci.* **2018,** *9*, 1757−1767.

(64) Poongavanam, V.; Namasivayam, V.; Vanangamudi, M.; Al Shamaileh, H.; Veedu, R. N.; Kihlberg, J.; Murugan, N. A. Integrative approaches in HIV-1 non-nucleoside reverse transcriptase inhibitor design. *WIREs Comput Mol Sci*, **2018**, *8*, e1328. doi:10.1002/wcms.1328.

(65) Murugan, N. A.; Halldin, C.; Nordberg, A.; Långström, B.; Ågren, H. The culprit is in the cave: the core sites explain the binding profiles of amyloid-specific tracers. *J. Phys. Chem. Lett.* **2016**, *7*, 3313−3321.

(66) Miller, B. R. 3rd; III, McGee, T. D. Jr; Swails, J. M.; Homeyer, N.; Gohlke, H.; Roitberg, A. E. MMPBSA.py: an efficient program for end-state free energy calculations. *J. Chem. Theory Comput.* **2012**, *8*, 3314−3321.

Table of Contents Graphic

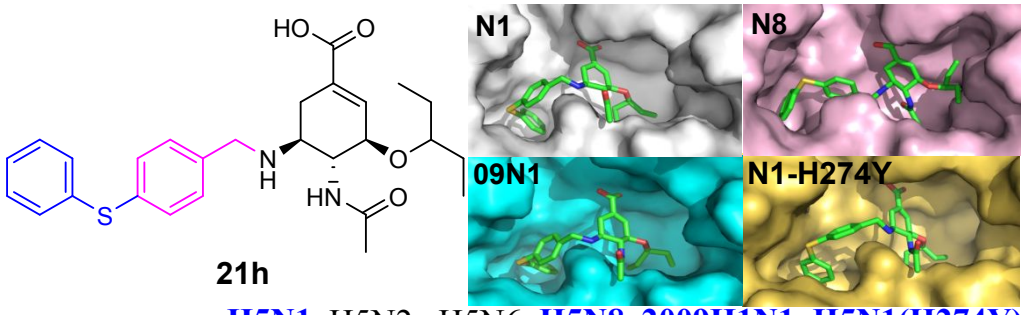

	H5N1	H5N2	H5N6	**H5N8**	**2009H1N1**	**H5N1(H274Y)**
IC_{50} (NA, nM)	**0.96**	896.9	3065	**1.89**	**5.57**	**32.81**
EC_{50} (μM)	**0.39**	0.09	0.52	**0.056**		

F (rat) = 10.30%; Metabolic stability: $T_{1/2}$ > 145 min, CL < 9.6 in human liver microsomes; intact after 120 min in human plasma